TAMPEREEN TEKNILLINEN YLIOPISTO
TAMPERE UNIVERSITY OF TECHNOLOGY

MD. LUSHANUR RAHMAN

# STUDY OF THE CYCLOSTATIONARITY PROPERTIES OF VARIOUS SIGNALS OF OPPORTUNITY

Master of Science Thesis

Examiners:
Associate Professor Dr. Elena-Simona Lohan
Professor Dr. Markku Renfors
Examiner and topic approved by the council of the Faculty of Computing and Electrical Engineering on 04 December 2013

# ABSTRACT

TAMPERE UNIVERSITY OF TECHNOLOGY
Master's Degree Programme in Electrical Engineering
**RAHMAN, MD. LUSHANUR**: Study of the cyclostationarity properties of various signals of opportunity
Master of Science Thesis, 119 pages.
May 2014
Major: Wireless Communication Circuits and Systems
Examiner(s): Associate Professor Dr. Elena-Simona Lohan
Professor Dr. Markku Renfors
Keywords: Signals of Opportunity (SoO), Cyclostationarity.

Global Navigation Satellite Systems (GNSS) offer precise position estimation and navigation services outdoor but they are rarely accessible in strong multipath environments, such as indoor environments. Fortunately, several Signals of Opportunity (SoO), (such as RFID, Wi-Fi, Bluetooth, digital TV signals, etc.) are readily available in these environments, creating an opportunity for seamless positioning. Performance evolution of positioning can be achieved through contextual exploitation of SoO. The detection and identification of available SoO signals or of the signals which are most relevant to localization and the signal selection in an optimum way, according to designer defined optimality criteria, are important stages to enter such contextual awareness domain. Man-made modulated signals have certain properties which vary periodically in time and this time-varying periodical characteristics trigger what is known as cyclostationarity. Cyclostationarity analysis can be used, among others, as a tool for signal detection. Detected signals through cyclostationary features can be exploited as SoO. The main purpose of this thesis is to study and analyze the cyclostationarity properties of various SoO. An additional goal is to investigate whether such cyclostationarity properties can be used to detect, identify and distinguish the signals which are present in a certain frequency band.

The thesis is divided into two parts. In the literature review part, the physical layer study of several signals is given, by emphasizing the potential of SoO in positioning. In the implementation part, the possibility of signals detection through cyclostationary features is investigated through MATLAB simulations. Cyclostationary properties obtained through FFT accumulation Method (FAM) and statistical performance of detection are studied in the presence of stationary additive white Gaussian noise (AWGN). Besides that, the performance in signal detection using cyclostationary-based detector is also compared to the performance with the energy-based detectors, used as benchmarks.

The simulated result suggest that cyclostationary features can certainly detect the presence of signals in noise, but simple cases, such as one type of signal only and AWGN noise, are better addressed via traditional energy-based detection. However, cyclostationary features can exhibit advantages in other types of noises and in the presence of signal mixtures which in fact may fulfil one of the preliminary requirements of cognitive positioning.

# PREFACE

The work for this Master of Science Thesis has been carried out at the Department of Electronics and Communication Engineering in Tampere University of Technology, Tampere, Finland during December 2013-May 2014. The funding has been offered by the Academy of Finland.

I am very much fortunate to have Dr. Elena-Simona Lohan as my supervisor. Firstly, I would like to express my deepest gratitude to her for enthusiastic encouragement, constant support, and precious guidance throughout this work. I am grateful to her for being available whenever I needed and also for offering me the opportunity to work in her research group.

I would like to thank Professor Dr. Markku Renfors for his constructive feedback and helpful comments being an examiner of this thesis. I am grateful to Pedro Silva and Dr. Mohammad Zahidul Hasan Bhuiyan, for offering me their help whenever I needed and sharing their technical opinions with me. I am very much pleased to find such a nice research environment and friendly colleagues within the research group.

I am deeply thankful to all my friends from Finland, for having such a great time in travelling around Europe and parties. Finally, I am thankful to my family and all of my friends in Bangladesh, for standing by me, for supporting me, for advising me, and last but not the least for believing in me.

Tampere, Finland, May 2014
Md. Lushanur Rahman

# TABLE OF CONTENTS

# LIST OF TABLES

# LIST OF FIGURES

# LIST OF SYMBOLS

| | |
|---|---|
| $a_k$ | Fourier coefficient |
| $b_n$ | Data bits for n$^{th}$ symbol |
| $c$ | Speed of light |
| $d_x$ | Deflection coefficient |
| $E_b$ | Bit energy |
| $f$ | Spectral frequency |
| $\Delta f$ | Spectral frequency resolution |
| $f_b$ | Symbol rate of data sequence |
| $f_c$ | Chip rate of spreading code |
| $f_{carrier}$ | Carrier frequency |
| $f_s$ | Sampling frequency |
| $f_{sym}$ | Subcarrier frequency |
| $\Delta f_{sym}$ | Subcarrier frequency separation |
| $H_0$ | Noise only hypothesis |
| $H_1$ | Signal in noise hypothesis |
| $M$ | Alphabet size |
| $N'$ | Length of short time FFT |
| $P$ | Size of second FFT point |
| $p(t)$ | Basic modulation pulse |
| $P_d$ | Probability of detection |
| $P_{fa}$ | Probability of false alarm |
| $R_y^{\alpha}(\tau)$ | Cyclic autocorrelation function |
| $S_y^{\alpha}(f)$ | Spectral correlation density function |
| $S_F$ | Spreading factor |
| $T_b$ | Symbol interval |
| $T_c$ | Chip interval |
| $T_{sym}$ | OFDM symbol duration |
| $\alpha$ | Cyclic frequency |
| $\Delta\alpha$ | Cyclic frequency resolution |
| $\gamma$ | Threshold |
| $\tau$ | Time delay |
| $\Psi(t)$ | Mother wavelet function |

## LIST OF ACRONYMS

| | |
|---|---|
| AOA | Angle of Arrival |
| AP | Access Point |
| AWGN | Additive White Gaussian Noise |
| CAF | Cyclic Autocorrelation Function |
| CDF | Cumulative Distribution Function |
| CDMA | Code Division Multiple Access |
| FAM | FFT Accumulation Method |
| FFT | Fast Fourier Transform |
| dB | Decibel |
| DVB | Digital Video Broadcasting |
| GMSK | Gaussian Minimum Shift Keying |
| GNSS | Global Navigation Satellite Systems |
| GPS | Global Positioning Systems |
| GSM | Global Systems for Mobile Communications |
| HOM | Higher Order Moment |
| ICI | Inter Carrier Interference |
| ISI | Inter Symbol Interference |
| MAC | Media Access Control |
| OFDM | Orthogonal Frequency Division Multiplexing |
| PDF | Probability Distribution Function |
| PSK | Phase Shift Keying |
| QAM | Quadrature Amplitude Modulation |
| RFID | Radio Frequency Identification |
| RSS | Received Signal Strength |
| RSSI | Received Signal Strength Indicator |
| ROC | Receiver Operating Characteristics |
| SCF | Spectral Correlation Density Function |
| SNR | Signal to Noise Ratio |
| SoO | Signals of Opportunity |
| TDOA | Time Difference of Arrival |
| TOA | Time of Arrival |
| UWB | Ultra Wideband |
| Wi-Fi | Wireless Fidelity |
| WLAN | Wireless Local Area Network |
| WWAN | Wireless Wide Area Network |

# 1. INTRODUCTION

## 1.1 Background and research motivation

Finding positioning solutions embedded to the wireless mobile terminals is becoming a key factor in recent years to drive location-aware and location-based services. The ultimate goal of such kind of localization solution is to provide position information anywhere anytime with sufficient accuracy. Global Satellite Navigation Systems (GNSS) such as the US Global positioning system (GPS) provide reliable, scalable and accurate position outdoors. The increasing demands for positioning solution worked as a driving force for the introduction of new satellite navigation systems such as the European Galileo system, the Russian GLONASS, and the Chinese Compass-Beidou 2 systems [1]. GNSS can be a more generic term to be used in conjunction with all the above-mentioned satellite systems. GNSS has become a popular choice due to its simplicity and low cost applications to the users. However, in specific environments, such as indoors and underground and sometimes even in dense urban scenarios, GNSS systems cannot provide good performance. Moreover, the accuracy of position estimation is degraded due to weak signals, multipath or non-line-of-sight signal propagation [2]. The indoor operational challenges of GNSS systems are the driving factors for finding complementary solutions. In addition, continuously available positioning solution is also a reasonable demand.

Signals of Opportunity (SoO) refer to any wireless signals initially not built for positioning. SoO are complementary solutions to GNSS, allowing continuous availability of localization solution regardless of the environment [3], [4]. To accomplish that, the mobile receiver needs first to identify all the available signals within its range of operation, then to select some of them for positioning purpose (according to certain optimality criteria defined by the designer), and then to combine them to form a hybrid positioning solution. The approach of receiving various signals for positioning leads to the concept of cognitive positioning or positioning with signals of opportunity [5]. However this approach involves the challenges of signal recognition and selection. A receiver able to capture various SoO must be a multi-mode multi-frequency receiver [6]. In such receiver, multiple active signals are simultaneously received at the front end [7]. The signal detection or identification is the first step in a cognitive positioning engine [8]. Indeed, the technique of effective signal recognition for accurate positioning estimation by selecting suitable signal is yet an open topic for research. Researchers around the world have put significant effort on modulation classification and feature-based signal detection [9]-[13]. One of the answers of signal selection resides in the signal's own features and the next step would be to sense such signal-related information by the receiver. The cognitive positioning aspects are inspired from the cognitive radio, where system is trying to find the absence of spectrum allocation so that secondary user can

use that unused band. However, in SoO-based positioning, the foremost need is to find out available signals which can be treated as candidates for positioning [14]. Looking back to 1960's, a statistical signal processing tool named cyclostationary signal analysis has been proposed by Dr. Gardner and his colleagues [15]-[18]. Cyclostationary process is defined by the periodical behavior of some of the signals' properties. Almost all types of modulated signals exhibit cyclostationarity as a result of periodicity associated with the modulation [19]. If the receiver measures cyclostationary attributes of received signals, then the signal recognition can be performed through its features. However, cyclostationary signal analysis has not been yet considered in navigation systems modeling. Recently, people are putting significant concentration on cyclostationary properties in the context of wireless communications, due to its remarkable distinguishing ability among multiple signals [20]-[23]. Consequently, cyclostationary signal analysis has a huge potential in future cognitive positioning receiver modeling where receiver has to deal with multiple signals of different types [7]. Moreover, the cyclostationarity property of SoO has been not studied (or studied very little) in literature so far, to the best of the author's knowledge. From this point of view, the research on cyclostationarity properties of various signals that are freely available within the mobile receiver range needs a crucial and timely contribution from the positioning context perspective. The author was motivated by these facts and the work presented in this thesis is related to studying cyclostationary-based signal detection for cognitive positioning systems.

## 1.2 Thesis objectives and contributions

The main objective of this research is to analyze the cyclostationary properties of various signals of opportunity. Comparison of cyclostationary properties among various signals and various ways of detection for signals of opportunity through this cyclostationarity property will be also demonstrated. After proper detection, the properties can be used for further cognitive positioning receiver modeling.

This work relates the signals of opportunity paradigm with the cyclostationary processes. Since future cognitive positioning receiver will have to process multiple signals, the spectrum recognition in terms of contextual information is a fundamental requirement for awareness about the available signals. Indeed, in the framework of seamless positioning of tomorrow, the focus will be on using the signals inherent features, which will make the acquisition and tracking process faster. Cyclostationary analysis is used in this thesis as a research method for having such spectrum awareness to decide which signal to select. Moreover, hybridization of existing technologies will be the most likely scenario of future positioning system where relevant information is used from co-operation of multiple systems. However, this hybridization problem is not addressed in the simulation of this work; rather we focus on individual signal detection through its cyclostationary properties. The detection of a signal is the first and foremost aspect towards the recognition of which SoO are available for positioning at the receiver

end. For that end, cyclostationary signal processing is used to detect the received individual signal. To accomplish the mentioned objective and motivation, the author points out main contribution as follows:

- Overview of the main SoO and their usage in environments where GNSS is not available, such as indoors.
- Seamless positioning framework formulation towards cognitive positioning.
- Literature review of exiting research methods for spectrum sensing and signal classification which gives a baseline for signal selection stage of SoO based positioning.
- General modeling of most common wireless signals namely CDMA and OFDM.
- Review of cyclostationary signal theory and characterization of cyclostationarity properties.
- Cyclic spectral analysis of individual signal at baseband and generation of cyclostationarity features-based detection statistics.
- Statistical performance analysis of cyclostationarity-based signal detection, at several cyclic frequencies in terms of receiver operation characteristics.
- Cyclostationary detection performance analysis for variation in test statistics formation.
- Drawing a comparison between cyclic features based detection and energy-based detection
- Finally, an overall explanation on cyclostationary-based detection performance with a view of simulation boundary and statistical analysis of the generated data.

The author submitted two publications at International Conference on Localization and GNSS 2014, one as the main author and one as co-author. The publication as the main author is related to the investigation on signal detection through its cyclic features in cognitive positioning framework for CDMA and OFDM signals. The author had a major contribution to the analytical derivation behind the explanation of results and performed the simulations.

## 1.3 Thesis organization

The thesis is organized in eight chapters. The subsequent chapters are as follows:

Chapter 2 familiarizes the reader with the concept of SoO. The process flow and challenges involved with SoO reception based future cognitive positioning receiver are also presented. The standard-related information of various SoO is overviewed which will lead the reader to the diverse use of signals' relevant parameters to location.

Chapter 3 discusses the typical modulations and multiple access techniques used in wireless signals nowadays.

Chapter 4 presents the spectrum sensing, signal detection and signal classification methods used in recent research on spectrum awareness of the navigation systems. This chapter also explains the necessity of selecting the signals which hold the best positioning capabilities.

Chapter 5 describes the theoretical definitions of cyclostationary processes and characterizes cyclostationarity properties. This chapter also focuses on the applications of the cyclostationary features in the context of signal-of-opportunity based positioning.

Chapter 6 discusses the different methods of cyclic spectral analysis. This chapter especially points out the simulation model used in implementation phase and specific criteria used for simulation with CDMA, OFDM signals in MATLAB.

Chapter 7 shows the main results that have been found from the simulations and also analyzes and compares the results. A brief overall discussion is also presented which is driven from the statistical analysis of generated data in simulation.

Chapter 8 finally draws conclusions from this research and makes recommendations for future work.

# 2. SIGNALS OF OPPORTUNITY

Signals of Opportunity (SoO) refer to all wireless signals that have not been originally intended for navigation systems but those are freely available to a navigation receiver within range. Signal-of-opportunity concept has opened a new paradigm for navigation solutions to find position through processing of SoO in cases where the GNSS has poor performance. SoO can be, for example, cellular telephone signals, digital TV signals, Radio Frequency Identification (RFID) signals, Wireless Local Area Network Signals (WLAN-Wi-Fi), Bluetooth signals or any other wireless signals which are accessible to the receiver to a certain time and location.

Positioning accuracy and seamless location between indoor and outdoor environments can be theoretically achieved through proper exploitation of SoO [3]. Identification or detection of available signals and selection in an optimum way for positioning solutions is playing key role on the activity of navigation system receiver. This thesis addresses the problem of signal identification and classification, by analysing and exploiting SoO cyclostationarity properties.

## 2.1 Prospects of SoO in positioning

Positioning is a key concern nowadays in the daily life easiness considering localization and location based service associated with it. GPS and other satellite positioning system can provide a precise localization and navigation service outdoors, where signals from the satellites are typically available at good Carrier to Noise Ratios (CNR). The main concern is in achieving also indoor positioning, where GNSS signals is scarcely present [24]. Moreover, indoor environment maps, topology and existing set-up can change frequently, which is a major obstacle in the path of obtaining accurate indoor positioning. Also, the presence of multipath effects, shadowing and fading is much more likely in indoor environments than in outdoor environments.

Most people spent nearly 80% of their time in indoor and which leads to a necessity of accurate indoor positioning solution to user. Fortunately, several wireless signals, such as wireless mobile communication signals and Wi-Fi signals are readily available in indoor [25]. Such signals can be used for positioning and commercial solutions are already available. Apparently, cellular signal and Wi-Fi signal based positioning has started to be adopted in indoor with few shortcomings in performance in an optimized manner [26].

Several research organization and institutions are now investigating the prospect of using SoO for indoor positioning, for example in [27]-[41]. Moreover, some authors have shown the potential for SoO based positioning in collaboration with GNSS, for example in [42]-[44].The sub-sequent section of this chapter describes the system specific information of those signals which have the prospect to be used in positioning estimation. A brief discussion on the deployment scenario of specific signal of opportunity in commercial and test set up will also be presented.

A block diagram for a receiver working with SoO is shown in *Figure 2-1*.The main structure and positioning computation concept are similar to the typical GNSS receiver, but the main difference stays in the way of processing the various SoO [7],[45]. After being received by the antenna, signals are processed in its baseband. In baseband processing, the signal is first identified, for example through its cyclostationarity properties studied in this, and then it is further processed for positioning purpose (for example via acquisition and tracking, or via Bayesian combining, etc). Signal selection unit selects the signal which has the best accuracy capability in positioning estimation while signal classification unit supports the selection through performing modulation recognition [7]. Post processing block computes the pseudorange between receiver and transmitter to find co-ordinate estimation. The navigation unit or the localization server converts the estimated coordinates into map position through the navigation software. Moreover, there might be a user interface, such as the map display present with the receiver system. Depending on the designer's choice, the position computation may take place either on the user receiver or at network side.

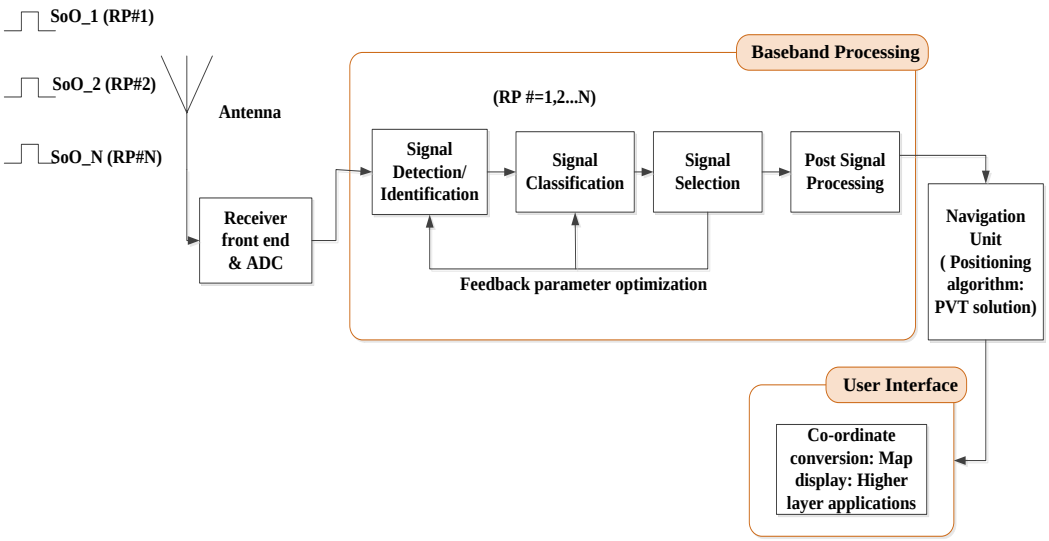


***Figure 2-1*** *Generic positioning receiver model for SoO reception [7]*

From a generic system point of view, according to the *Figure 2-2*, mobile user nodes communicate to the server through wireless switches or access points. These user nodes are capable to receive different SoO from several known transmitters and process that

signals for estimating position from the estimation of distance or pseudorange between receiver and transmitter. The distance estimation can be done in several ways, such as, based on Received Signal Strength Indicator (RSSI) and path loss models, based on timing estimation (such as time of arrival /time difference of arrival), or based on angle of arrival (AOA) or other spatial information [6]. Trilateration principle or least square methods may be for example used to find the user location coordinates from the estimated distance of receiver to the several transmitters.

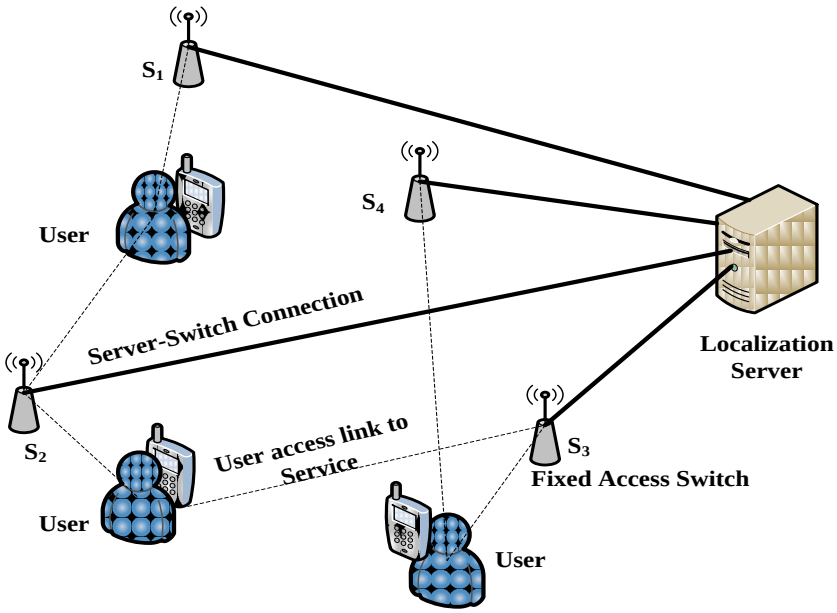


***Figure 2-2*** *Generic positioning system architecture based on SoO reception*

The main localization principles are briefly described in what follows:

- **TOA/TDOA:**

The time of arrival (TOA) is defined by the simple formula of finding the travel time of signal as,

$$\begin{cases} TOA = T_{received\ time} - T_{transmit\ time} \\ wave\ speed * TOA = distance \end{cases} \quad (2\text{-}1)$$

Where, $T_{received\ time}$ is the signal reception time at the receiver, $T_{transmit\ time}$ is the signal transmit time from the transmitter, and wave speed is equal to the speed of light (about $3 \times 10^8\ ms^{-1}$).

When the distance is derived from the above eq. (2-1), errors may occur due to imperfect timing synchronization or due to clock error and multipath effect. Clock errors are common to all transmitters, while multipath errors are transmitter dependent. If the transmitters are not synchronized, it is more common to use time difference of arrival (TDOA) instead of TOA [6], [24]. TDOA measures the time difference of one signal arrival at the same receiver from several transmitters. From the TDOA value, the distance between known transmitter and receiver can be again calculated [24], [46], [47].

- **RSSI:**

Received Signal strength Indicator (RSSI) provides the Received Signal Strength (RSS) averaged over a period of time at a certain location [6], [26]. This received power can be used to estimate the distance between receiver and transmitter with the help of propagation model [6]. After that, the estimated distances can be used to determine the receiver position by trilateration or multilateration principle.

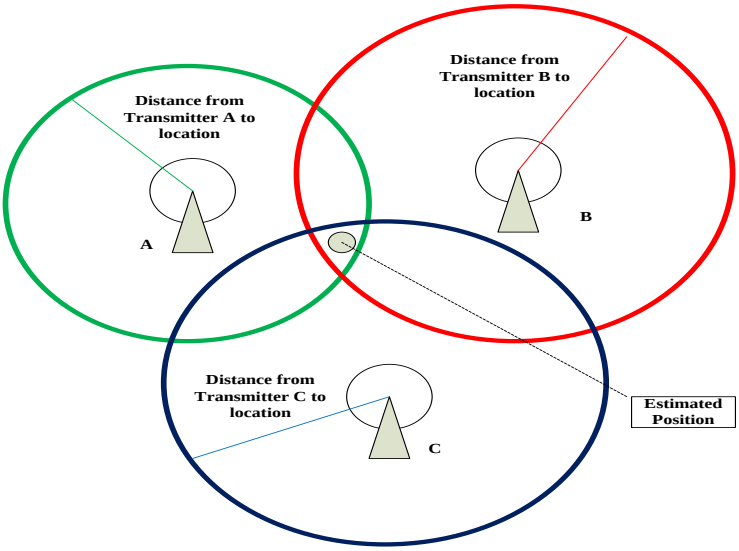


***Figure 2-3*** *Trilateration principle* [1], [6]

- **Trilateration principle:**

Trilateration principle can be used to determine the user position from the distance estimation made based on TDOA, TOA, RSS or AOA. The main idea is to build a circle or radius equal to the computed distance around each transmitter. The user position can be found at the intersection point of the circles drawn. Trilateration refers to the use of three transmitters with known location for the position estimation [1], [6]. The drawn circles and estimated user position concept can be observed in *Figure 2-3*. The same concept can be extended to more than 3 transmitters, and in this case we would talk about multi-lateration.

The signals of opportunity can be categorized in two types according to their deployment aspect. Some signals may use to make position estimation through its existing infrastructure, while some other SoO signals need to deploy new or partial infrastructure [24], [48]. According to this concept, SoO can be divided as below:

- Requiring a (large) specific infrastructure, examples belonging to this category are Active Badge (infrared) [49], Bat System (ultrasound) [44], Smart Floor (pressure sensors) [50], RFID [34], cameras [51], and so on.

- Using the existing wireless telecommunication networks, such as Wi-Fi (802.11) [27], Bluetooth [29], [30], RADAR [52], DTV [40], [41], UWB [38], [39] communications satellite signals, celestial and other signals from nature, and so on.

There are several challenges related with positioning estimation through the available SoO signals. The main ones are summarized below:

- Identification of SoO reaching the receiver (the topic of this thesis focuses in fact on challenges related to this identification of SoO)
- Relevant signal selection from the received numerous signals for accurate positioning. This challenge is better addressed by relevant signal selection problem
- Practical implementation of the hybridization algorithms for localization based on different types of signals
- Parameter optimization at various stages involved in positioning (signal detection, signal selection, hybridization, etc.)
- The absence of synchronization between the transmitters and the typical lack of reference points (unknown location of transmitters)
- Limited infrastructure deployments for SoO
- Achieving low implementation cost and user friendly interfaces
- Initially, the SoO systems were not built and maintained for positioning solution, which may lead sometimes to the need of having a complex remodeling and modification of the system for using such signal for navigation purposes.

Evolutions in positioning systems are considering contextual information, such as signal identification, classification and selection. In theory, such system could be capable of adapting the signal acquisition and tracking accordingly [7], [8]. This adaptation can result in the hybridization of several technologies or selecting the most viable for that time and location [53]. According to the previous discussions, a simplified block diagram of the steps involved in SoO-based positioning is illustrated in *Figure 2-4*.

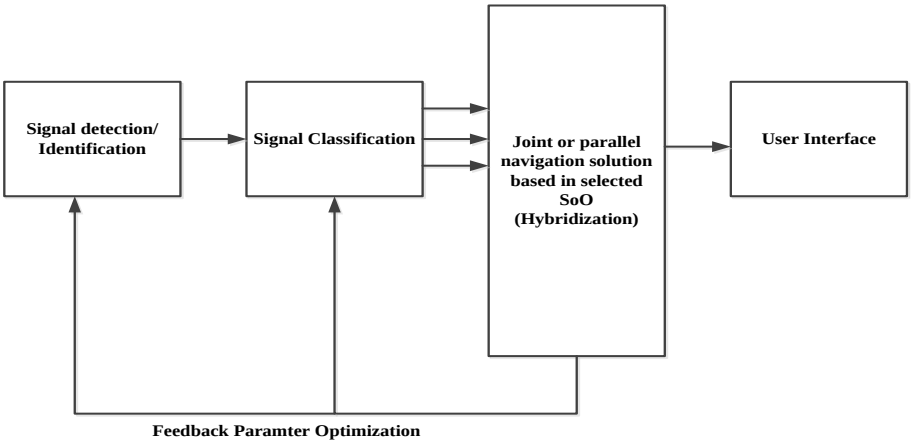


***Figure 2-4*** *Illustration of the steps involved in a SoO-based positioning [7]*

This thesis focuses on the first step involved in a SoO-based positioning mentioned in *Figure 2-4* which is SoO detection. Intuitive study on the SoO provides us the fact that, they can be analyzed according to their modulation types being used and possibly according to the multiple access types as well. Cyclostationarity analysis is one of the existing tools which can be used to identify various signals according to their modulation type. Apparently, by investigating the baseband cyclostationary properties of CDMA, OFDM signals, we can obtain a clear idea on detection and positioning prospects of SoO. This is the goal of this thesis and this analysis will be explained in detail in chapters 5, 6, 7.

Many wireless network technology including WLAN, WPAN, and WWAN operate in ISM bands (Industrial, scientific, medical). *Figure2-5* shows ISM frequency bands which provide unlicensed shared access to wireless activity [54]. ISM bands are separated in three different frequency bands, namely 900 MHz, 2.4 GHz, and 5.7 GHz. Several common wireless technologies operate in ISM band, as described below.

- **WPAN, Wireless Personal Area Network**
  - IEEE 802.15: Bluetooth [30], ZigBee [55], WiMedia/UWB [38]
  - Infrared Data Association (IrDA) [56], RFID [34]
- **WLAN, Wireless Local Area Network**
  - IEEE 802.11: Wi-Fi [24]
- **BWA, Broadband Wireless Access/WMAN, Wireless Metropolitan Area Network**
  - IEEE 802.16: WiMAX (also WiBRO in South Korea) [57]
- **WWAN, Wireless Wide Area Network**
  - IEEE 802.20: MBWA (Mobile Broadband Wireless Access) [58]

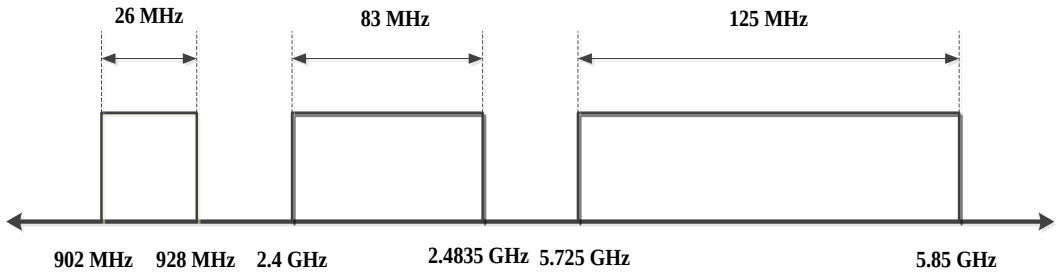


***Figure2-5*** *ISM frequency band* [54]

The next sections investigate the prospect of SoO as positioning signals. Positioning accuracy depends on the effective extraction of useful information from the signal which is available. In order to achieve that, individual study on the different signals is needed, in order to know which signal has a better performance in which aspect of positioning. As a matter of fact, this type of idea will lead us to the diverse use of signals' relevant parameter for a better estimation of position. The estimation needs to be done in a seamless manner from indoor to outdoor [5], [42] and [43].

The standard-related information of various SoO is overviewed in the next sections, focusing on physical layer. This means that, we will mainly describe the signals modulation type, the frequency band of operation, and their basic operation procedure. This is done for the following signals, WLAN, WPAN (Bluetooth, RFID, UWB), and digital TV signals.

### 2.1.1 WLAN (Wi-Fi) signal

Wireless Local Area Network (WLAN) signals (also referred to as Wi-Fi signals) stand for IEEE 802.11x signals. IEEE 802.11 set of standard covers the 5 GHz and 2.4 GHz public spectrum bands, and more recently extensions to 60 GHz frequency bands. WLAN signals are used to provide high speed internet access to the indoor users. WLAN signals are easily available to the standard mobile devices or stations through the numerous access points in indoor environments [26]. Each access point has its unique identification MAC address which in fact refers to access ID. Access points controls the traffic in the wireless medium. *Figure 2-6* illustrates basic components required to set up WLAN network. Access points are connected to the internet through broadband connection with firewall and provide access to internet for the user station [48].

Nowadays, wireless LAN cards are integrated with the end stations devices to get access to the WLAN signal. Transmission power level for the most common band of 2400-2483.5 MHz is limited to maximum 1W in USA and to maximum 10 mW/MHz in Europe (although it may vary ). WLAN signal can be used to estimate the location of a mobile user within the network. WLAN can act as signal of opportunity as it is available indoors through the existing fixed access points for positioning [25]-[27]. The existing high density of access points is the key factor motivating the use of WLAN as a supplementary of GNSS in indoor [48].

In general, the distance measurement take place in WLAN based positioning through RSSI extracted from network or through access points ID [6], [26]. Multipath environments in indoor and time-varying features of the received signal strength are the main bottleneck in WLAN-based indoor positioning [24]. The accuracy of typical WLAN positioning systems using RSS is approximately 3 to 30 m with the current state-of-art approaches [59], [60] and [61]. The main WLAN standard details about data rate, modulation, frequency band are shown in *Table 2-1*.

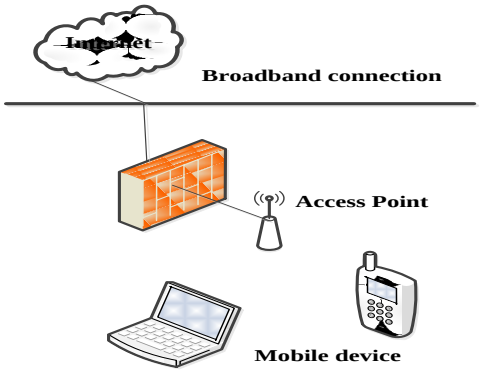


***Figure 2-6*** *A typical WLAN network setup*

***Table 2-1*** *System parameters of WLAN-Wi-Fi standard*

| **Parame-ter/system** | **802.11** | **802.11a** | **802.11b** | **802.11g** | **802.11n** | **802.11ac** [62] | **802.11af** [63] | **802.11ad** [64] |
|---|---|---|---|---|---|---|---|---|
| Approved since | July 1997 | September 1999 | September 1999 | June 2003 | September 2009 | January 2014 | February 2014 | December 2012 |
| Frequency bands cen-tered around, (GHz) | 2.4 | 5 | 2.4 | 2.4 | 2.4, 5 | 5 | TV white space | 60 |
| Maximum supported data rate | 2.1 Mbps | 54 Mbps | 11 Mbps | 6-54 Mbps | 108-600 Mbps | 6.93 Gbps | 600 Mbps | 6.76 Gbps |
| Modulation types | FHSS, DSSS | OFDM | FHSS, DSSS | DSSS, OFDM | OFDM | BPSK, QPSK, 16QAM, 64QAM | OFDM | OFDM |

### 2.1.2 WPAN: Bluetooth, RFID, UWB

Wireless Personal Area Network (WPAN) operates in a short range of radius of about few meters to tens of meter. WPAN signals have diversity in signal types and data rate and good prospect in indoor positioning. IEEE 802.15x standard covers Bluetooth, UWB, ZigBee signals whereas systems like RFID, IrDA, and home RF also belong to WPAN [54]. Bluetooth, RFID, UWB signals based positioning provides significant development in recent days and in the next subsections a brief description on those signals is presented.

#### 2.1.2.1 Bluetooth signal

Bluetooth aims for a personal local area network to connect small devices through radio-based wireless technology. Bluetooth operates in the 2.4 GHz ISM band. Bluetooth devices have a range of up to 10 m (or even up to 100 m with special transceivers) with transmitting power of up to 100 mW [24]. A frequency-hopping (FHSS)/time-division duplex (TDD) scheme is used for transmission with a fast hopping rate of 1,600 hops per second [29]. The time between two hops is called a slot, which has an interval of 625μs. Each slot uses a different frequency. All devices using the same hopping sequence with the same phase form a Bluetooth piconet. One device within piconet act as a master and others act as slaves for the connection set up. *Figure 2-7* points out different kinds of Bluetooth piconet arrangement for connection set up.

Nowadays Bluetooth chips are embedded in most of the smart phones due to Bluetooth short range connectivity and ease of integration facility. Bluetooth has a short range with low power consumption and can act as a signal of opportunity [30], [65].

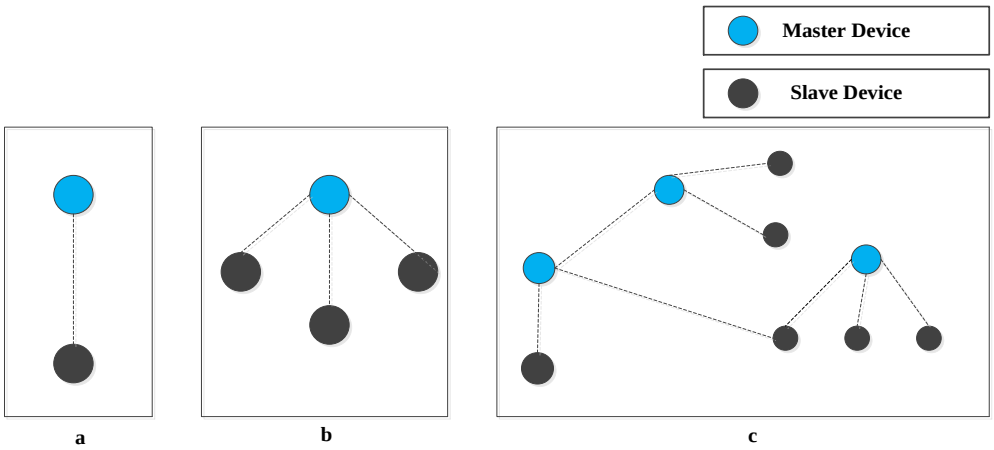


***Figure 2-7*** *(a) Single-slave piconet, (b) multiple-slave piconet and (c) scatternet [65]*

Advantages of using Bluetooth technology in positioning [24], [48]:

- Low-cost technology
- Low transmitted power (lower interference)
- Many smart phones already have a Bluetooth chip

Disadvantages of using Bluetooth technology in positioning [24], [48]:

- Very short range solutions (typically below 10m)
- Accuracy limited by multipath and shadowing (same as in WLAN)
- Typically, existing mobile transmitters lead to new stationary transmitter installation in case of RSS based positioning solution.

#### 2.1.2.2 RFID

RFID system offers storing and retrieving data through electromagnetic (EM) transmission which can be use a means of identification and tracking purposes. RFID systems operate in frequency ranges from a few hundred kHz to several GHz. A typical RFID system is presented in *Figure 2-8*. It consists of several basic components, including RFID readers along with antennas, RFID tags and servers or data management systems [32]. A RFID tag attached to the tracked object holds a unique data or a serial number or other unique attribute of the item. RFID reader transmits and receives simultaneously at the same frequency and able to read the data emitted from RFID tags from a distance [33]. RFID system uses a defined radio frequency and protocol to transmit and receive data. RFID tags can be either passive or active. In passive system, the tag is powered by the high power electromagnetic field generated by the reader antennas. After the tag IC is activated, the tag antenna reflects back a weak modulated signal containing the data back to the reader. On the other hand, tags in the active system are powered by own

internal battery. A comparison of several parameters between active RFID and passive RFID system is presented in *Table 2-2* for better understanding.

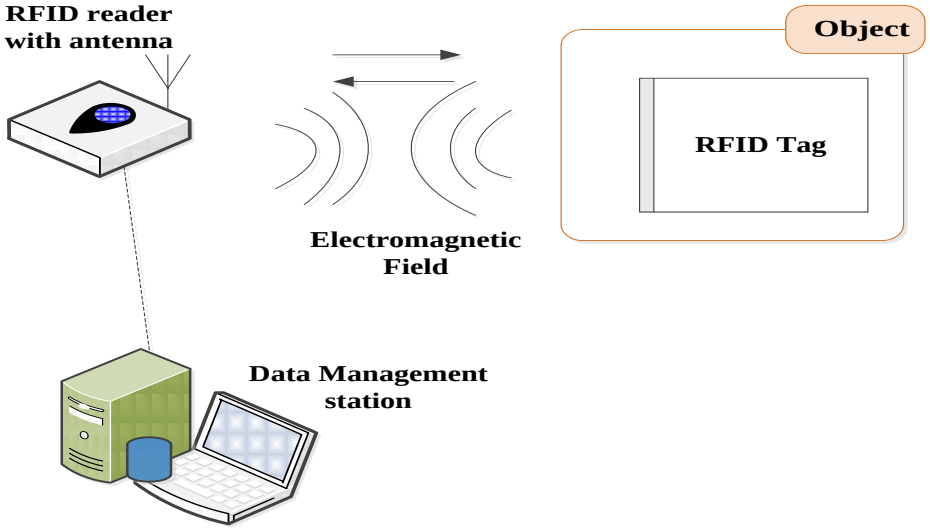


***Figure 2-8*** *Components of a RFID system* [24], [34]

***Table 2-2*** *Comparison between active and passive RFID system*

| **Type/ Parameter** | **Active RFID** [24] | **Passive RFID** [24] |
|---|---|---|
| Tag power source | Internal tag battery | Eternal power from EM wave |
| Tag battery | Yes | No |
| Availability of power | Continuous | Once EM field apply |
| Required signal strength to tag | Very low | Very high |
| Communication range | Up to 100m | 10-30 m |

***Table 2-3*** *RFID system based on different frequency range of operation [24]*

| **System/Parameter** | **LF** | **HF** | **UHF** |
|---|---|---|---|
| Frequency | 125-134 KHz | 13.56 MHz | 860-960 MHz |
| Wavelength | ~2400 m | 22m | ~0.33m |
| Read range | Up to 1m | Up to 1m | Up to 20 m |
| Data range | Up to 9.6 Kbps | Up to 64 Kbps | Up to 640 Kbps |

In an RFID system, the data reading range vary with the system that is being use based on frequency as shown in *Table 2-3*. RFID based positioning can be accomplished through TOA, TDOA, or RSS [31]-[36]. In indoor, RFID can give higher than 1m accuracy for positioning [24]. However RFID-based TDOA estimation process needs additional infrastructures such as sensor nodes or a stationary reader to be deployed in order to measure the reader tags inter distance for estimating the position. In contrast, in RSSI-based system, the received signal strength indicators are commonly built into the transceiver chips used in commercial RFID readers. Thus this measurement method does not require additional hardware [24], [36]. The reader diversity, data

storing capability of tag, tag types, reader range, whether reader is moving or tag is moving, all of these factors need to take in consideration while designing a state of art RFID-based localization scheme [24]. A performance comparison table on several parameters in RFID-based positioning is presented in *Table 2-4* which basically refer to several companies owning RFID commercial set ups for positioning purpose.

***Table 2-4*** *Comparison among different RFID based positioning system* [66]

| **Systems/Parameters** | **Axcess View** [67] | **Honeywell Asset Locator** [68] | **SpotON** [36] | **WhereTag** [66] |
|---|---|---|---|---|
| Positioning method | Proximity (node–ID) | Proximity (node–ID) | RSS | TDOA |
| Positioning accuracy | Zone/room | Zone/room | 1-2 m | 1-3 m |
| Positioning range (m) | 10 | 20 | 30 | 300 |

#### 2.1.2.3 UWB signal

UWB system falls into the category of high data rate example of WPAN systems. UWB was introduced to download or exchange digital image or video [38]. UWB system is based on sending ultra-short pulses whose duration is typically below 1 ns [39]. As a result, in spectral domain, the UWB spectrum uses a very wide bandwidth (> 500 MHz) [24], [39], [69] and [70]. UWB system transmits a signal with low duty cycle over multiple bands of frequencies simultaneously, from 3.1 to 10.6 GHz [38]. UWB signal can easily pass through the wall, clothes, and equipments. Moreover, UWB short duration pulses are easy to filter in order to determine correct signal in a multipath environment [24]. In UWB communication system, a number of UWB pulses are transmitted per information symbol and information are being carried by the timing or polarities of the pulses [71]. A simple description on two main existing standards on UWB system is presented in *Table 2-5*.

***Table 2-5*** *Different parameters of UWB standard [24], [48]*

| **System/Parameter** | **IEEE 802.15.4a** | **IEEE 802.15.4f** |
|---|---|---|
| Description | UWB with ranging capability | UWB RF-ID tags |
| Transmission range | <100 m | Few m |
| Ranging accuracy | ~ several cm | ~ cm order |

The usefulness of UWB signals can be realized from the Shannon capacity formula. The maximum data rate $C$ for signal transmission in a channel with bandwidth $BW$ and signal to noise ratio as $SNR$ is given by,

$$C = BW \log_2(1 + SNR) \qquad (2\text{-}2)$$

According to eq. (2-2), as the bandwidth is large in UWB system, more information can be sent from transmitter to the receiver compared to other narrowband transmission system [71].

UWB system covers a wide spectrum range and coexists with other system without having significant interference. According to the Federal Communications Commission (FCC) regulations, UWB systems transmit below certain power levels in order not to cause significant interference to the existing systems in the same frequency spectrum [24], [71]. The average power spectral density (PSD) remains below $-41.3\ \mathrm{dBm/MHz}$ over the frequency band from 3.1 GHz to 10.6 GHz which can be seen from *Figure 2-9* [71]. In *Figure 2-9*, a UWB signal is defined to have an absolute bandwidth, $B = f_H - f_L$, where $f_H$ and $f_L$ represents the upper and lower frequency of the $-10\ dB$ emission points respectively.

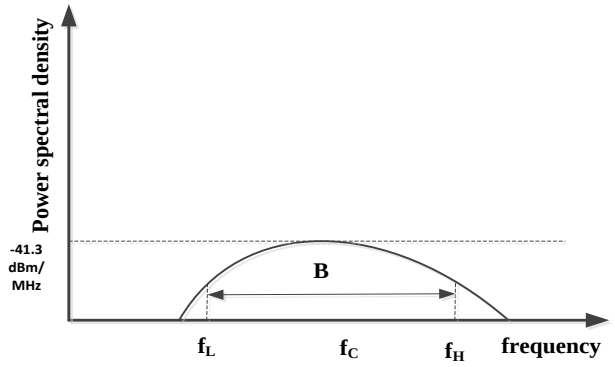


***Figure 2-9*** *UWB power spectral density [71]*

Research worlds is currently putting significant interest on UWB based positioning capability due to its low power, large bandwidth, and high accuracy operation [24], [37] and [38]. UWB system transmits UWB signals to the network receivers and the receiver position can be estimated typically through TDOA or AOA. From the positioning prospective, UWB based location estimation provides very high indoor location accuracy (20 cm) because of the short pulse -based precise estimation [24]. However to overcome interference, strategic placement of UWB readers require high implementation cost. On the other hand, as UWB signal can transmit without carrier modulation, baseband processing of UWB received signal requires simple navigation receiver structure which reduces cost indeed [71]. From the positioning point of view, even though UWB system provides high accuracy, this system requires complete new set up which involves infrastructure cost.

### 2.1.3 Digital TV signal

Digital TV (DTV) infrastructure are readily available at indoor to apply as a mean of positioning scheme [8]. The digital TV system uses OFDM techniques for transmission. Digital Video Broadcasting (DVB) is the digital TV standard [40]. There are four variants of DVB,

- DVB-T (Digital Video Broadcasting – Terrestrial)

- DVB-T 2 (Digital Video Broadcasting – Terrestrial Enhanced)
- DVB-S (Digital Video Broadcasting – Satellite)
- DVB-H (Digital Video Broadcasting – Handheld)

DVB-T is a digital broadcasting standard created by the European Telecommunications Standards Institute (ETSI). DVB-H (Handheld) is another available standard for mobile services which derived from DVB-T. The next generation DVB-T2 standard was published by ETSI in April 25, 2009 [72]. DVB-S is a standard for digital TV distribution via satellite. Evolution of DVB-S standard is considering a new standard named DVB-S2. An overview of several system related parameters of different digital TV signal standard is presented below in *Table 2-6* and in *Table 2-7*.

***Table 2-6*** *System parameters of different DTV standard [72]*

| System/Parameter | DVB-T | DVB-T2 | DVB-H |
|---|---|---|---|
| Modulation | QPSK,16 QAM, 64 QAM | QPSK,16QAM,64QAM, 256QAM | QPSK,16QAM,64QAM |
| FFT size | 2K, 8K | 1K,2K,4K,8K,16K,32K | 2K,4K,8K |
| Bandwidth | 8 MHz | 8 MHz | 8 MHz |
| Service rate | ~22.1 Mb/s | ~32.4 Mb/s | ~8.3 Mb/s |

***Table 2-7*** *System parameters of DVB-S standard [73]*

| System/Parameter | DVB-S | DVB-S2 |
|---|---|---|
| Bandwidth | 2 MHz | ~30 MHz |
| Compression technique | MPEG2 | MPEG4 |
| Modulation | QPSK,16QAM | BPSK,QPSK,8PSK, 16APSK, 32APSK |
| Pilots | Not applicable | Pilot symbols |
| Bit rate | 33.8 Mbps | 46 Mbps |

Digital TV signals can be used to estimate the user position in indoors, where GNSS signal is rarely available. DTV signals have several advantages such as high transmission power, fixed known transmitter location, synchronized emitters, high SNR [40], [41]. However the initial position of user needs to be found out through the GPS signal in an aided manner [48]. The typical scenario where DTV position can be applied is the following: the user will move from outside to a GNSS blocked area and in indoor the DTV signals act as a signal of opportunity for positioning. The OFDM-modulated transmitted digital TV signal contains scattered pilot subcarrier from which time of arrival can be estimated and pseudo-range between receiver and transmitter calculated for position solution [41].

DVB-T signal has a non-negligible prospect for positioning solution which can be summarized below [48]:

- DVB-T signal has high transmission signal power: 10 KW- 15 KW
- Frequency diversity, 6-8 MHz signal BW
- Existing system provides fixed transmitter which reduce Doppler effects
- Low frequency of operation: UHF (50-750 MHZ), VHF (1775–2265 MHz)
- Horizontal signals provides  less attenuation from walls than roof
- Existing infrastructure can serve the purpose which provides savings.

Nevertheless, there is not much research nowadays focusing on DTV positioning solutions, and one of the pioneer companies who offered commercial DTV positioning solutions (Rossum) is currently bankrupt.

## 2.2 Comparison among SoO

In general, SoO has prospect of being used as an alternative to GNSS in indoor. Combining various type of signals which contain relevant information towards a cooperative positioning where all the devices interact with each other can also increase the accuracy of the positioning estimation [24], [42]. Better positioning accuracy can be achieved with a tradeoff in the implementation cost through UWB and RFID-based solutions compared to WLAN and DTV solutions. WLAN-based positioning solution is already running with an accuracy of 3 to 30 m whereas demand of more accuracy can be mitigated by UWB and RFID-based solutions which give accuracy in cm scale. A comparative summary of previous sections description on positioning based on several types of wireless signals with respect to range of accuracy and operating environment is presented in *Figure 2-10* [24]. *Figure 2-10* points out the potentiality of UWB, RFID, Bluetooth and WLAN signals for accurate indoor positioning with their accuracy range while GPS, cellular based positioning and wireless signals assisted GPS can support outdoor and rural open areas.

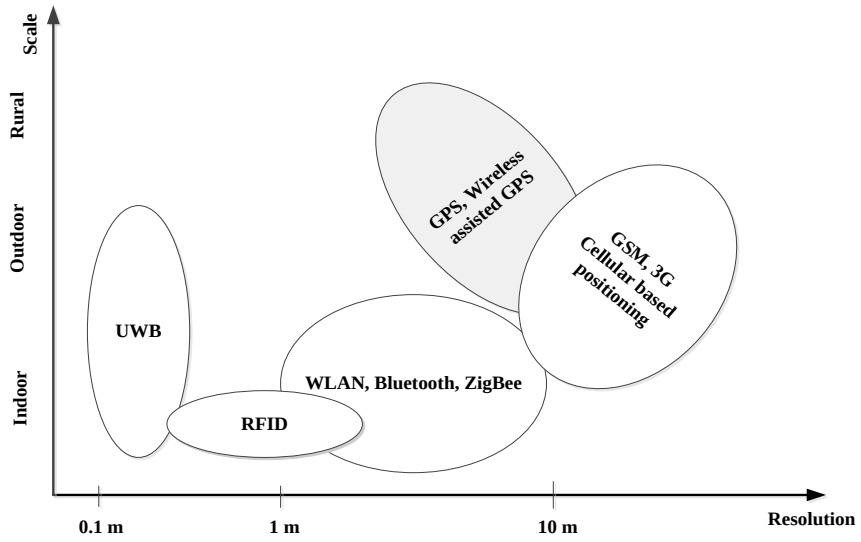


***Figure 2-10*** *Overview of positioning based on several wireless signals* (reproduced from [24])

# 3. MODULATIONS AND MULTIPLE ACCESS TECHNIQUES

This chapter presents the theoretical description of most common multiple access methods namely Code Division Multiple Access (CDMA), Orthogonal Frequency Division Multiplexing (OFDM).This chapter will also give a view on several linear and non-linear modulation methods adopted in positioning and communication systems. Moreover, recent wireless research steps consider Ultra Wideband (UWB) system for its low power, high bandwidth and this will be presented in a brief manner.

## 3.1 Multiple access techniques

Multiple access techniques enable multiple users to share the common medium. Multiple access techniques typically refer to the sharing of a communication channel such as a satellite or radio channel by users in highly geographically isolated locations. Multiple access techniques allow efficient wireless transmission system through handling highly frequency selective channel. CDMA and OFDM are two most common access method used in recent wireless applications. The subsequent sections will describe their general modeling including signal structure and system block diagram.

### 3.1.1 CDMA basic principles

CDMA is a multiple access procedure implemented by spread spectrum techniques. Most of the 3G cellular communication, GPS, some WLAN standard use spread spectrum technology. In CDMA, all users share the same frequency band simultaneously with having a unique pseudorandom code sequence [74]. *Figure 3-1* shows the concept of code division multiplexing used in CDMA. In *Figure 3-1*, users (1, 2… N) are separated from each other through the unique codes. Users may transmit at the same time using the same frequency which in fact allows multiple users to use the same transmission bandwidth. Spread spectrum technique is used in many wireless systems such as,

- CDMA2000( UMTS/WCDMA) cellular standard
- CDMAone cellular standard
- GPS, Galileo, Compass satellite navigation systems
- Some of the WLAN standard
- ZigBee

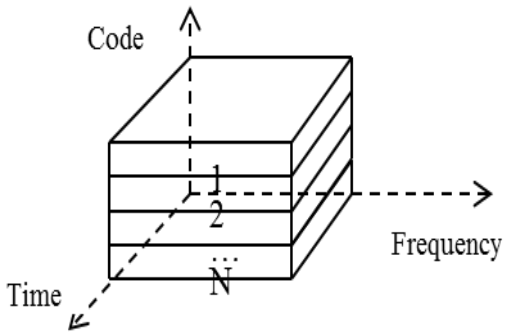


***Figure 3-1*** *Code division multiplexing concept*

#### 3.1.1.1 Spread spectrum techniques

In spread spectrum techniques, the narrowband signal spectrum spreads to a wider bandwidth using a spreading code before transmission [75]. Spreading allows the signal not to be destroyed by the narrowband and broadband interference encountered in channel. The de-spreading operation at receiver recovers the desired signal followed by a bandpass filter. The transmission bandwidth is maintained larger than the information bandwidth to achieve spreading operation [54]. The processing gain achieved from spreading reduces the impact of narrowband interference. The spectrum spreading can be performed using three basic methods, such as,

- Direct Sequence Spread Spectrum (DS-SS)
- Frequency Hopping Spread Spectrum (FS-SS)
- Time Hopping Spread Spectrum (TH-SS)

**Direct Sequence CDMA (DS-CDMA or DS-SS)**:

DS-SS is the most used form of spread spectrum. The original data signal is multiplied directly with the spreading code at a chip rate higher than the symbol rate [76]. In DS-SS, the user bits are mainly multiplied with binary Pesudonoise (PN) sequence as spreading code such as, Gold sequences, Kasami sequences [54]. However, DS-SS method is not limited to binary sequences; it can be also used with QPSK, QAM modulated spreading codes. More details on the types of spreading codes used in different systems can be found in literature, for example, in [77], [78]. The bits of the spreading code are called chips. The chip rate is typically much higher than user bit rate [54]. At the receiver side, the received spread signal is again multiplied with the same spreading code to get the actual transmitted signal. *Figure 3-2* illustrates the basic principles of direct sequence spread spectrum operation. In *Figure 3-2*, the certain user data is spread to a wider bandwidth by multiplication with a higher frequency code sequence. In bit domain, the spreading operation is following XOR operation between data sequence and chip sequence.

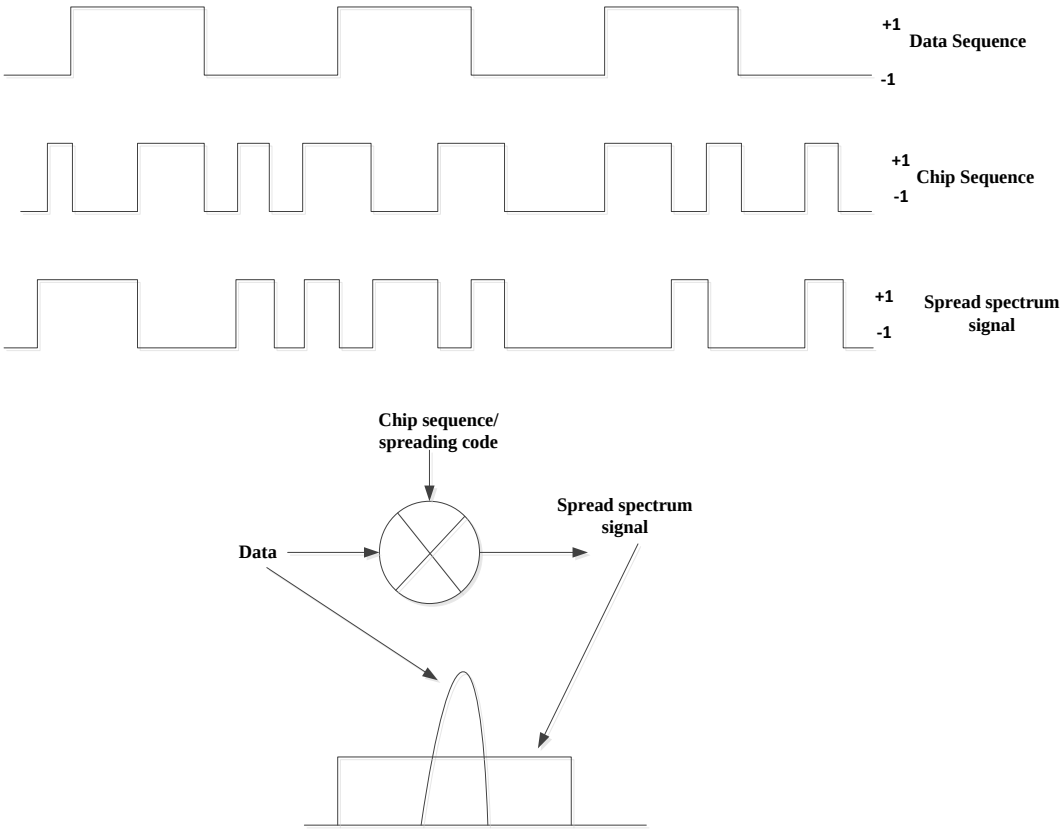


***Figure 3-2*** *DS-SS basic principle [54]*

**Frequency Hopping CDMA (FH-CDMA or FH-SS):**

In FH-SS, the carrier frequency at which the original data signal is transmitted is frequently changed according to the spreading code or the PN sequence used in spreading. Eventually, the spreading code controls the sequence of carrier frequencies. As a result, the data signal will spread over a wide range of frequencies without changing the original bandwidth of the data [54]. A frequency synthesizer generates hopping signal according to the PN sequence. The pre modulated data signal will multiply with hopping signal to generate FH-SS signal. The main advantage of FS-SS includes the possibility of having simpler implementation, frequency diversity and simple detection compared with other two techniques [80]. However, this method is not that much robust as DS-SS.

**Time Hopping CDMA (TH-CDMA or TH-SS):** Having discussed DS-SS and FH-SS, we would also like to briefly describe TH-SS. In TH-SS**,** the signal is transmitted in short bursts where the times of the transmitter to switch on and off are decided by the specific PN code sequence [80]. This technique can be implemented in visible light communication systems, as studied in [81]. However, TH-SS is not as popular as the

other two techniques. The main reasons are implementation difficulties and lack of robustness.

In the case of CDMA implementation through spread spectrum, DS-SS is the most used and popular method due to the following advantages,

- In DS-SS, the orthogonality condition for the spreading sequences can be relaxed [76]. This implies asynchronous users much simpler access to the medium.
- Frequency planning can be relaxed
- Reduces the effects of frequency selective fading
- In DS-SS implemented cellular network, soft or softer handover and frequency reuse can be possible [83].

Under the above circumstance, DS-SS method is selected in CDMA signal implementation for this thesis simulation purposes. Section 3.1.1.2 will present DS-CDMA signal model and section 3.1.1.4 will illustrate the DS-CDMA general block diagram which is used in chapter 7 for CDMA signal generation. However, section 3.1.1.3 will cover the signal models for remaining two types namely FH-SS and TH-SS.

#### 3.1.1.2 DS-CDMA signal model

In order to characterize the DS-CDMA signal, the signal model is explained in this section. If the user data sequence is denoted $d(t)$, $b_n$ are data bits for n$^{th}$ symbol, $T_b$ is the symbol interval, and $p(t)$ is modulation pulse, then the data sequence can be written as,

$$d(t) = \sum_{n=-\infty}^{n=+\infty} b_n p(t - nT_b) \quad (3\text{-}1)$$

In DS-CDMA, if $f_c$ is the chip rate of spreading code, $f_b$ is the symbol rate of data sequence, $T_c$ is the chip interval then the spreading factor $S_F$ can be written as in eq. (3-2),

$$S_F = \frac{f_c}{f_b} = \frac{T_b}{T_c} \quad (3\text{-}2)$$

The CDMA baseband signal with BPSK modulation, expressed as the spread nal $x(t)$, at the output of the spreading operation can be modeled as,

$$x(t) = \sqrt{E_b} \sum_{n=-\infty}^{n=+\infty} \sum_{k=1}^{+S_F} c_k(n) p(t - kT_c - nS_F T_c) \quad (3\text{-}3)$$

Where, $c_n(k)$ is code value (+1 or -1) for k$^{th}$ chip during the n$^{th}$ symbol, $E_b$ is bit energy.

#### 3.1.1.3 Other spread spectrum signal model

In FS-SS system, the initial M-FSK modulated data signal can be exressed as,

$$s_n(t) = \sum_{n=-\infty}^{\infty} p(t - nT_{FS})\cos\,(2\pi f_n(t)t)$$

Where, $T_{FS}$ is the symbol duration, $f_n \in \{f_{s0}, f_{s1}, \dots\dots, f_{sM-1}\}$. The output of frequency synthesizer can be writen as,

$$c_h(t) = \sum_{l=-\infty}^{\infty} p(t - lT_{hop})\cos\,(2\pi f_{hop}(t)t)$$

Where, $T_{hop}$ is the hopping chip duration, $f_{hop} \in \{f_{c0}, f_{c1}, \dots\dots, f_{cL-1}\}$, $L$ is non-overlapping frequency bins. The FH-SS signal is a high-pass filtered product of $s_n(t)$ and $c_h(t)$, giving,

$$S_{FH-SS}(t) = \cos\,(2\pi\left(f_n(t) + f_{hop}(t)\right)t)$$

On the other hand, TH-SS signal can be constructed by modulating the data signal by a pseudorandom pulse position modulated spreading signal [80]. The resulting TH-SS signal can be given by,

$$S_{TH-SS}(t) = \sum_{u=-\infty}^{\infty} b_u p(t - uT_{TH} - c_j T_{c,TH-SS} - \Delta)$$

Where, $b_u$ is the data sysmbols, $T_{TH}$ is the symbol duration, $T_{c,TH-SS}$ is the chip time, $c_j$ is an integer specified by the pseudorandom code, $\Delta$ is the propagation delay.

#### 3.1.1.4 DS-CDMA system block diagram

*Figure 3-3* shows DS-CDMA system block diagram considering transmitter and receiver operations. According to the *Figure 3-3*, the channel-coded user data spread with the chip sequence and passed to the channel modulation as a spread spectrum signal. After that, DS-CDMA modulated signal passes though the wireless channel and it is converted back into digital form after being received in the receiver. At the receiver side, the signal received from several mutipaths and multipath estimator provides estimation on that receptions. Rake receiver deployment can be beneficial in case of wireless communication where energy gathered from all the paths will certainly influences the overall signal estimation [84]. On the contrary, in positioning, rake receiver is not beneficial, rather multipath mitiation techniques needs to incorporate with the system [85]. The received signal again multiplied with the same chip sequence in order to get the same transmitted signal as a output from receiver.

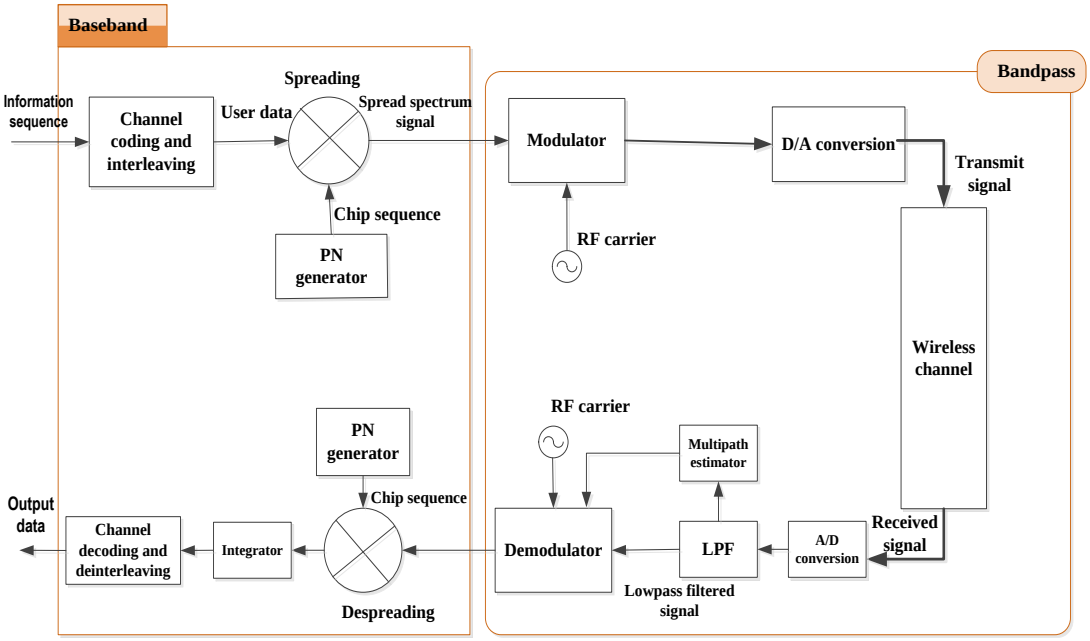


***Figure 3-3*** *DS-CDMA system block diagram*

### 3.1.2 OFDM basic principles

Orthogonal Frequency Division Multiplexing (OFDM) is a multicarrier modulation technique which has significant advantages for high data rate transmissions in multipath environments. OFDM has been chosen in many communication systems, such as Long-Term Evolution (LTE) for 4G communications systems, WLAN, WiMAX, and DVB-T for its robustness in multipath channels. The main idea behind the multicarrier modulation is to subdivide the available bandwidth into a number of sub-channels, such that each sub-channel is nearly ideal.

#### 3.1.2.1 Multicarrier techniques

Multicarrier technique is a special form of Frequency Division Multiplexing (FDM). In OFDM system, high spectral efficiency is achieved by selecting a specific (orthogonal) set of overlapping subcarrier frequencies [54]. OFDM permits overlapping between the subcarrier through the orthogonality without corrupting the user data, which is the main feature of OFDM. Orthogonality can be explained through the sub-channel response as when the response of any one sub-channel is at its maximum, the collection of spurious responses from all the remaining sub-channels is zero [76]. The orthogonality between the subcarriers provides less interference of other carriers in the detection of the information in a particular carrier [67], [86]. As a result, inter carrier interference (ICI) free reception can be possible at the receiver. In addition, orthogonality between the subcarriers allows carriers to be closer to each other in the frequency domain and such arrangement reduces required bandwidth. Multicarrier or multichannel signal

transmission can be also efficient in case of dealing with fading channel effect on transmission [54].

In multicarrier modulation scheme, the high bit rate serial data stream is divided into a number of parallel data streams at a much lower symbol rate, which are modulated on a set of subcarriers distributed within a specified frequency band [87]. The parallel subcarrier modulated data streams exhibits low rate transmission in multipath environment which generates less interference. As a result, this process will give higher bit rates with less interference at the receiver after the overall transmission.

In OFDM, the multiplexing and de-multiplexing can be implemented by IDFT and DFT operations respectively. In practice, this is accomplished in the baseband prior to RF section through the effective use of digital signal processing techniques, such as Inverse FFT (IFFT) at the transmitter side and FFT at the receiver side [86].

#### 3.1.2.2 Guard interval (GI) and pilot subcarrier

OFDM signal provide robustness against multipath by introducing the so-called guard intervals (GI) as part of its signal structure [54]. Peled and Ruiz proposed a method to cyclically extend the OFDM time signal by replicating the last part of the OFDM time signal at the front of the OFDM symbol during the transmission [54], [86]. *Figure 3-4* shows the replication procedure to extend the time domain signal by means of GI. Moreover, the orthogonality between subcarriers is maintained through inserting a guard interval lager than channel delay spread. This selection of GI will assure that the multipath components of the symbols will not interfere with the useful symbol and which in fact eliminate the inter symbol interference (ISI) [54], [76] and [87].

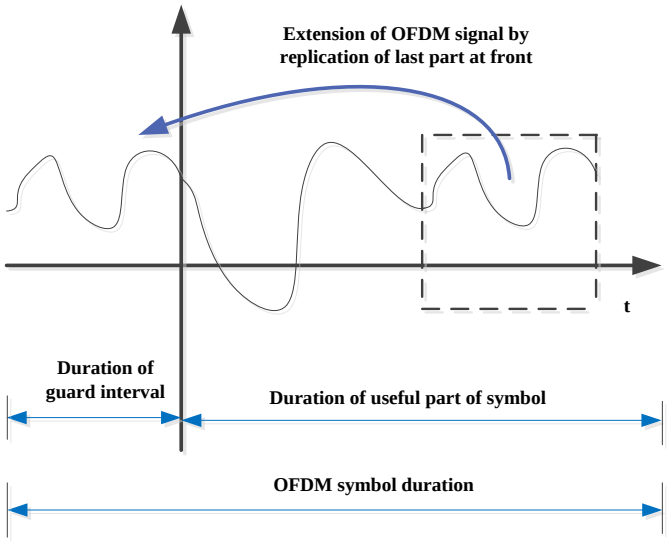


***Figure 3-4*** *Guard interval principle*

Another key element in the structure of OFDM signals is the existence of pilot subcarriers. Channel estimation can be possible from inserted pilot subcarriers through interpolation [76]. Frequency estimation and in some cases data management can also be

possible by pilot in receiver as inserted pilot symbols are already known by the receiver [86]. Usually some of the subcarriers are chosen as pilots and are modulated by BPSK or QPSK modulation and placed every $n^{th}$ subcarrier. As a result, the used total subcarriers consist of data subcarriers and pilot subcarriers. An example is shown in *Figure 3-5*. Receiver can equalize the frequency response in a frequency selective channel through exploitation of pilot subcarrier. This is the reason why pilot subcarriers are used in OFDM.

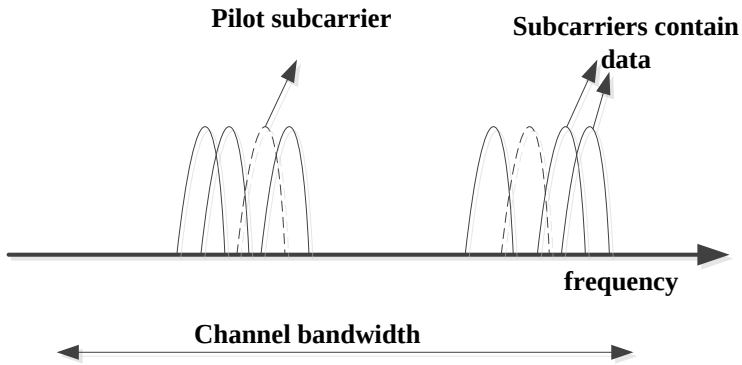


***Figure 3-5*** *Pilot (dashed) and data (continuous lines) subcarriers [86]*

#### 3.1.2.3 OFDM signal model

If OFDM symbol duration is $T_{sym}$, the number of subcarriers is $N$, subcarrier frequencies is $f_{sym}$, subcarrier frequency separation is $\Delta f_{sym}$, then the continuous time domain OFDM signal $x(t)$ is given by,

$$x(t) = \sqrt{E_b}\frac{1}{N}\sum_{k=1}^{N} X(k) e^{j2\pi k \Delta f_{sym} t} \qquad t \in [0, T_{sym}] \tag{3-4}$$

Here $X(k)$ is the complex data symbol at $k^{th}$ subcarrier and $E_b$ is the bit energy. The frequency domain symbols $X(k)$ are obtained from the data bits after being digitally modulated using one of the modulation schemes such as Binary Phase Shift Keying (BPSK), Quadrature Amplitude Modulation (QAM), etc.

If $f_{sym\_0}$ is the subcarrier center frequency, the subcarrier frequency is given by,

$$f_{sym} = f_{sym\_0} + k\Delta f_{sym} \tag{3-5}$$

Orthogonality between subcarriers can be achieved by having subcarrier spacing $\Delta f_{sym} = \frac{1}{T_{sym}}$ . If *N*-point parallel data streams are used in IDFT, the total bandwidth of the OFDM signal will be, $BW = N * \Delta f_{sym}$.

#### 3.1.2.4 OFDM system block diagram

*Figure 3-6* indicates an OFDM transmission system as described in earlier sections. Channel coding and interleaving are performed initially to have less bit error in OFDM symbol [87]. After that, modulated subcarriers produce parallel low rate data streams through IFFT operation. OFDM symbol is then created along with GI from the summation of parallel data subcarriers. OFDM symbol shaping procedure applies time domain windowing function to reduce the out-of-band spectrum. OFDM symbol is converted to the analog domain and transmitted through the wireless channel after being processed at the RF front end. On the other hand, at the receiver side, OFDM symbol demodulation is performed through FFT operation. GI is removed at the receiver side before demodulating the signal. Channel estimation can be performed before having symbol demapping. Channel decoding and de-interleaving are performed at the very end to extract the user data bit from the received OFDM symbol at receiver. In a nutshell, in OFDM system, *N* data subcarriers carry *N* data symbols in parallel and these data transmitted simultaneously. Once the *N* data symbols are modulated to their respective subcarriers, the modulated subcarriers are summed and formed one OFDM symbol [86].

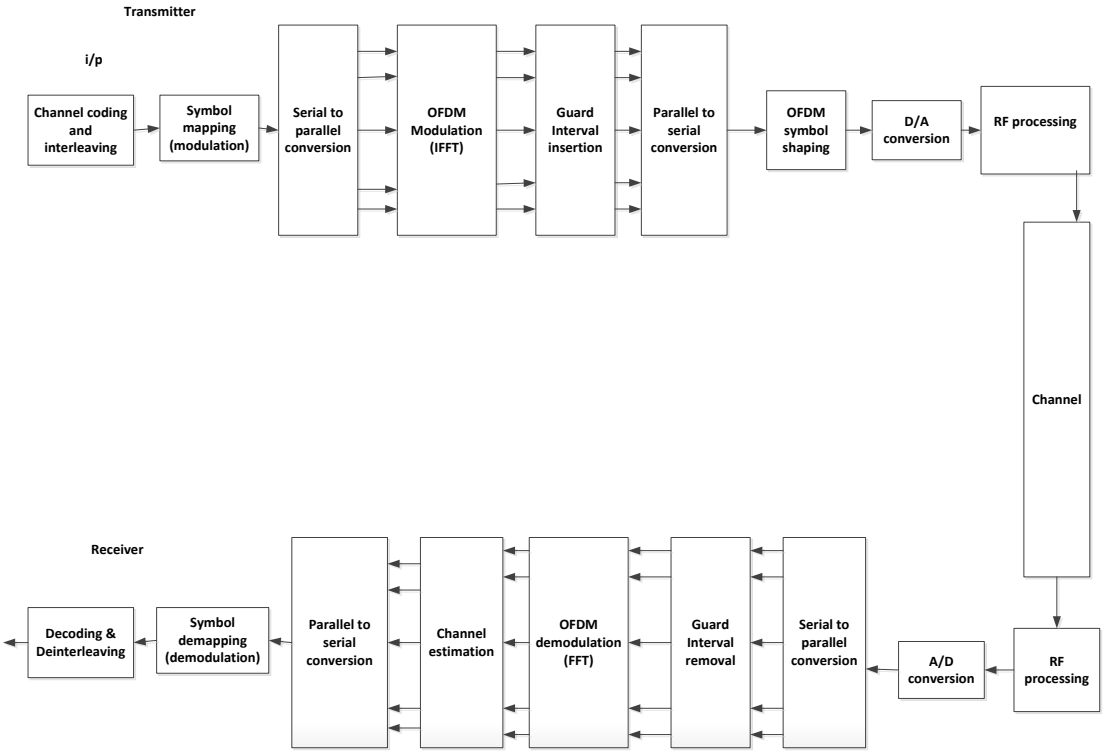


***Figure 3-6*** *OFDM system block diagram [54], [76]*

The quality of the transmitter and receiver oscillators could influence in phase noise [87]. In addition, large Peak-to-Average Power Ratio (PAPR) of the OFDM signal requires high quality power amplifiers with large linear ranges [76].

## 3.2 Modulation techniques

According to modulation concept, information is transmitted through the time varying fading channel as a form of data enveloped with certain continuous pulse to reduce the effect of noise, interference on data. The next sections will demonstrate different types of modulation schemes used in wireless communication and positioning systems.

### 3.2.1 Linear modulations

In linear modulation schemes, the amplitude of the modulated transmitted signal varies linearly with the modulating digital signal. The input-output relation of linear modulator satisfies principle of superposition. There are many linear digital modulation techniques possible to implement in signal transmission, such as, Binary Phase Shift keying (BPSK), Quadrature Amplitude Modulation (QAM), M-PSK, M-QAM etc. Linear modulations can be represented through constellations.

#### 3.2.1.1 BPSK

BPSK is the simplest form of digital modulation [6]. If $p(t)$ represents the basic modulation pulse is used to construct binary data stream, $T_b$ is the bit interval, $b_n$ is the $n^{th}$ data symbol, then the bipolar data stream can be expressed as,

$$m(t) = \sum_n b_n \, p(t - kT_b) \qquad (3\text{-}6)$$

Where $b_n = \begin{cases} +1\,, for\ binary\ symbol\ "1" \\ -1\,, for\ binary\ symbol\ "0" \end{cases}$

The binary symbol “1” is obtained by setting the carrier phase $\theta(t) = 0\ rad$ , and the binary symbol “0” is obtained by setting the carrier phase $\theta(t) = \pi\ rad.$

Modulation pulse $p(t)$ used in BPSK modulation can be of different shapes such as, rectangular pulses, Nyquist pulses (e.g. root raised cosine pulse), depends on the applications [89]. For example, fundamental rectangular pulse can be shown below,

$$p(t) = \begin{cases} +1\,, for\ 0 \le t \le T_b \\ 0, \qquad otherwise \end{cases} \qquad (3\text{-}7)$$

The passband signal $x(t)$ can be written as,

$$x(t) = A_c cos\ (2\pi f_{carrier} t) \qquad (3\text{-}8)$$

Where, $f_{carrier}$ is the carrier frequency, $A_c$ is the amplitude of carrier frequency. Then, the BPSK modulated signal expressed in passband (at carrier frequency) becomes,

$$y(t) = A_c\ m(t)\ cos\ (2\pi f_{carrier} t) \qquad (3\text{-}9)$$

Or in more specific way,

$$y(t) = \begin{cases} A_c\, m(t)\, cos(2\pi f_{carrier} t)\,, & for\ binary\ symbol\ "1" \\ A_c\, m(t)\, cos(2\pi f_{carrier} t + \pi)\,, & for\ binary\ symbol\ "0" \end{cases}$$

*Figure 3-7* shows the constellation plot of BPSK modulated signal with zero phase offset.

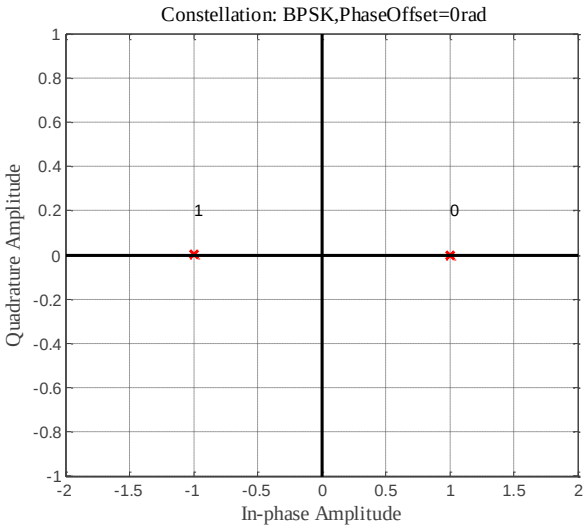


***Figure 3-7*** *BPSK constellation diagram*

### 3.2.1.2 M-PSK

The aim of M-PSK modulation is to increase the bandwidth efficiency of PSK modulation scheme [90]. Bandwidth efficiency or spectral efficiency refers to the information transmission rate for a specific channel bandwidth. In that aspect, spectral efficiency is the characterization of utilization of channel bandwidth. If the alphabet size is *M*, then the maximum possible spectral efficiency for linear passband modulated signal is $\log_2 M$ bps/Hz. In BPSK, a data bit is represented by a symbol, whereas in M-PSK, $B = \log_2 M$ data bits are represented by a symbol. So, the bandwidth efficiency is increased by *B* times through this multilevel modulation technique [90].

Quadrature Phase Shift keying (QPSK) is a type of M-PSK where alphabet size, M=4 (two bits per symbol). QPSK is the most used method among all other M-PSK (8-PSK, 16-PSK and 32-PSK) methods. According to the explanation, it is a fact that, QPSK is two times more bandwidth efficient than BPSK [90]. In the case of M-PSK, the constellation points are uniformly distributed in a circle where M is the alphabet size.

*Figure 3-8* shows the constellation plot of QPSK signal with gray mapping and 0.785 rad phase offset.

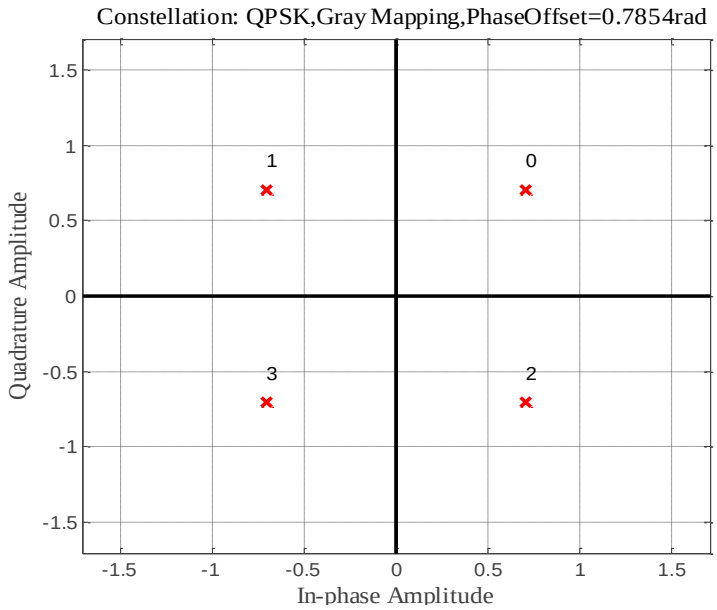


***Figure 3-8*** *QPSK (M=4) constellation diagram*

*Figure 3-9* presents the constellation plot of 16-PSK signal with gray mapping and 0.1963 rad phase offset. *Figure 3-9* indicates that, constellation points are uniformly distributed in a circle.

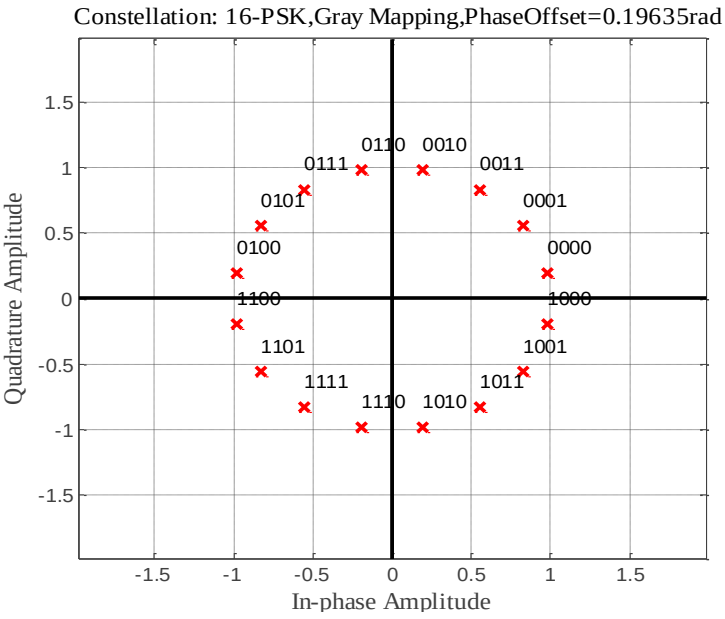


***Figure 3-9*** *16-PSK constellation diagram*

### 3.2.1.3 M-QAM

Quadrature amplitude modulation (QAM) is a linear digital modulation scheme where two independent real baseband signals are transmitted by modulating them into sine and cosine waveforms (I/Q) of the carrier waveforms [91], [92]. *Figure 3-10* shows a complex Quadrature modulation model which can be used for M-QAM generation.

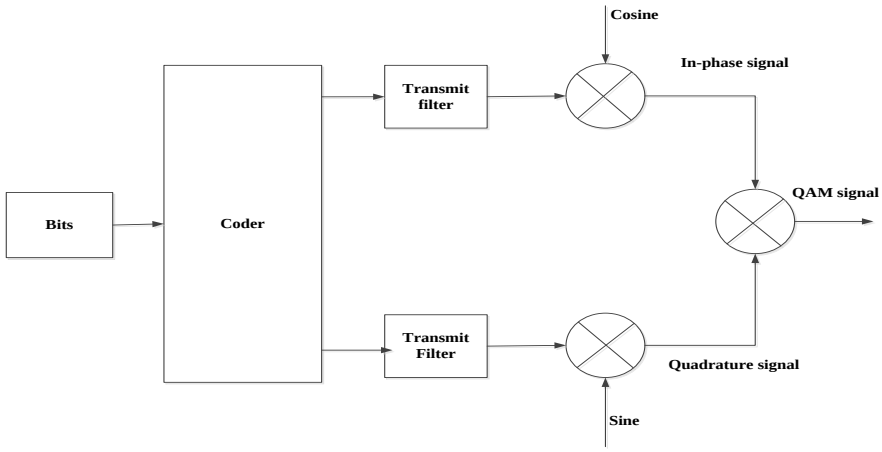


***Figure 3-10*** *General QAM scheme block diagram*

M-QAM represents the M-ary modulation of QAM for better bandwidth efficiency. If the alphabet size is *M* and number of bits per symbol is *B*, then for M-QAM,

$$2^B = M \qquad (3\text{-}10)$$

In case of M-QAM, the constellation points are distributed in regular rectangular shape. Constellation plots for 4-QAM, 8-QAM, 16-QAM and 32-QAM are shown in *Figure 3-11*.

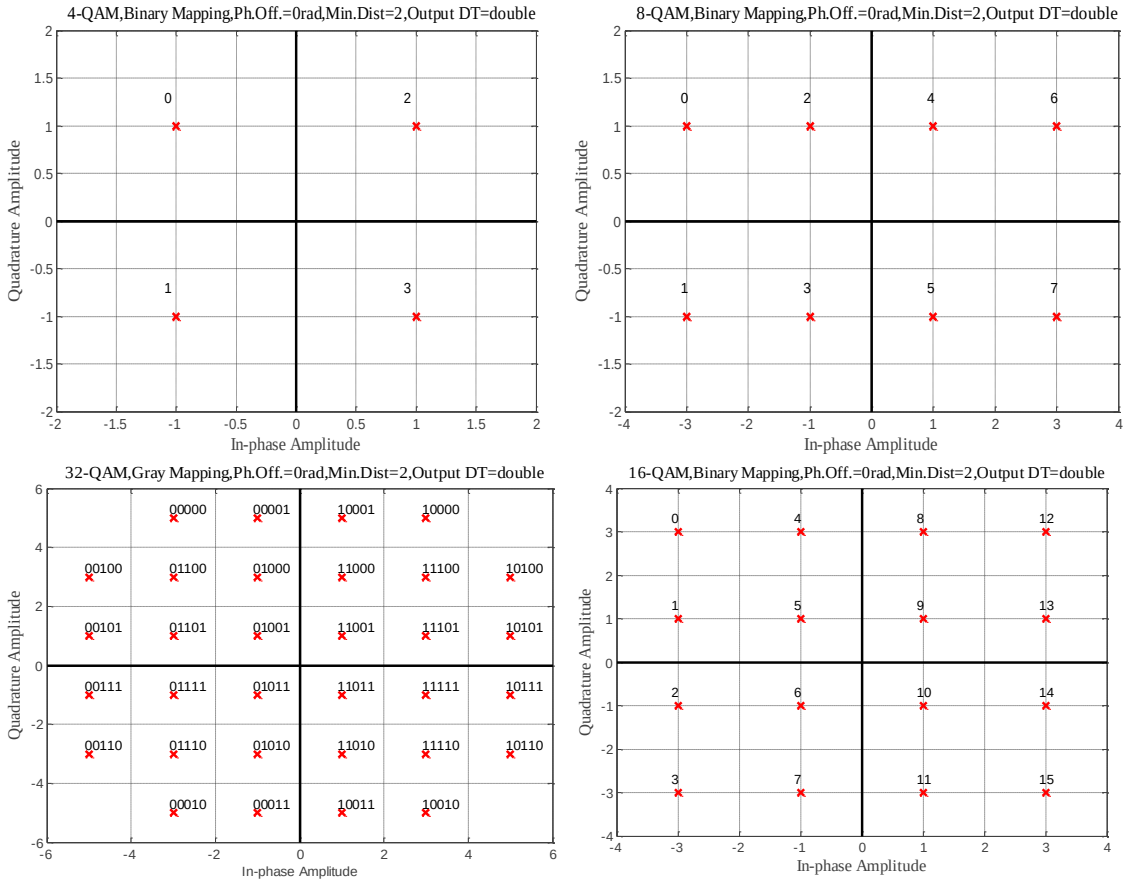


***Figure 3-11*** *M-QAM constellation: 4-QAM (upper left plot), 8-QAM (upper right plot), 16-QAM (lower right plot), and 32-QAM (lower left plot).*

### 3.2.2 Non-linear modulations

In non-linear modulation, the input-output relation does not follow the principle of superposition. Non-linear modulation includes, for example, Frequency shift Keying (FSK), Minimum Shift Keying (MSK), Gaussian Minimum Shift Keying (GMSK) etc. Non-linear modulation methods can be modelled in polar form as [92],

$$y(t) = \mathrm{a}(t)\cos(2\pi f_{carrier}t + \theta(t)) \qquad (3\text{-}11)$$

Where, $a(t) = \sqrt{y_I^2(t) + y_Q^2}$ is the time-varying amplitude, $\theta(t) = \tan^{-1}(\frac{y_Q(t)}{y_I(t)})$ is the time varying phase, and $f_{carrier}$ is the un-modulated carrier frequency.

#### 3.2.2.1 FSK

FSK is the most common non-linear digital modulation method. The principle of creating FSK modulated signal is that, *M* different frequencies are used for presenting *M* different symbols. Provided that, *M* is the alphabet size, hence, there are $\log_2 M$ bits per symbols. Symbols are created from consecutive bits. The simple form is the binary FSK, where 0 and 1 values correspond to different frequencies as shown in *Figure 3-12*.

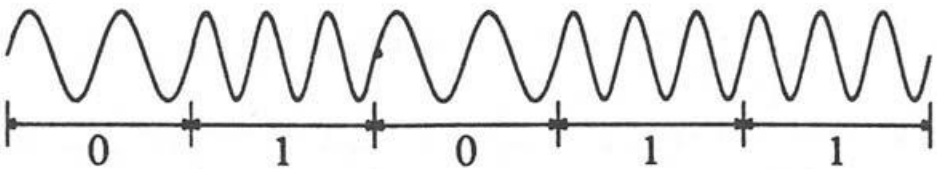


***Figure 3-12*** *FSK principle*

In some cases carrier synchronization is extremely hard to implement in receiver. Non-coherent detection does not require carrier synchronization [93]. Non-coherent detection is possible for FSK modulated signal [93]. In that context, FSK modulated signal opens the possibility of using non-coherent detection. However, coherent detection can also be possible for FSK modulated signal.

FSK modulated signal is less sensitive to nonlinearities. Since FSK is a nonlinear modulation method, non-linear power amplifier with high efficiency can be used in wireless transceiver design. FSK transceiver consumes less power from hardware point of view. However, spectral efficiency is poor with FSK modulated signal compared to amplitude modulation. In addition, nonlinearities involved with FSK bring difficulty in channel equalization. This topic can be found in more details, for example in [94], [95].

The phase of FSK may be continuous or discontinuous. Continuous phase is better in terms of bandwidth because discontinuities cause high frequency components to the spectrum. Continuous-phase is also better when the transmission link has nonlinearities, for example in the transmitter power amplifier.

FSK is used in caller ID applications of telecommunication systems and remote metering purposes [96]. Moreover, research for using FSK modulation conducted for localization where fluorescent light is modulated by FSK scheme. The demo of this work can be found, for example, in [82]. In that experimental setup, every fluorescent lamp of the building is equipped with FSK modulated ballast and location ID is assigned to it. Once the receiver will be at the area covered by the lamp, the receiver can extract location information.

In FSK, if symbol interval is $T_{FSK}$, then the FSK frequencies $f_i$ satisfy the below condition,

$$f_i T_{FSK} = K_i \qquad (3\text{-}12)$$

Where $K_i$ are integers, and $i = 1,2, \dots M$

It is sensible with this choice of the frequencies to minimize the frequency separation in order to obtain minimum bandwidth while maintaining continuous phase and orthogonality of pulses.

The minimum shift keying (MSK) is a specific kind of continuous phase FSK where this minimum frequency separation is used and hence the bandwidth is narrower. The minimum frequency separation $|f_1 - f_2|$ is achieved when$|K_1 - K_2| = 1$. More generally, to achieve orthogonality of pulses, the condition becomes,

$$f_i - f_{i-1} = \frac{1}{T_{FSK}} \qquad i = 1,2, \dots \dots M \qquad (3\text{-}13)$$

MSK is used in maritime navigational security systems namely Differential GPS (DGPS) in many counties including Canada, Australia, and Singapore [97], [98]. The DGPS provides differential corrections to a GPS receiver to improve navigational accuracy by using MSK modulation for transmitting radio signals [97]. In addition, GSM system uses Gaussian MSK (GMSK) modulation scheme which is a special form of the MSK modulation.

#### 3.2.2.2 GMSK

The GMSK is a special type of MSK modulation method. In order to reduce adjacent channel interference in MSK, a better pulse shaping is used instead of square pulse and the pulse shape is determined by Gaussian low pass filter (LPF) [99], [100]. Gaussian filter has a narrow bandwidth and sharp cut off properties which are required to reduce the high frequency components. The Gaussian LPF is used before modulation stage and this differentiates GMSK from MSK [101]. This pre-modulation filter makes the output power more compact [92]. The time domain impulse response of Gaussian filters to rectangular pulse of unit amplitude and duration of *T* can be expressed by eq.( 3-14 ).

$$g(t) = \sqrt{\frac{2\pi}{\log 2}} BW \int_{-\frac{T}{2}}^{\frac{T}{2}} \exp\left(-\frac{2\pi^2}{\log 2} BW^2 (t-\tau)^2\right) d\tau \quad (3\text{-}14)$$

Where, $BW$ is the 3 dB baseband bandwidth of used Gaussian LPF, $\tau$ is the time delay realization of filter.

In GMSK, the Gaussian pulse shaping is used for getting smooth control signal. There are two methods to generate GMSK signal from that smooth control signal, namely FSK modulation based method and Quadrature modulation method [102], [103]. In FSK modulation based method, the obtained control signal from Gaussian LPF is fed into a voltage control oscillator (VCO) core to get GMSK signal as output. An example of the basic structure of GMSK signal generation with VCO and Gaussian LPF is shown by *Figure 3-13* [101]. The structure of *Figure 3-13* is simple but the component tolerance of VCO creates deviation from desired output. Moreover, modulation index of VCO needs to be exactly 0.5 and it is difficult to maintain during implementation [103].

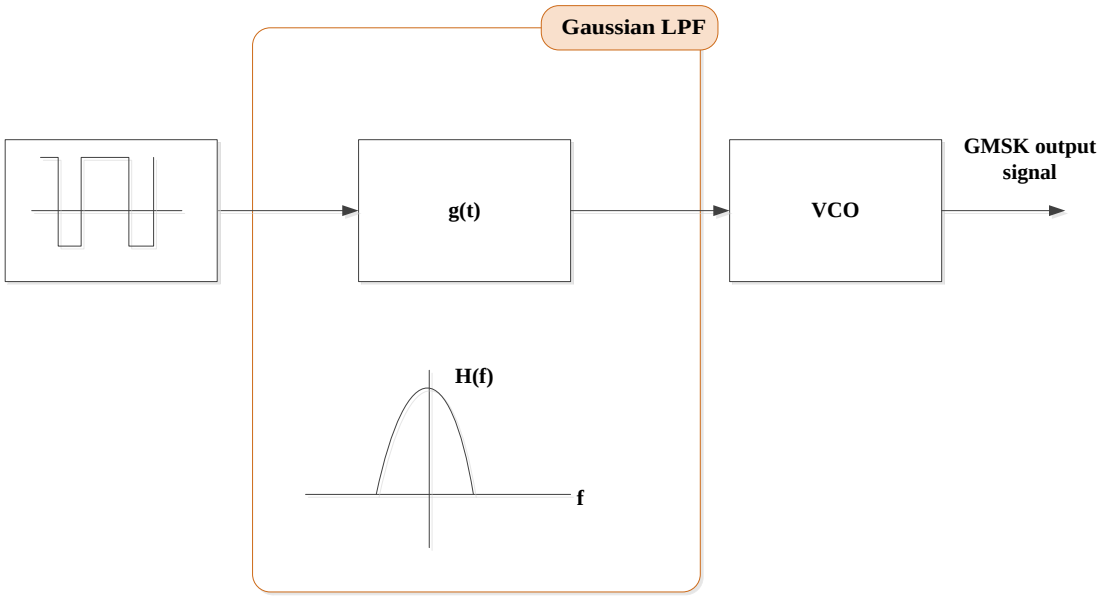


***Figure 3-13*** *GMSK signal generation*

The second method of GMSK signal generation based on Quadrature modulation method is shown in *Figure 3-14*, which is widely used for GMSK baseband signal creation. It is possible to maintain the modulation index of VCO core exactly at 0.5 by this structure. Moreover, this approach is much simpler compared to VCO implementation [103]. In this approach, the data bits converted to Gaussian pulses $b(t)$ by Gaussian LPF. The function $b(t)$ is then integrated with respect to time which produces the function $c(t)$ as shown in *Figure 3-14*. The function $c(t)$ is then further modulated in the Quadrature modulator blocks. Quadrature modulator consists of two major blocks, a Quadrature baseband processing followed by I/Q modulator. In the Quadrature baseband processing, I and Q baseband signals are produced from Cosine and Sine functions of $c(t)$.

The I and Q baseband signals are then passed through the I/Q modulator and the GMSK output signals $k(t)$ can be written as,

$$k(t) = \sin[c(t)]\sin(wt) + \cos[c(t)]\cos(wt) = Q(t)\sin(wt) + I(t)\cos(wt) \quad (3\text{-}15)$$

Where, $w = 2\pi f_{c,vco}$ and $f_{c,vco}$ is the carrier frequency used in I/Q modulator.

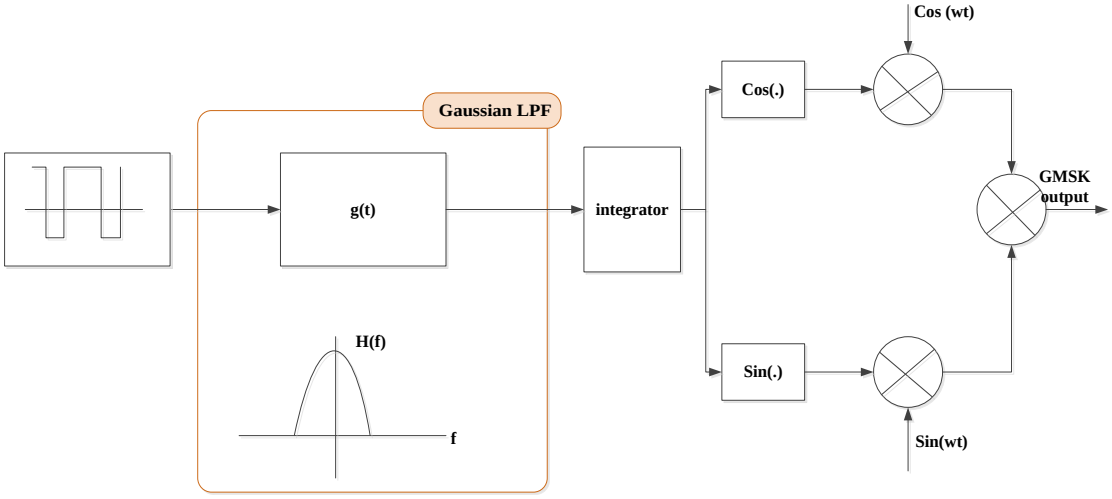


***Figure 3-14*** *GMSK signal generation with I/Q modulator concept [103]*

The multiplication between the bandwidth of the filter $BW$ and the bit duration $T$ defines the bandwidth time parameter $BT$ of the system. The selection of the bandwidth time product parameter value plays an important role in reducing side-lobes and having compact spectrum. GMSK is the basic modulation method utilized in the GSM system, with the bandwidth time product parameter value, $BT = 0.3$ (compromise tradeoff value between spectral compactness and receiver performance) [102]. *Figure 3-15* shows the power spectral density of GMSK modulated signal.

GMSK modulation can be used in navigation systems for its characteristics of minimum bandwidth to transmit signal at reduced power. For example, United states coast guard unit uses GMSK modulation for their maritime positioning solution named Automatic Identification System (AIS). AIS transponder transmits 9.6 Kb GMSK signal over the channel to identify the position and speed of vessels [104]. There is still further modifications need to be done to release international AIS standard using GMSK signal. More details on GMSK modulation based satellite communication receiver design can be found in [104], [105].

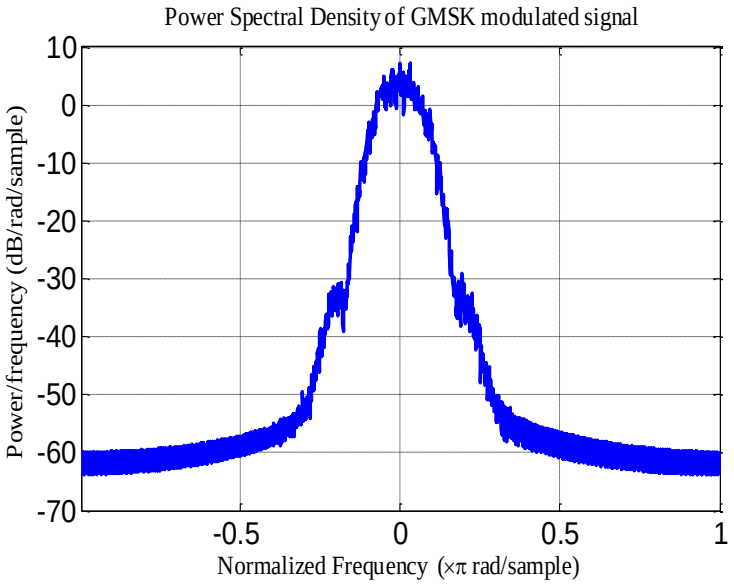


***Figure 3-15*** *Power spectral density of GMSK signal*

## 3.3 UWB principles

UWB technology is different from narrowband wireless transmission system. In UWB, signal spreads over a very wide range of frequencies instead of broadcasting on separate frequency band [69]. Several pulse generation techniques may be used to satisfy the UWB signal requirements. Time-based modulation method and shape-based modulation method are two basic modulation techniques used in UWB system [69]. Time-based UWB is based on emission of very short Gaussian pulse as illustrated in *Figure 3-16*. The first derivative of Gaussian pulse provides ideal monocycle pulse as shown in *Figure 3-17* , which has single zero crossing.

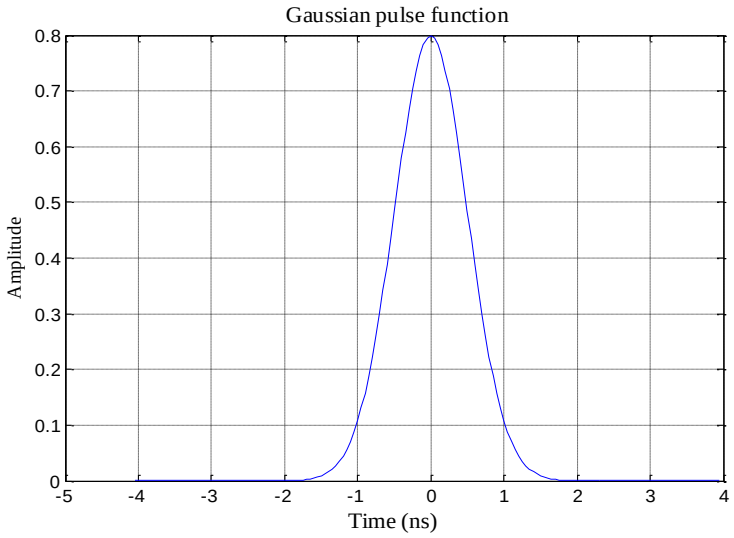


***Figure 3-16*** *Gaussian pulse function*

UWB based radio concept is implemented in baseband approach. The most common data modulation method used in time based UWB system is Pulse Position Modulation (PPM) [106]. In PPM, each pulse is delayed or sent in advance of a regular time scale. TH-SS and DS-SS are the most popular multiple access method used in UWB systems. Information bit is spread over multiple monocycles in order to achieve processing gain in reception through this multiple access.

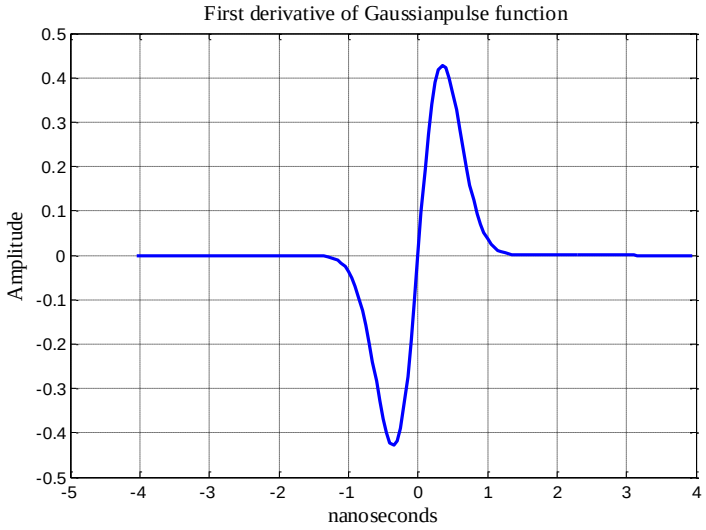


***Figure 3-17*** *UWB monocycle pulse (based on the derivative of a Gaussian function)*

A general UWB pulse train signal $s(t)$ can be modeled as a sum of pulses shifted in time by,

$$s(t) = \sum_{uw=-\infty}^{\infty} a_{uw} p(t - t_{uw}) \qquad (3\text{-}16)$$

Where, $p(t)$ is the basic pulse shape, $a_{uw}$ and $t_{uw}$ are the amplitude and time offset for each individual pulse.

Recent research methods for accurate positioning approach are considering this UWB system for its high bandwidth characteristics [107]. In time based positioning approach, such as, by TOA and TDOA, ranging and positioning accuracy depends upon signal bandwidth. In fact, as the bandwidth of UWB system is order of 2-3 GHz, the ranging accuracy is of the order of 1cm. Therefore, the characteristics of UWB signals provide the potential of accurate positioning of user. This fact on ranging accuracy $d$ can be observed by eq.( 3-8 ),

$$d = \frac{c}{BW} \qquad (3\text{-}17)$$

Where, $c$ is the speed of light ($3 \times 10^8 ms^{-1}$), $BW$ is the bandwidth of UWB signal.

A simple general block diagram of UWB system is presented in *Figure 3-18* [108]. According to this block diagram, the generated Gaussian pulses are modulated and pass through the channel. In receiver, multiband low noise amplifier (LNA) and Automatic Gain Control unit (AGC) plays important role in signal processing [108]. A control unit derived from the cross-correlator generates pulse to decode the user data in receiver section.

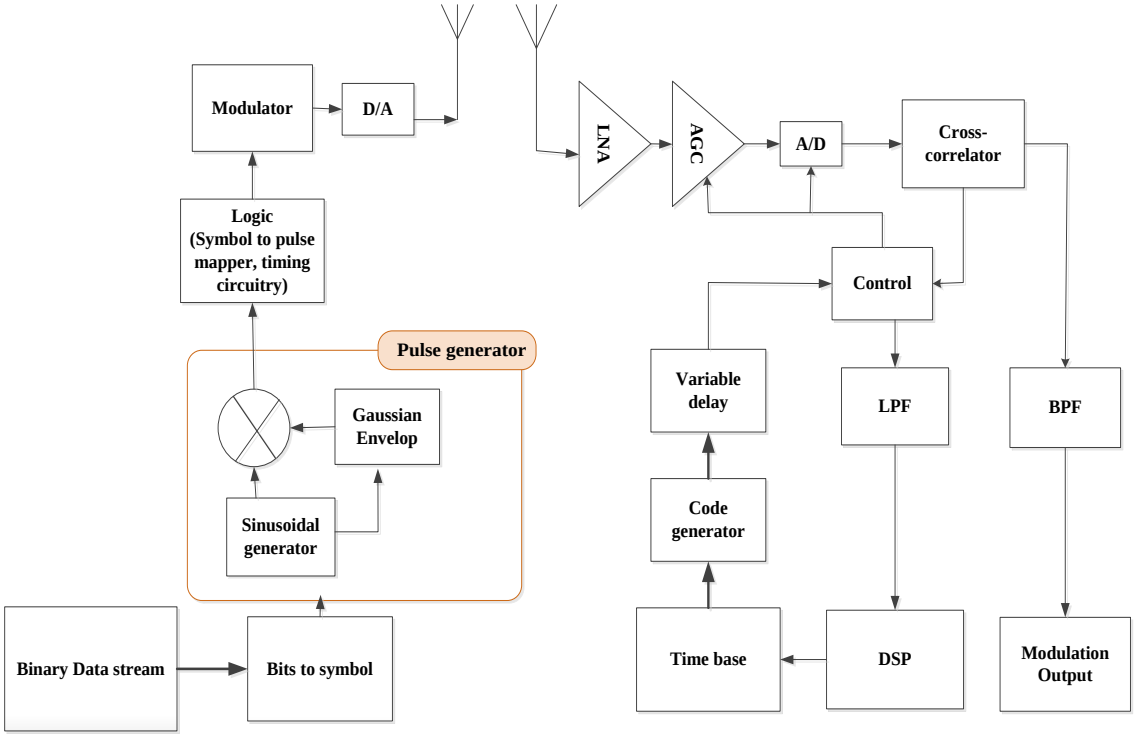


***Figure 3-18*** *UWB system block diagram [69], [108]*

# 4. SIGNAL DETECTION AND SELECTION IN COMMUNICATION AND NAVIGATION APPLICATIONS

Awareness of the radio environment is of great interest in cognitive wireless domain. Efficient and opportunistic usage of spectrum needs signal detection and then proper identification will lead accurate solution. Also, what is currently named as cognitive positioning in [8], [42], [43], [44], [109] and [110] may require a certain type of signal selection. In addition, recent advances in wireless communications use the so-called Non-Orthogonal Multiple Access (NOMA) concept, which is also relying on some form of signal separation from a signal mixture [111], [112]. This chapter will focus on this signal detection, signal classification and signal selection fundamentals. Our thesis focus is on the emerging positioning solution based on signals of opportunity, but most of the issues presented in this chapter apply as well to various challenges in wireless communication domain.

## 4.1 Spectrum sensing

Spectrum sensing is an elementary requirement for wireless solutions which meet spectrum awareness feature. The detection of the presence of signals in noisy environment is called spectrum sensing [113]. In a broader view, spectrum sensing is used to detect and identify whether a certain frequency band contains a strong wireless signal (a signal is present or not in a certain spectral band over noise level) that can be further used for communication or positioning purposes. The signal identification from the available signals is the first concern for successful cognitive radio and cognitive positioning solutions.

Cognition refers to the awareness achieved by an adaptive feedback and statistical learning in a system and that system is called cognitive approach-based system. To achieve awareness in positioning, spectrum sensing process may comprises different spectrum awareness criteria, such as, signal recognition, classification and selection from a pool of available signals [44], [53]. The spectrum awareness features of the cognitive approach-based hybridized positioning solution can be accomplished by contextual information. The detection of signal from available ones in a certain time and location provides a part of such contextual information. The aspect of contextual information-based signal detection is taken into consideration in this thesis.

Spectrum sensing is one of the crucial functionalities of a cognitive radio in order to learn the radio environment. Wasteful static spectrum allocations and inefficient utilization creates spectral congestion. Cognitive radio with respect to spectrum sensing can achieve efficient spectral usage through allocating free spectrum to the secondary users. A conceptual view on spectrum sensing for signal detection in cognitive radio can be presented by *Figure 4-1*. The plot of *Figure 4-1* shows the allocation of a free band (in case of cognitive radio) to a secondary user, while the primary user was allocated certain bands previously with priority [114].

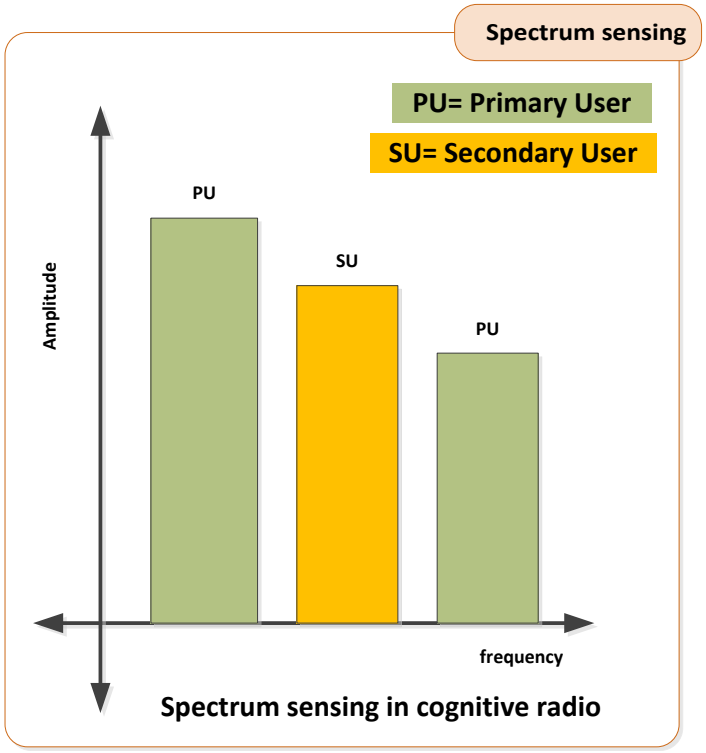


***Figure 4-1*** *Spectrum sensing in cognitive radio [114]*

A high level view of cognitive radio system can be shown in *Figure 4-2*. The spectrum sensing engine receives signals and performs dynamic spectrum allocation to users. The system can have a cognitive engine which defines the adaptability [115]. According to the *Figure 4-2*, a learning unit accumulate the information based on experience (past values) which helps in adaptive change of resource allocation and component configuration. Finally, a software defined radio completes the concept of cognitive radio by adaptively changing of parameter such as frequency, bandwidth, modulation order, etc based on each situation [116]. In cognitive radio approach, a dynamic spectrum allocation procedure followed by free band detection offer the user an opportunistic usage of the band for radio applications [116]. Literature study of cognitive radio opens a wide research area and more information can be extracted from for example [115], [116] and [117].

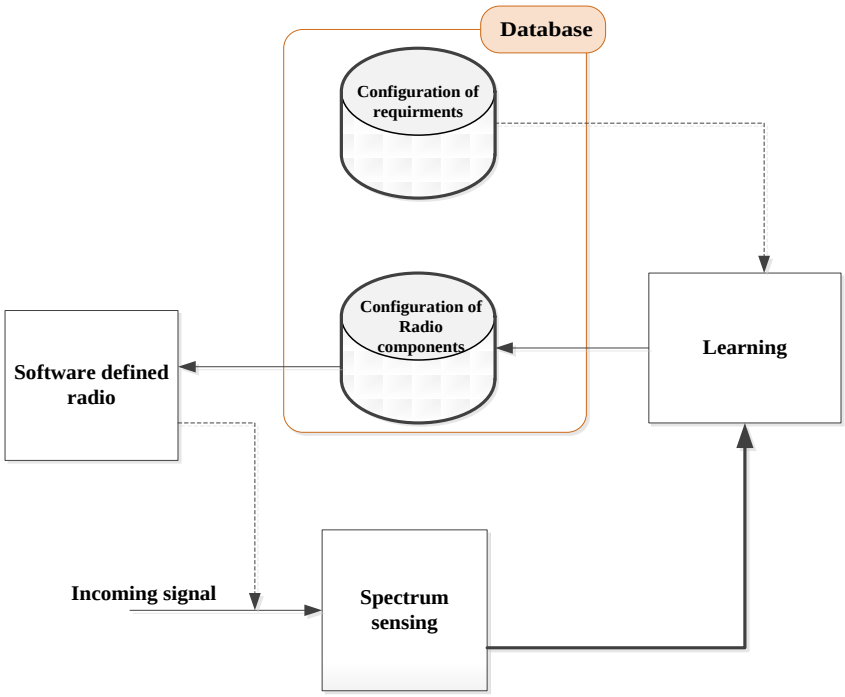


***Figure 4-2*** *Cognitive radio high level diagram (reproduced from [116])*

On the other hand, in a positioning system, the purpose of spectrum sensing is to detect or identify whether a signal is available or not in a certain frequency band. Cognitive positioning needs to incorporate a spectrum sensing unit to create awareness about the surrounding radio spectrum. Further processing such as, signal classification, selection has to be taken into consideration to achieve required contextual awareness in positioning solution. A state of art model for cognitive approach based positioning system embedded with spectrum sensing techniques is proposed by the author in *Figure 4-3*. The idea of the proposed model is inspired from several published research articles on cognitive positioning, for example [7], [43], [118]. According to the *Figure 4-3*, since there are many signals available through simultaneous reception at the receiver front end, a first step is to identify the most relevant to location. Signal types also need to be distinguished from the combination of all localization sources. After relevant signal selection at the spectrum sensing unit, metric value is obtained from selected signal. After that, in post signal processing, pseudorange calculation is performed from obtained metric value. Finally, position estimation of users can be obtained from pseudorange.

Furthermore, scientific research in literature is going on to combine spectrum sensing and location awareness positioning engine in a single compressed sensing based formalism in the cognitive radio context, for example in [119]. Several IEEE standards, for example IEEE 802.22 (WRAN) are also considering location aware spectrum efficient cognitive radio system.

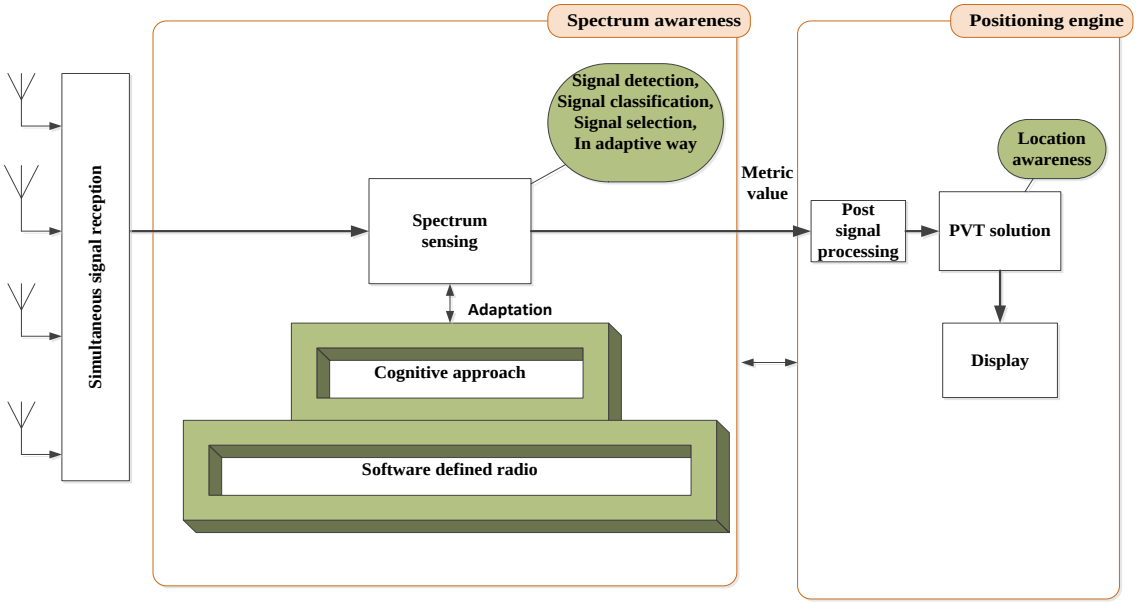


***Figure 4-3*** *Spectrum sensing in positioning through software defined radio*

Summing up, in cognitive positioning, the system tries to detect the presence of signals in order to select the relevant ones for positioning purposes, whereas in cognitive radio, system tries to detect the free spectrum (not used by primary user) in order to establish transmission for secondary users in an opportunistic manner.

## 4.2 Detection problem

In general, the spectrum sensing is basically a statistical detection problem which boils down to a binary hypothesis testing problem. To detect the signal of interest, the detector must decide between two hypotheses. The hypotheses can be formulates as below by eq. ( 4-1**)**, where hypothesis $H_0$ (noise only) is tested against hypothesis $H_1$ (signal plus noise present).

$$\begin{cases} H_0: & noise\ only \\ H_1: & signal\ in\ noise \end{cases} \qquad (4\text{-}1)$$

If the signal of interest is $x(t)$, noise is $n(t)$, the received signal can be modeled as in eq. ( 4-2 **)** according to the hypotheses considered above in eq. ( 4-1),

$$z(t) = \begin{cases} n(t), & if\ H_0 \\ x(t) + n(t), & if\ H_1 \end{cases} \qquad (4\text{-}2)$$

In the detection stage, a test statistic is computed based on the detector's observation value for signal detection [1]. In general, a test statistic is a function of the received signal [120]. After that, this test statistic is compared to a pre-defined threshold $\gamma$ in order to decide whether the signal is present or not. Eq. ( 4-3 ) gives the decision structure for

the test statistic to be compared with a threshold. The threshold $\gamma$ is typically computed adaptively according to a fixed false alarm value [121].

$$T_{statistics} \underset{H_0}{\overset{H_1}{\gtrless}} \gamma \qquad (4\text{-}3)$$

The result of the comparison of test statistics with the threshold in eq. ( 4-3 ) is obtained from the Probability Density Function (PDF) under $H_1$ versus PDF under $H_0$. The PDF under each hypothesis can be obtained from a high enough number of random realizations of the simulated test statistics. *Figure 4-4* shows a binary hypothesis decision example of CDMA signal, where both PDFs are used in detection stage with the threshold placement. The probability of detection ($P_d$) and the probability of false alarm ($P_{fa}$) are the parameters for the detection performance of spectrum sensing. In other words, for the signal detection, the main objective is to maximize the probability of detection with a lower probability of false alarm. The probability of detection and probability of false alarm can be computed according to the threshold as,

$$P_d = proba(T_{statistics} \geq \gamma | H_1) = 1 - F_{H_1} \qquad (4\text{-}4)$$

$$P_{fa} = proba(T_{statistics} \geq \gamma | H_0) = 1 - F_{H_0} \qquad (4\text{-}5)$$

Where $F_{H_1}$ and $F_{H_0}$ are the cumulative distribution functions derived from the respective PDFs.

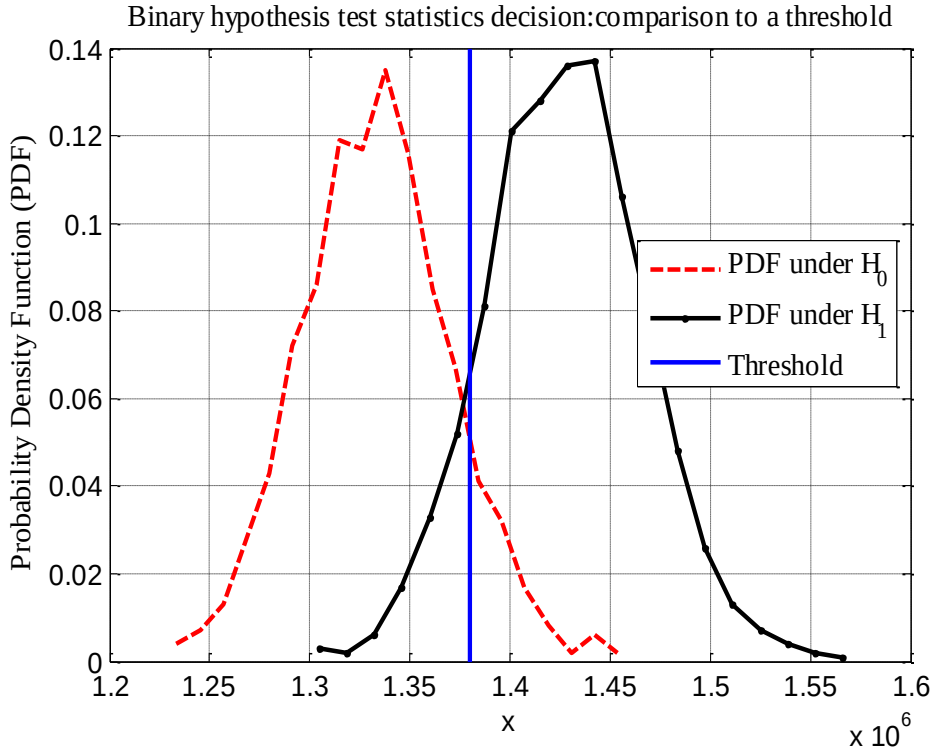


***Figure 4-4*** *Illustration of PDFs for binary decision (CDMA signal)*

The choice of suitable threshold has an important contribution in the signal detection process [122]. It can be noticed from the *Figure 4-4* that, if the threshold is set too low, the probability of detection increases. However, probability of false alarm also increases as well and vice versa [1]. There is a tradeoff between probability of detection and probability of false alarm value derived from the selected threshold [123].

*Figure 4-5* shows the cumulative distribution functions comparison with the threshold in order to detect the presence of signals.

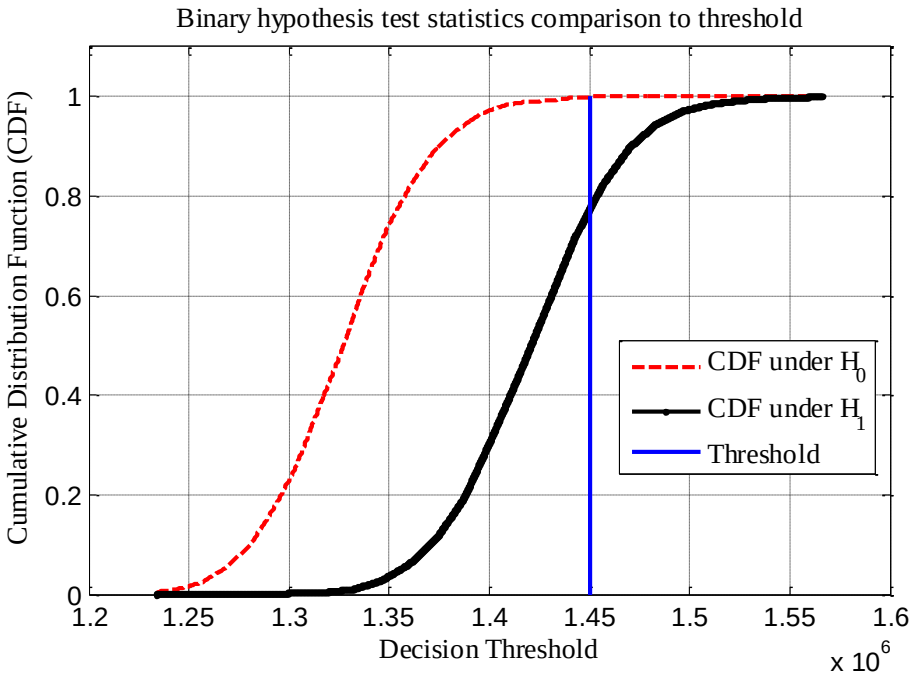


***Figure 4-5*** *Illustrative example for the CDFs of test statistics (CDMA signal)*

The detection probability in this thesis is defined as the probability of signal being detected (i.e., the value of test statistics is higher than the threshold), given the event $H_1$ hypothesis is true. A false alarm situation occurs when the event $H_0$ hypothesis is true and the test statistics is higher than the threshold. It may be also possible that signal is present but not detected (miss-detection). This may happen if the threshold is set too high or the environment noise is too high, that the signal is lost in noise. This phenomenon is counted in the missed detection probability $P_m$. The usual way of illustrating the detector performance is the Receiver Operating Characteristics curve (ROC) which describes the relation between $P_d$ and $P_{fa}$ for all possible values of threshold. *Figure 4-6* indicated the binary hypothesis conceptual steps flow diagram where all possible probabilities are shown depends on the threshold comparison.

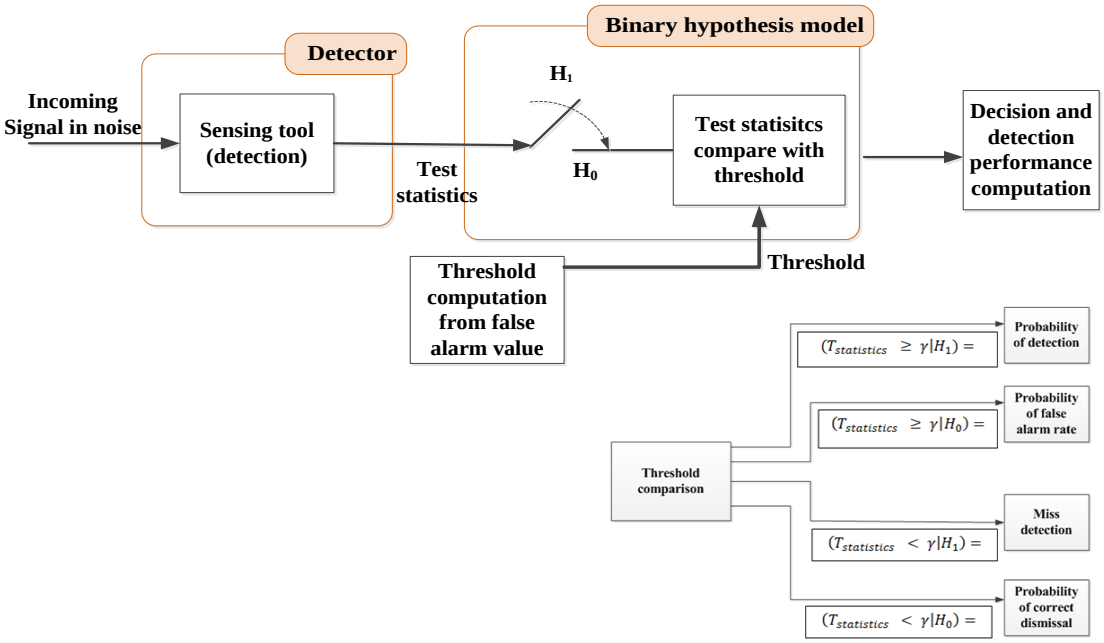


***Figure 4-6*** *Binary hypothesis model for signal detection performance observation*

## 4.3 Signal classification and selection

Typically, several signals of opportunity can be available over the wireless channel for positioning purposes in a cognitive positioning system. Signals of opportunity may create an opportunity to do better positioning estimation in multipath environments (e.g. by optimal combining or hybridization of the available signals). Having different and high number of signals also raises the problem of selecting the most worthy one corresponding to accurate positioning [7]. So, in a first step of a cognitive positioning engine, it is important for the system to be able to select the signal with the best positioning capabilities among the available signals.

In the context of cognitive wireless navigation, the relevant signal selection refers to the process of selecting potential signals from all the available signals [53]. Selection of relevant signals will reduce the receiver complexity [7]. The final goal is to be able to increase the location estimation accuracy. However, the hybridization part is not within the scope of this thesis. The concept address here in this section is the problem of relevant signal selection, where the term ‘relevant’ signal can be defined in various ways,

1) as the signal which has the highest positioning accuracy capability among the available in a pool of available signals
2) as the signal having the highest signal to noise ratio among the received signals
3) as the signal having the lower Cramer Rao Lower Bound (CRLB).

It is not however within the scope of our thesis to investigate the different relevance criteria above, but rather to show that signal detection in noise is indeed possible based on the cyclostationary signal features. The future steps would be to investigate and op-

timize the different ‘relevance’ criteria, but this is not addressed in here. An example based on the second criterion above-mentioned (signal-to-noise power ratio relevance criteria) can be found for example in our submitted work [124].

Several parameters may influence the accurate positioning estimation capability of signal, such as, transmit power, Signal to Noise Ratio (SNR) or Carrier-to-Noise Ratio (CNR), modulation order, channel co-efficient parameter, channel bandwidth, multipath effects and so on. One statement could be that, a stronger signal with higher modulation order has a higher positioning capability among available signals. This is an intuitive statement and its validation is again outside the scope of this thesis.

In order to find out the positioning capabilities of signals, it is necessary to know some of its features such as carrier frequency, symbol rate, cyclic frequency, phase information of the signal prior to selection for using in position estimation [42]. However, the navigation part, such as the pseudorange calculation procedure may also influence in the accurate estimation.

Cognitive positioning research challenges can be divided into three areas namely:

1) Channel modeling,
2) Location engine design,
3) Positioning algorithm development.

Channel modeling deals with the required bandwidth design in order to achieve target location accuracy [44]. As a consequence, the channel modeling influences the signal selection. The required bandwidth is formulated in an adaptive way, using as a cost criterion based on the accuracy-related decision handshaking between transmitter and receiver of cognitive system [44], [125]. A cognitive positioning system can select the signal based on its accuracy capabilities. The system can agree on a desire accuracy level prior to selection of signal [125]. Afterwards, it will select the signal which will meet the desired accuracy level for positioning solution. The adaption of accuracy and bandwidth requirements take place automatically depending on the channel situation and environment. Location core design is another important challenge to achieve location and environment awareness of cognitive positioning system. Location aware core engine needs to be able to track the users by maintaining the history profile of previous locations from statistical learning and by sensing the location whether urban, indoor or outdoor [44]. The purpose of this learning and sensing about user locations is to achieve location awareness. Location aware core also influences the decision about the signal selection in adaptive way derived from the achieved location awareness to achieve the desire accuracy level for positioning solution [44]. Finally, an adaptive positioning algorithm needs to develop for processing various kinds of signals and estimate location from obtained metric value [125]. Since there will be different signals, metric value formation and pseudorange calculation will be conducted adaptively according to the selected signal to meet certain accuracy.

The situation addressed above about cognitive positioning can be better visualized by *Figure 4-7*. *Figure 4-7* shows the signal selection stage which is basically depends on the signal classification stage. Cognitive positioning system will classify signals and give identification for the best possible signal out of available signals. The identified signal which has highest positioning capability (high accuracy) will be selected as a next level candidate for position estimation [7].

A better suited equation to this signal selection problem and its bandwidth estimation can be written as in eq. ( 4-6) derived from the Cramer Rao Lower Bound (CRLB) method [125], [126].

$$\beta = \sqrt{\frac{c^2 M(w)}{\varphi^2\, SNR}} \qquad (4\text{-}6)$$

Where, $\beta$ is the required bandwidth, $M(w)$ is the certain accuracy with adaptive parameter $w$, $w$ is the estimated distance between transmitter and receiver, $\varphi$ is the channel co-efficient, SNR is signal to noise ratio, $c$ is the speed of light taken as $3 \times 10^8 m/s$ .

It seems that, to achieve certain level of accuracy from a selected signal with high positioning capability will require $\beta$ bandwidth and overall system has to provide this bandwidth allocation [126].

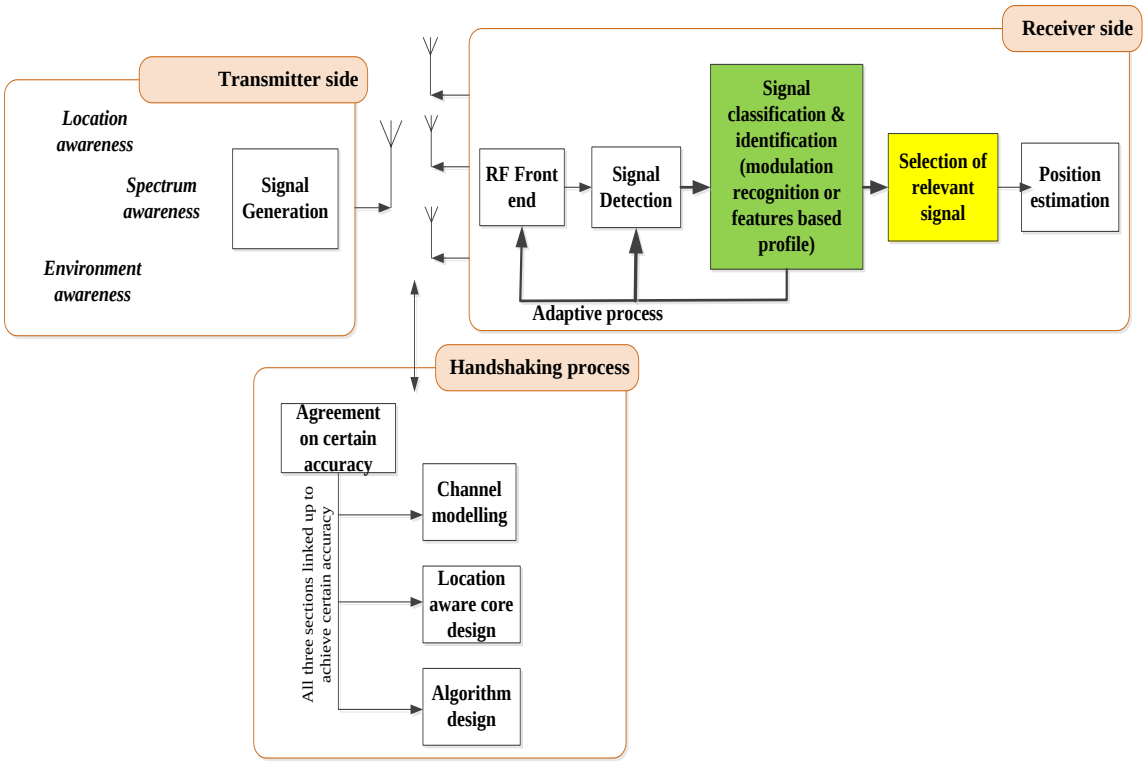


***Figure 4-7*** *Signal selection in a cognitive positioning system*

## 4.4 State-of-art detectors

Spectrum sensing can be implemented by several detection methods, such as, energy detector, matched filer, cyclostationary properties, higher order moment detector etc. Different techniques serve different purposes based on their principles. Various methods for signal detection are presented in this section. However, cyclostationary detector will be described in chapter 5.

### 4.4.1 Energy detector

The energy-based spectrum sensing and detection is the simplest method to detect signals in the environment. The underlying idea is to detect the energy of signal at the receiver side; if the energy is higher than a threshold, then the signal is detected; otherwise only noise is present in that band [76]. In general, the time domain implementation of energy detector consists of averaging the square of the signal to get the test statistics.

In the continuous-time domain implementation of energy detectors, if the observation time is $T$, the energy metric of the received signal $z(t)$ modeled in eq. ( 4-2 ) can be used as a test statistics for signal detection. Test statistics for the energy detector is given by,

$$\xi = \int_{t_0}^{t_0+T} z(t)z^*(t)\,dt \qquad (4\text{-}7)$$

Where, $t_0$ is random starting time for observation, $z^*(t)$is the complex conjugate of received signal.

In discrete time domain, if the observation is performed over total $N$ complex samples, at a sampling period of $T_s$ , then for the discrete signal $z[n] = z(nT_s)$, the energy-based test statistic is given by,

$$\xi \approx T_s \sum_{n=0}^{N-1} z[n]z^*[n] = T_s \sum_{n=0}^{N-1} |z[n]|^2 \qquad (4\text{-}8)$$

The detection criteria based on the energy-based test statistic is then given by,

$$\varpi = \begin{cases} H_0; & \xi < \gamma \\ H_1; & \xi \geq \gamma \end{cases} \qquad (4\text{-}9)$$

*Figure 4-8* shows a digital implementation of the energy based detection. Eq. ( 4-10 ) and eq. (4-11 **)** indicate the probability of detection and probability of false alarm, respectively.

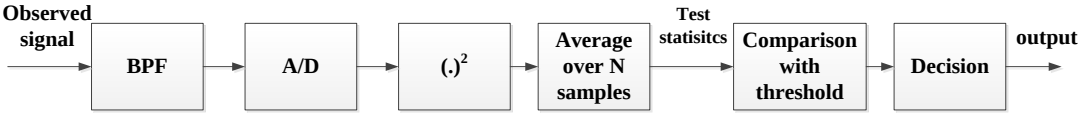


***Figure 4-8*** *Energy detector*

The detection and false alarm probabilities depend on the threshold $\gamma$, and hence it is necessary to choose an appropriate value. One approach of selection of threshold is to select $\gamma$ to meet a predefined desire false alarm probability. There are many evolutions over the basic idea of energy detector that mainly focuses on the adaptive threshold calculation [87]. More details on appropriate threshold selection based on noise power estimate value can be found [127]. Moreover, the energy detector performance varies when the received signal undergoes different types of fading channels with AWGN, such as, Rayleigh, Rice, and Nakagami. More details can be found in [127].

$$P_d = Prob(\xi \geq \gamma | H_1) \quad (4\text{-}10)$$

$$P_{fa} = Prob(\xi \geq \gamma | H_0) \quad (4\text{-}11)$$

The detection performance of energy detector affects in a negative way when the noise variance is unknown to the receiver. The prior knowledge of the noise power can be used to improve the detection performance in a low SNR situation. However, in real systems prior perfect knowledge of the noise power level may not possible, causing degradation in energy detection performance [127]. Another disadvantage of energy detector is that, it does not recognize the difference between signal of interest, noise and interference [9]. A strong noise or interference can be easily mistaken as a signal presence. Moreover, making a separation among different kind of noise present in environment is not possible with this detector.

### 4.4.2 Matched filter detector

The matched filter based signal detection requires prior knowledge of the signal, for example, information of modulation, data rate, carrier frequency, and even the presence of some training or pilot sequences [114], [127]. Matched filter detector is widely used in GNSS as an optimal choice for signal acquisition. This approach involves demodulation of the observed signal in order to get the prior knowledge of signal [87]. The idea is to maximize the SNR at the output of the filter corresponding received signal $z(t)$ over observation period $T$. The output of the filter is given by,

$$h(t) = \begin{cases} x(T-t), & 0 \leq t \geq T \\ 0, & otherwise \end{cases} \quad (4\text{-}12)$$

Here, $x(t)$ is the signal of interest.

In order to present a fundamental view of matched filter based spectrum sensing, a block diagram is shown in *Figure 4-9*.

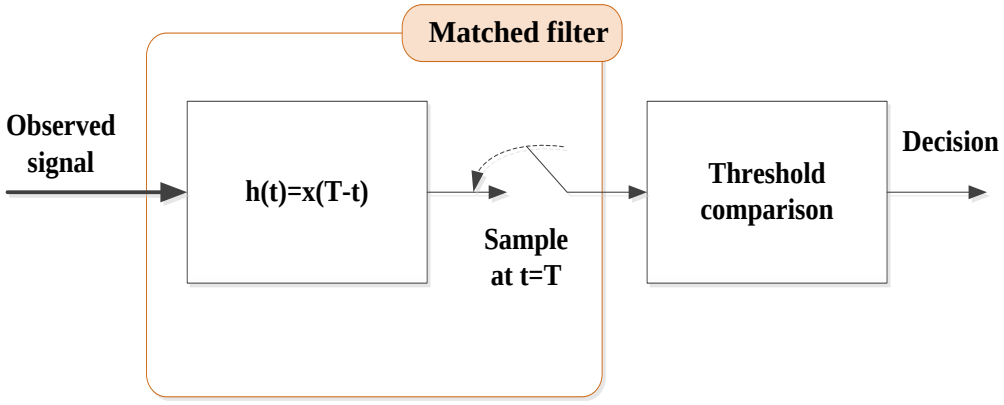


***Figure 4-9*** *Matched filter based spectrum sensing [76][127]*

The matched filter-based detector gives better detection probability compared to the previously discussed energy detector. However as mentioned, it requires the complete signal information and needs to perform the complete receiver operations in order to detect the signal.

### 4.4.3 Higher-order moment detector

Higher-order moment (HOM) of a signal is a statistical tool which describes the shape of the probability distribution obtained from the signal samples [128]. The higher-order moment detector uses the higher-order autocorrelation value obtained from signal as a test statistic and compares it to a predetermined threshold. Decision is made as to whether the test statistic contains a signal in noise or only noise based on that comparison. A $P^{th}$-order moment detector can be modeled as in eq. (4-13),

$$\zeta = T_s \sum_{n=0}^{N-1} |z[n]|^P \tag{4-13}$$

Where, $P$ is the order of the moment [P=1, 2, 3, 4……e.g. first order moment ($P$=1; mean), second order moment ($P$=2, variance)], $T_s$ is the sampling period, $N$ is the size of the population.

In the same way, fourth order moment detector ($P$=4) can be derived from eq. (4-13) as,

$$\zeta = T_s \sum_{n=0}^{N-1} |z[n]|^4 \tag{4-14}$$

The performance of detection for HOM detection can be obtained from the previously explained binary hypothesis model in section 4.2.

### 4.4.4 Other signal detection methods

Covariance based, eigenvalue based, waveform based, wavelet transform, filter bank method, radio identification based, random Hough transform based detection are some of the other different approaches found in the literature that are applied for spectrum sensing as well. In here, we are giving very brief introduction per each method enumerated. More details about these methods with a comparison among them can be found in [114], [121] and [127].

Covariance of signal of interest and the AWGN is different and this statistical difference is used to detect the presence of signal. In the covariance detector, the test statistics are derived from the covariance matrix of the received signal. Eigenvalue based signal detection uses the eigenvalue of the covariance matrix of the received signal as a test statistics for signal detection. In waveform based detection, patterns corresponding to the signal, such as, pilot pattern, spreading code sequence, etc are utilized to detect the presence of signal. Wavelet transform based spectrum sensing is used to detect the edges on the power spectral density of a wideband spectrum. Detection of edges will determine the presence of signals. In the filter bank method, a set of bandpass filters with low side-lobes are used to detect the signal spectra. Radio identification based method uses several features extracted from the received signal, such as transmission frequency, transmission range, and modulation techniques for spectrum sensing. Random Hough transform is a well-known image processing techniques and can be used as a signal detection method. In this method, random Hough transform of the received signal is used to identify the signal.

## 4.5 Signal classification methods

Eventually, automatic recognition of the modulation used by a signal is an important aspect of signal processing in spectrum-aware systems. The purpose of signal classification in a receiver is to determine the modulation type being employed in the spectrum. A large number of modulation classification methods have been developed in recent years, namely spectrogram analysis, cumulant feature based classification, Kolmogorov-Smirnov test, wavelet analysis, cyclostationary classification etc. In general, classification methods are grouped into two broad categories, likelihood-based and feature-based methods. This section focuses on those classification methods in brief manner. However, cyclostationary classification method will be described in chapter 5.

### 4.5.1 Spectrogram analysis

Signal modulation can be recognized by spectrogram analysis. Spectrogram is defined as the graph of the energy content of a signal expressed as function of frequency and time [129]. In more specific way, spectrogram represents how the frequency content of a signal changes with time. The classification method based on spectrogram image analysis can discriminate between various digital signal modulations such as, FSK,

BPSK, MSK, QPSK, and 16-QAM. Signals spectrogram analysis can be divided into module spectrogram analysis and phase spectrogram analysis. In module spectrogram, the modulated signal gives a unique spectrogram graph as a form of maxima peak at distinct frequency. FSK and MSK modulated signal can be differentiate by using this module spectrogram analysis.

On the other hand, in phase spectrogram, the observation of phase state and occurrence count of phase difference is used for signal classification. For example, BPSK signal has two phase states and two differences of phase while QPSK signal has four phase sate and four changeovers.

The test statistics for detection performance calculation can be obtained from histograms of spectrograms. It is necessary to estimate symbol length of received signals to obtain required spectrogram through which the classification of modulation will be performed. In fact, classification performance is strongly depends on the segment size used for spectrogram calculation. The segment size used in spectrogram formation is taken equal to the symbol length of the received signals [129]. This method cannot provide reliable classification performance in the presence of frequency and phase offset, timing error and unknown symbol arriving sequence. Moreover, due to the resolution limitation of spectrogram, this method is not beneficial to classify modulation patterns of signals with high bit rate [129]. However, spectrogram analysis can be used as an initial stage modulation classifier with cooperation of other features based classifier scheme for example wavelet based classification. The scope of spectrogram analysis can be extended by this type of joint classifier arrangement. Detail description of this spectrogram analysis can be found in several research articles, for example, in [130].

### 4.5.2 Kolmogorov-Smirnov tests

Cumulants feature based classification method can be used to distinguish modulation formats. The $r^{th}$ order cumulants $k_r$ of a random variable $X$ can be defined via so-called cumulant generating function $g(t)$ as,

$$g(t) = \log E[e^{tX}] = \sum_{r=1}^{\infty} k_r \frac{t^r}{r!} \qquad (4\text{-}15)$$

Where, $E[e^{tX}]$ is the moment generating function, for integer $r = 0,1,2,\ldots$ and $t \in R$ .

Higher-order cumulants (e.g. $r = 4$; fourth order cumulants) can discriminate PSK and QAM modulations [131]. PSK and QAM modulated signals have identical theoretical cumulant values. The cumulant based classification method compares the received signal's cumulant value with the corresponding theoretical cumulant value and find the modulation format. However, cumulants feature based method does not give precise discrimination of modulation patterns in presence of noise. Moreover, classification between different series of QAM (16-QAM, 64-QAM) and PSK (8-PSK, 16-PSK) is also difficult through this cumulants based method.

Kolmogorov-Smirnov (K-S) is a statistical test which can be used in effective classification between several series of QAM and PSK [132]. In fact, both cumulant based method and K-S test can be used in a hybrid manner to achieve effective modulation classification. In that hybrid implementation, the cumulant test will decide the modulation pattern whether PSK or QAM and the K-S test will classify between different series of PSK or QAM. This type of hybrid modulation classification scheme can be found in [133].

In K-S test, it is assumed that, the empirical cumulative distribution function of the received signal and cumulative distribution function of the theoretical reference signal is same. In other words, for ideal classification scheme, it is more likely that, received signal distribution is identical to reference signal distribution. However, due to noise injected from wireless channel makes an alternation from this equal distribution assumption between received and reference signals. The assumption can be formulated as in eq. ( 4-16 ),

$$F(z) = S_m(z) \tag{4-16}$$

Where, $F(z)$ is empirical cumulative distribution function of received signal, $m$ is the modulation format of reference signal and $S_m(z)$ is the cumulative distribution function of the reference signals.

The K-S test statistics is the maximum absolute different between $F(z)$ and $S(z)$ and written as,

$$D = \max|F(z) - S(z)| \tag{4-17}$$

The decision of the classification can be characterized based on the K-S test statistics. More details on the implementation of K-S test based signal classification can be found for example in [133].

### 4.5.3 Wavelet analysis

Digital modulation classification can be also performed through discrete wavelet transform (DWT) [134], [135]. Digital wavelet techniques can be applied to the signal for feature extraction. Wavelet transform of a signal $x(t)$ can be written as,

$$CWT(a,\tau) = \frac{1}{\sqrt{a}} \int x(t) \Psi_a^*(t - \frac{\tau}{a}) dt \tag{4-18}$$

Where, $CWT(a,\tau)$ is the wavelet transform co-efficient, $a$ $(a > 0)$ is a scale parameter, $\tau$ is a translation variable,* denotes complex conjugate, $\Psi_a(t)$ is a baby wavelet function which is derived from mother wavelet, $\Psi(t)$ [136]. Baby wavelet is a translated and scaled version of mother wavelet as follows,

$$\Psi_a(t) = \frac{1}{\sqrt{a}}\Psi\left(\frac{t-\tau}{a}\right) \quad (4\text{-}19)$$

There are different kinds of mother wavelets available is literature, such as, Morlet, Haar, Daubechies, Shannon etc [137]. For example, if Haar wavelet is chosen as the mother wavelet, $T$ is the symbol duration, mother wavelet $\Psi(t)$ can be written as,

$$\Psi(t) = \begin{cases} 1\,, if\ 0 \le t < \frac{T}{2} \\ -1, if\ \frac{T}{2} \le T < T \\ 0,\ \ otherwise \end{cases} \quad (4\text{-}20)$$

DWT method can recognize the transients of several signals which created due to the change in symbols of different signals. DWT can characterize the transient value to classify signal effectively based on modulation used. DWT decompose signal into a set of detail component of various sizes as signal contains information of different scales. Decomposition set of signal helps in modulation recognition. DWT process employ two set of co-efficient derived from signals components [138]. This wavelet co-efficient can be act as feature to classify signals. The formulated features basically indicate time and frequency information of signals under consideration. Performance of modulation classification based on DWT process can be observed by Monte Carlo simulation with setting up a threshold value according to the SNR [137], [138]. Otherwise, extracted features can be fed into the so called pattern recognition subsystem for making better decision on modulation classification [138]. Basically, classification of modulation falls into a pattern recognition problem. Pattern recognition use received signals feature which are obtained in advance for example from wavelet transform method [138].

Many researchers have proposed pattern recognition using artificial neural network (ANN) [9], [138], [139]. Using of ANN in the pattern recognition problem is a recent phenomenon. It is worth to mention that, ANN learns the modulation pattern and other signal parameter specific to the requirements by a training phase with standard learning algorithm. ANN makes decision on classification performance based on matching the received signals wavelet co-efficient with training phase co-efficient. More details on the implementation of wavelet based signal classification with ANN can be found for example in [138].

# 5. CYCLOSTATIONARY PROCESSES

Cyclostationarity can be a perfect probabilistic approach to model wireless man-made signals where certain periodicity comes from coding, modulation, multiplexing, sampling etc. Cyclostationarity can also be observed in nature-originated signals, such as in climatology, atmospheric, or biomedicine signals, due to their rhythmic or seasonal behavior. Stationary processes exhibit a time-invariant mean and auto-correlation function, whereas a cyclostationary process has a time periodical probability distribution function. In addition, a cyclostationary process exhibits the so-called spectral correlation property. Spectral correlation means that the signal and its frequency shifted version are correlated.

A random process is cyclostationary if its mean and autocorrelation vary periodically in time. In the context of stationary signals, wide-sense stationary refers to time-invariant moments (such as mean, variance and higher order moments), whereas strict-sense stationary refers to time-invariant probability distribution function. A stationary random process is cyclostationary in strict sense if its probability distribution function is periodic in time. Wide-sense cyclostationarity means that the mean and the autocorrelation function of the signal is periodic [140], [141]. This chapter presents the theoretical definitions of cyclostationarity and the properties of cyclostationary signals from mathematical point of view. Cyclostationary detector and cyclostationary classification method are also described in details. Finally, the later part of this chapter will focus on the applications of the cyclic spectral analysis in the context of signal-of-opportunity selection.

## 5.1 Definition of cyclostationary signal

From mathematical point of view, if any higher order nonlinear transformation of a random signal generates a spectral line at cyclic frequencies other than zero, the signal is called cyclostationary [16], [17].The cycle frequencies are the integer multiples of the reciprocal of the period of the cyclostationarity. A cyclostationary signal exhibits spectral correlation between the spectral components of that signal at the position of non-zero cyclic frequency. In contrast, for a stationary signal, only one spectral line can be generated at zero cyclic frequency [18].

A signal $x(t)$ is said to be cyclostationary with a cycle frequency $\alpha$ , delay $\tau$ and period $T_0$ if and only if its delay conjugate product $y(t) = (x(t)x^*(t-\tau))$ produces a spectral line at frequency $\alpha$.

If the signal exhibits cyclostationarity with cyclic frequency $\alpha$ in time domain, then it also exhibits a spectral correlation at shift equal to $\alpha$, in frequency domain. There is a fundamental link between the creation of a spectral line at a cyclic frequency and the spectral correlation of two frequency components of the cyclostationary signal. A spectral line is generated at the cyclic frequency through nonlinear transformation of the main modulated signal. The value of the cyclic frequency at which a spectral line is created is exactly the same as the frequency difference of the two frequency components which are correlated [15].

Man-made signals are periodically correlated signals. This is because their mean and autocorrelation function are periodic and this periodicity is born from processes such as coding, multiplexing, or modulation. Such inherent property of the man-made signals can be used in signal detection, recognition, or classification. However, the noise is random in nature and a stationary random noise does not exhibit a peak at non-zero cyclic frequencies [18]. As a result, man-made signals can be separated from the background additive noise at non-zero cyclic frequencies.

Fourier analysis is a strong tool for extraction of some features of periodic deterministic signal (such as their period). On the other hand, a random signal which exhibits cyclostationarity properties can be detected through the extraction of its cyclic features [9]. The spectral correlation of a cyclostationary signal cannot be visible through conventional Power Spectral Density (PSD) function [18]. Cyclic spectral analysis or cyclostationary processing are the tools for investigating and extracting of such cyclic features.

Cyclic peaks of non-linear quadratic (squared) transformed modulated signals form together the spectral density. The spectral density is explained and compared with Fourier analysis for a periodic signal in the next part of this section. The motivation of such kind of explanation is to mention the necessity of higher-order statistical analysis of a signal in order to get the inherent periodicity created by modulation, coding or training sequences of the signal.

A simple periodic signal with period $T_0$ and fundamental frequency, $w_0 = \frac{2\pi}{T_0}$ can be expressed as eq. ( 5-1 ),

$$x(t) = x(t + T_0) \qquad (5\text{-}1)$$

The Fourier series expansion of $x(t)$ is,

$$x(t) = \sum_{k=-\infty}^{\infty} a_k \, e^{jkw_0 t} \qquad (5\text{-}2)$$

Where, $a_k$ is the Fourier coefficient.

The Fourier series expansion extracts certain features, in this case the period of the periodic signal. This is illustrated in *Figure 5-1*, with a sine wave as the signal $x(t)$. In frequency domain, the spectral lines of *Figure 5-1* are related with the Fourier coefficient $a_k = \frac{1}{T_0} \int x(t) e^{-jkw_0 t} \, dt$.

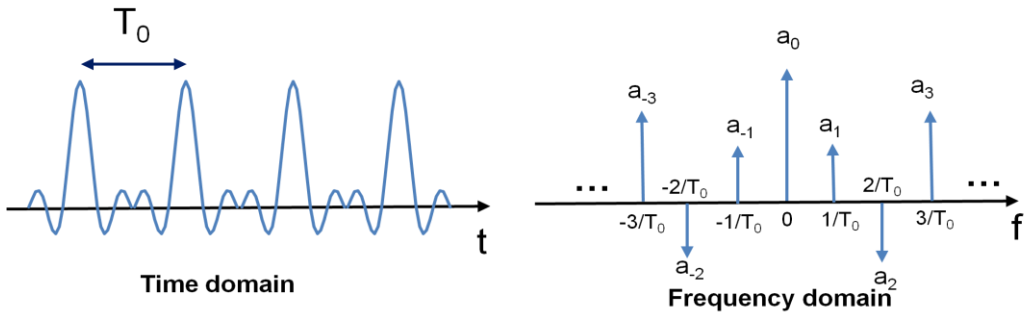


***Figure 5-1*** *Fourier expansion of periodic signal for feature extraction*

If we apply a quadratic transformation to our signal, we can extract its hidden periodicity due to the presence of modulation.

The simple quadratic transformation of an amplitude-modulated (AM) signal, $x(t) = a(t)\,cos(2\pi f_0 t)$ with $a(t)$ being a zero mean stationary random process and $f_0$ being the carrier frequency creates the signal $y(t)$ as in eq. ( 5-3 ),

$$y(t) = x(t)^2 = \frac{1}{2}[b(t) + b(t)\,cos(2\pi(2f_0)t)] \qquad (5\text{-}3)$$

Where, $b(t) = a(t)^2; b(t) = \{a^2(t)\} > 0$

The power spectral density function, $S_y(f)$ of $y(t)$ given in eq. ( 5-4 ) will exhibit spectral lines at cyclic frequencies 0, $\pm 2f_0$. This is shown in *Figure 5-2*.

$$S_y(f) = \frac{1}{4}[S_b(f) + \frac{1}{4}S_b(f \pm 2f_0)] \qquad (5\text{-}4)$$

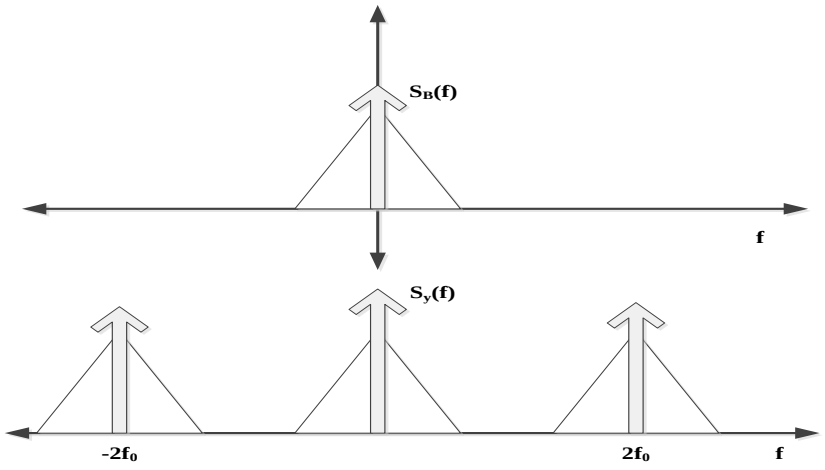


***Figure 5-2*** *Spectral line creation through non-linear transformation of signal* $x(t)$ *into* $y(t)$ *(reprodued from [15], [54])*

The spectral lines at the cyclic frequencies 0, $\pm 2f_0$ represent the cyclostationary characteristics of the modulated signal. The inherent (hidden) periodicity of the AM signal can be extracted through the quadric transformation and hence spectral lines are visible at cyclic frequencies.

## 5.2 Characterization of cyclostationary signals

General properties of cyclostationary processes are derived starting from the Fourier series expansion of the autocorrelation function, which is periodical. The Fourier coefficient of the Fourier expansion of the periodic autocorrelation function of a cyclostationary signal is called the Cyclic Autocorrelation Function (CAF). The Fourier transform of CAF is called the Spectral Correlation Density Function (SCF).

### 5.2.1 Cyclic Autocorrelation Function (CAF)

The CAF is a measure of the spectral correlation between time shifted versions of a cyclostationary process. The periodic autocorrelation function for a cyclostationary signal can be written as,

$$R_y(t,\tau) = E\left[(x(t)x^*(t-\tau)\right] \quad (5\text{-}5)$$

Here in eq. ( 5-5 **)**, E[.] stands for the statistical expectation operator and $\tau$ is a time delay.

If the autocorrelation function $R_y(t,\tau)$ is periodic, then the Fourier series decomposition can be performed and it yields:

$$R_y(t,\tau) = \sum_{\alpha} R_y^{\alpha}(\tau) e^{j2\pi\alpha t} \quad (5\text{-}6)$$

Where $\alpha$ is the cyclic frequency and it ranges over all integer multiples of the fundamental frequency $\frac{1}{T_0}$ . The Fourier coefficient $R_y^{\alpha}(\tau)$ is called CAF and it can be defined according to eq. ( 5-7 ),

$$R_y^{\alpha}(\tau) = \lim_{T\to\infty} \frac{1}{T} \int_{-\frac{T}{2}}^{\frac{T}{2}} R_y(t,\tau) e^{-j2\pi\alpha t} dt \quad (5\text{-}7)$$

Where , $T$ is an observation interval.

Autocorrelation function $R_y(t,\tau)$ of eq. ( 5-7 **)** can be replaced by symmetric delay conjugate product and expressed as in eq. ( 5-8 **)**,

$$R_y^{\alpha}(\tau) = \lim_{T\to\infty} \frac{1}{T} \int_{-\frac{T}{2}}^{\frac{T}{2}} x\left(t+\frac{\tau}{2}\right) x(t-\frac{\tau}{2})^* e^{-j2\pi\alpha t} dt \quad (5\text{-}8)$$

CAF may be viewed as the correlation in time domain between two frequency-shifted values of $x(t)$ separated in frequency by $\alpha$ as below in eq. ( 5-9 **)**.

$$R_y^{\alpha}(\tau) = \lim_{T\to\infty} \frac{1}{T} \int_{-\frac{T}{2}}^{\frac{T}{2}} u\left(t+\frac{\tau}{2}\right) v(t-\frac{\tau}{2})^{*}\, dt \qquad (5\text{-}9)$$

Where $u(t) = x(t)e^{-j\pi\alpha t}$ and $v(t) = x(t)e^{j\pi\alpha t}$ are two shifted version of $x(t)$.

### 5.2.2 Spectral Correlation Density Function (SCF)

The Spectral Correlation Density Function (SCF) is defined as the Fourier transform of cyclic autocorrelation function of $x(t)$. The SCF of a signal $x(t)$ is given by,

$$S_y^{\alpha}(f) = \int_{-\infty}^{\infty} R_y^{\alpha}(\tau) e^{-j2\pi f\tau}\, d\tau \qquad (5\text{-}10)$$

SCF with the spectral components of $x(t)$ at frequencies $\left(f+\frac{\alpha}{2}\right)$ and $\left(f-\frac{\alpha}{2}\right)$ over an observation interval of $T$ given below in eq. (5-11),

$$S_y^{\alpha}(f) = \lim_{\Delta t\to\infty} \lim_{T\to\infty} \frac{1}{\Delta t}\frac{1}{T} \int_{\Delta t/2}^{\Delta t/2} X_T(t, f+\frac{\alpha}{2}) X_T^{*}\left(t, f-\frac{\alpha}{2}\right) dt \qquad (5\text{-}11)$$

Above, the spectral component of $x(t)$ at frequency $f$ with period $T$ is:

$$X_T(t,f) = \int_{t-\frac{T}{2}}^{t+\frac{T}{2}} x(t) e^{-j2\pi f}\, dt \qquad (5\text{-}12)$$

The cyclic spectrum at a given cycle frequency represents the density of correlation between two spectral components of the process which are separated by an amount equal to the cycle frequency. The SCF is typically plotted on a bi-frequency plane as a function of spectral frequency $f$ and cyclic frequency $\alpha$. The range of values of $f$ (normally, $-\frac{f_s}{2}$ to $\frac{f_s}{2}$, where $f_s$ is the sampling frequency) and $\alpha$ (normally, $-f_s$ to $f_s$) for which $S_y^{\alpha}(f)$ exists is referred to as the region of support on bi-frequency plane [21]. *Figure 5-3* indicates a typical bi-frequency plane for the range of $f$ and α.

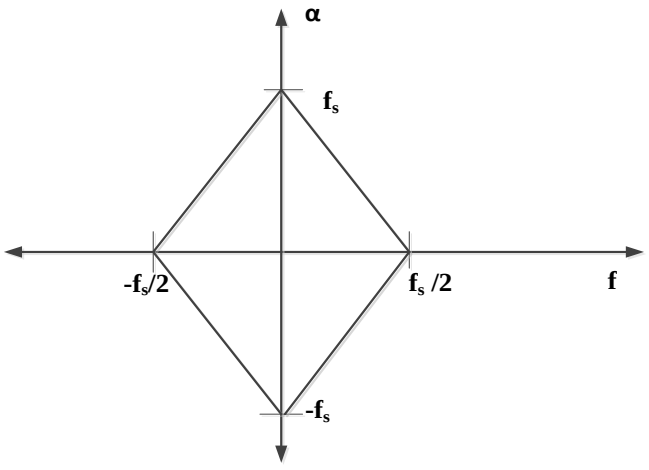


***Figure 5-3*** *Bi-frequency plane [21]*

For a purely stationary random process, CAF reduces to autocorrelation function $R_y(t)$ and SCF reduces to the PSD function $S_y(f)$ [120].This corresponds to $\alpha = 0$. Starting from eq. (5-10) and choosing $\alpha = 0$, we get,

$$S_y^{\alpha}(f) = \frac{1}{T_0}\int_{-\infty}^{\infty}\int_{-T_0/2}^{T_0/2} R_y(\tau)e^{-j2\pi f\tau}\,dtd\tau = \int_{-\infty}^{\infty} R_y(\tau)e^{-j2\pi f\tau}d\tau = S_y(f)$$

SCF of different modulated signals creates unique patterns which are modulation dependent. Thus, SCF can be used as a signal classifier based on signals' modulation scheme [139]. More details on applications of cyclostationary processing including signal detection and signal classification will be discussed in next sections of this chapter.

Time-smoothing and frequency-smoothing methods are mainly two basic approaches to determine the cyclic spectral estimate [139]. FFT Accumulation method (FAM) is a particular implementation of SCF. FAM is based on time smoothing in order to obtain the spectral correlation function more efficiently. In FAM, the frequency components of a cyclostationary signal are evaluated over a time window for a specific observation time, through short time Fourier transform procedures. Then, in each window, two frequency components are multiplied to get the autocorrelation product of sequences. The sequences are then further passed through a Fast Fourier Transform (FFT) operation to evaluate the SCF [139]. In a nutshell, the idea of FAM is to divide the bi-frequency plane into several parts, in order to get a discrete-channel-pair area. The generated areas are passed through an FFT operation to estimate cyclic spectral function. More details on FAM and different other methods of cyclic spectral estimation and implementation set for SCF based signal detection will be discussed in chapter 6.

## 5.3 Cyclostationary detector

As explained earlier in section 5.1, statistical characteristics of the manufactured wireless signals encountered in signal processors vary periodically with time and this time-varying characteristic is known as cyclostationarity. If the wireless signal which has periodicity property is modeled as a cyclostationary signal, then extraction of the cyclic feature is the key to enhance the functionalities of that signal processor through feature-based signal detection.

The cyclostationary feature analysis is a well-developed topic in the literature of signal processing, but it has been traditionally used in the context of wireless communications only (and not of wireless navigation). The cyclostationary theory was first introduced by Gardner in his paper series about the exploitation of the cyclostationary features in random processes [15], [16]. So, the exploration of signal detection through cyclostationary features in the context of wireless navigation opens a wide research scope. In this section, the main ideas behind the cyclostationary feature analysis are

presented and it is shown how the cyclic properties of a signal can be used as a spectrum sensing technique. To implement the cyclostationary detector, the main idea is to use the cyclostationarity features of the signals [19]. When the signal is present, this method gives the peak in cyclic spectral correlation value. If there is no such peak, the method implies that the given spectrum band is idle or there is no signal at given time and location.

Test statistics can be formed from the spectral correlation values. It is important to have a sufficient number of samples in order to get better estimation of spectral correlation value, which will lead better signal detection. The probability of detection and the probability of false alarm can be obtained by comparing the test statistics with a defined threshold similarly with the model described earlier in section 4.2. Cyclostationary detector can be implemented via FFT operations. An example of a digital implementation of cyclostationary detector is depicted in *Figure 5-4*.

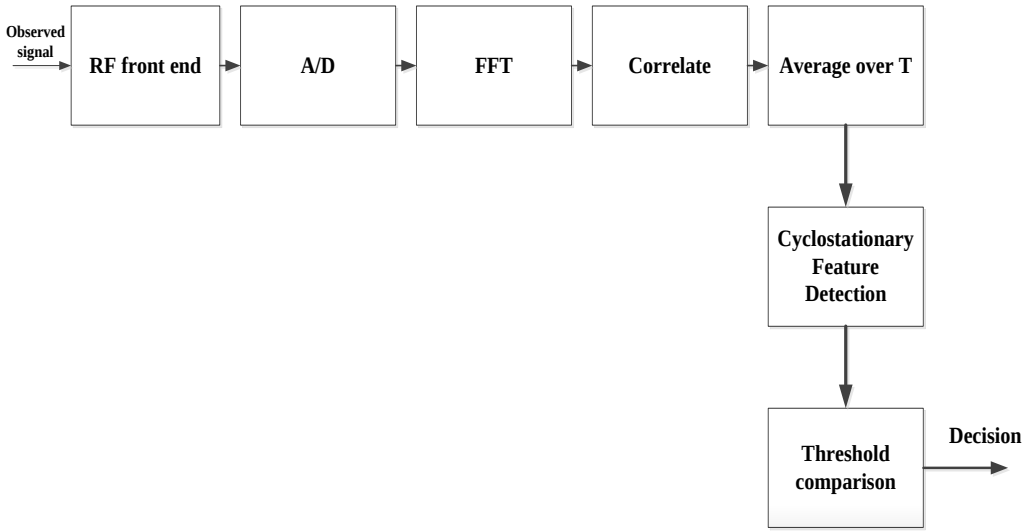


***Figure 5-4*** *Cyclostationary detector*

Cyclostationary processing is beneficial because of its insensitivity (or low sensitivity) to SNR and detection capability without demodulation of the received signal [127]. From the implementation point of view, cyclostationary detector is based on FFT and effect of SNR issues can be avoidable as the noise variance is not needed in cyclic spectral analysis. This confers a benefit over the energy-based detection. The tradeoff between performance and efficiency always arises for this kind of implementation of detection system. It has been suggested in the literature to have a longer length of observation in order to have better estimation for signal detection [127]. However, the performance of the detector degrades in the presence of timing and frequency jitters and RF nonlinearities [127].

## 5.4 Cyclostationary feature based signal classification

Recognition of the modulation format of a sensed signal in a spectrum aware receiver can be performed using cyclostationary features. This technique falls under the category of feature-based methods. Cyclic feature based approach for classification contains many advantages, including reduced sensitivity to noise and the ability to differentiate overlapping signals [115]. The key advantages of using cyclostationary feature is to having non zero correlation value between certain frequency components. Moreover, such cyclic feature gives specific information about modulation. As a result, cyclostationarity properties can be applied to design signal selective algorithms where detector can distinguish signals based on features observed. In turns, cyclic features can act as discriminator in the classification process [139]. In general, this classification process uses lager set of cyclostationary features of signal.

Cyclostationary feature detection on the receiver side is able to classify among BPSK, QPSK, FSK, and MSK modulation schemes [9], [10], [11] and [127]. The performance of signal classification mainly depends on the feature extraction stage which collects distinctive features from the incoming signal. The receiver extracts the detected received signals cyclostationary features and performs classification of the modulation schemes, for example through a pattern recognition method. In general, modulation recognition is a pattern recognition problem [9], [139]. Research was conducted for modulation recognition by using different pattern matching techniques, such as supported vector machine, hidden Markov models, neural network, for example, in [9], [10] and [139]. An example implementation set up for modulation classification by cyclostationary feature and neural network will be presented in this section.

*Figure 5-5* depicts modulation recognition through signal's cyclostationary features with artificial neural network. In this neural network-based pattern recognition, the neural network is trained on a pre-defined theoretical cyclostationary feature profile of signal of interest. Training sequences are used initially to get the networks familiarized with the patterns associated with different modulation schemes. Such trained network is used to classify the received signal based on the cyclostationary feature. In more details, the classifier system processes the received signal by using features extracted from the cyclic spectral analysis of the signal and uses them in a neural network to perform pattern matching. In turns, the classifier system can be divided into several parts, namely feature extraction, classifier design, classification decision, as shown in *Figure 5-5*.

More details on the spectral correlation pattern of different modulation schemes and cyclostationary classification can be found in [9], [11], [12] and [86].

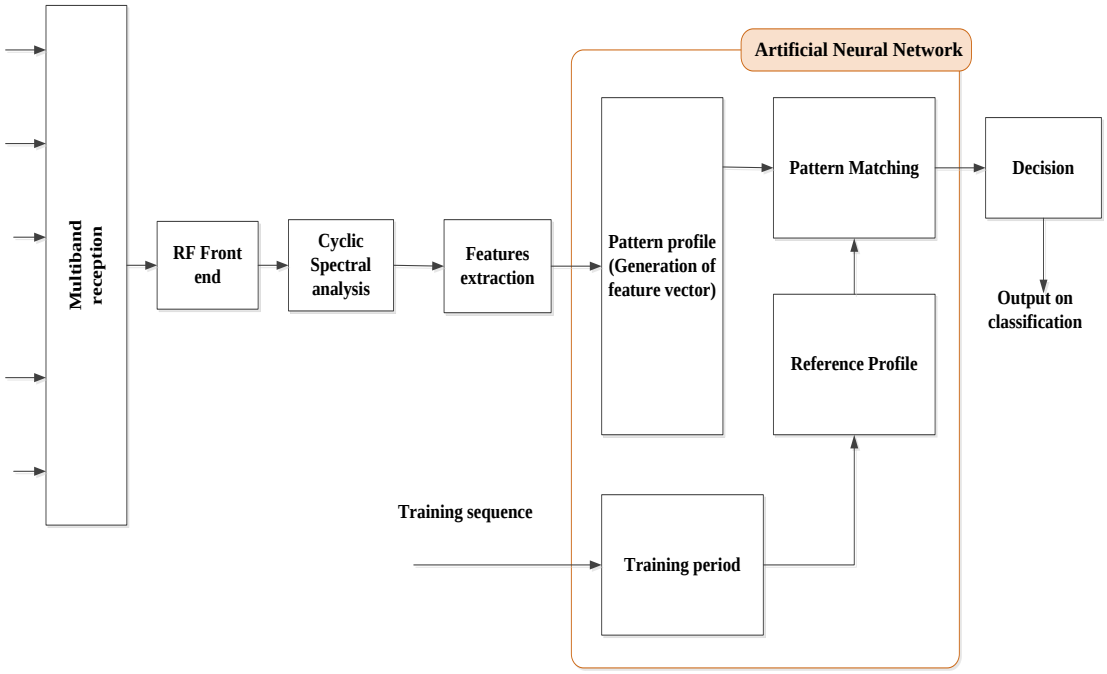


***Figure 5-5*** *Cyclostationary feature based modulation recognition [9]*

## 5.5 Application of cyclostationarity in SoO selection

As described earlier in section 5.1, cyclic spectral analysis can be performed to find different cyclostationary features, such as the location of the cyclic frequencies and the spectral correlation amplitude of the signals present in a mixture of signals plus noise. The peaks at cyclic frequencies help in determining whether the signal is present or not. This is due to the fact that the noise, being random in nature, does not exhibit peaks at non-zero cyclic frequencies. As a result, the signals of interest which are present in the considered frequency band can be separated from the noise. Spectral correlation means spectral redundancy and the exploitation of such signal redundancy will enhance the detection accuracy and reliability of information [15].

The spectral correlation characteristic of cyclostationary signals is a rich signal detection method. The detection process is done by searching the cyclic frequencies of different kinds of modulated signals. In addition, some parameter such as carrier frequency or chip rate can be also calculated according to the cyclic frequencies [54]. Moreover, different signals produce unique SCF patterns and these patterns can be used as a tool for signal classifier [10]. From the positioning point of view, the signal detection could be employed in a cognitive framework, in order to identify the available signals for positioning. Selection of signal with the best positioning accuracy can be also performed based on classification information obtained from cyclostationary features [7].

Let's illustrate the benefit of SCF analysis in the context of SoO detection. For this purpose, we start from eq. ( 5-13 ), which shows a signal present in additive noise,

$$z(t) = x(t) + n(t) \quad (5\text{-}13)$$

Where $x(t)$ and $n(t)$ represents the signal of interest or signal of opportunity and the additive noise, respectively. Cyclostationary processing is a linear operation, thus we can compute the SCF of $z(t)$ as,

$$S_z(f) = S_x(f) + S_n(f) \quad (5\text{-}14)$$

From the above eq. ( 5-14 ), if we focus at non-zero cyclic frequency ($\alpha \neq 0$), then the noise SCF will be zero: $S_n(f) = 0$ for $\alpha \neq 0$. Therefore, at non-zero cyclic frequency ($\alpha \neq 0$), the SCF of the observed signal becomes equal with the SCF of the transmitted signal without noise.

$$S_z(f) = S_x(f) \quad (5\text{-}15)$$

Thus, in theory, the SCF at non-zero cyclic frequencies may provide an excellent detection tool [120]. In consequence, cyclostationary processing may be beneficial because of its insensitivity to low signal to noise ratios (SNRs) and to its detection capability without requiring the demodulation of the received signal.

In summary, the inherent spectral redundancy (the cyclostationary processing) can be useful for various signal processing tasks such as:

- Detection of signal in the presence of noise and other modulated signal based on modulation used [19].
- Estimation of the TDOA, carrier phase, direction of arrival, cyclic frequency, classification of multiple received signals in noise according the modulation type [142].
- Selection of best signal for positioning estimation among the detected available signals [53].
- Reduction of co-channel interference and channel fading affects for single receiver system (channel impairment) [15].
- Prediction of random signal (future value of signal) [15].

# 6. SIMULATION MODEL

The cyclic spectral analysis refers to the process of detecting the presence of signal via the cyclic features. In this thesis, we work with the spectral correlation density function. The deterministic approach of SCF algorithm was implemented in MATLAB language. This chapter will discuss several methodologies for the implementation of SCF, with a particular attention to the implementation selected in this thesis, namely FFT Accumulation Method (FAM).Then, the implemented set-up is described, together with the meaning of the parameters used for simulation. Furthermore, the implementation of the cyclic spectral analysis test bench and simulation criteria will be presented in a detailed manner.

## 6.1 Methodology of cyclic spectral analysis

The theoretical methods behind cyclic spectral analysis can be basically divided into two types as time smoothing and frequency smoothing method [139].

In time smoothing method, the procedure to estimate the cyclic spectral density of the signal is simply by passing overlapping pieces of the signal through several FFT transforms [139]. A general process flow with the signal processing block diagram of time smoothing method is shown in *Figure 6-1*. According to the process flow, spectral components of signal are firstly extracted through a BPF which are then down-converted through multiplication of exponential components [13]. One down-converted spectral component is multiplied with the conjugate of another down-converted spectral component and the multiplication product is averaged over time to get the time smoothed SCF estimation [20].

One algorithm based on this time smoothed method is called time soothed FFT method, and it will be described in section 6.1.1 [143]. Further developments based on time smoothed FFT method are FFT Accumulation Method (FAM) and Strip Spectral Correlation Algorithm (SSCA) method and they will be described in Sections 6.1.2, 6.1.3 respectively.

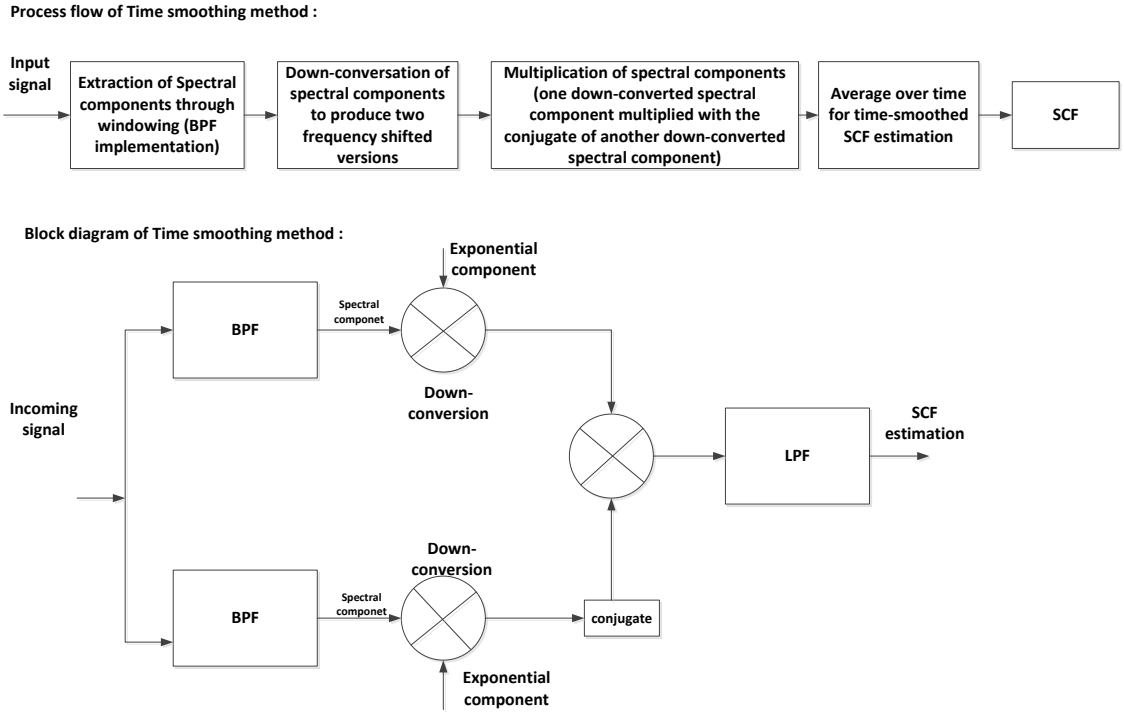


***Figure 6-1*** *Time smoothing method for cyclic spectral analysis [13], [143]*

On the other hand, frequency smoothing method is based on the frequency smoothed process. A block diagram of frequency smoothing method is shown in *Figure 6-2*. In frequency smoothed process, the bandpass filtered signal samples are first Fourier transformed and down-converted to baseband and averaging of frequency shifted components in done over frequency [139], [144]. The frequency smoothed estimation of SCF can be carried out by multiplication of down-converted spectral components with averaging over frequency [144]. However, this approach is not that much effective from computational point of view to use in general cyclic spectral analysis, as mentioned in several research articles, mainly in [139], [143] and [144].

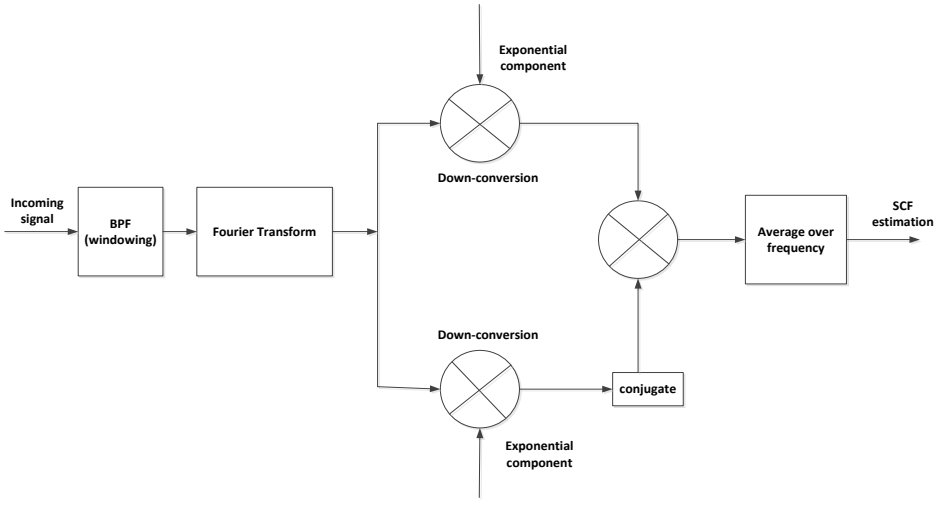


***Figure 6-2*** *Frequency smoothing method for cyclic spectral analysis*

This thesis focuses on the time smoothing method based implementation for a computationally efficient SCF estimation from the received signal. Time smoothing method is considered to be more computationally efficient for general cyclic spectral analysis as described in [139], [143] and [144]. The next sections describe briefly the existing time smoothed approach algorithms for SCF implementation.

### 6.1.1 Time smoothed FFT method

In time smoothing FFT method, spectral components of signal $x(t)$ are determined over a data tapering window of length $T$ with overlapping ($L$) sliding (short time) Fast Fourier Transform (FFT) over the entire observation time window $\Delta t$ of received signal. The practical approach for sliding the time window for determining frequency components of $x(t)$ is shown in *Figure 6-3.*

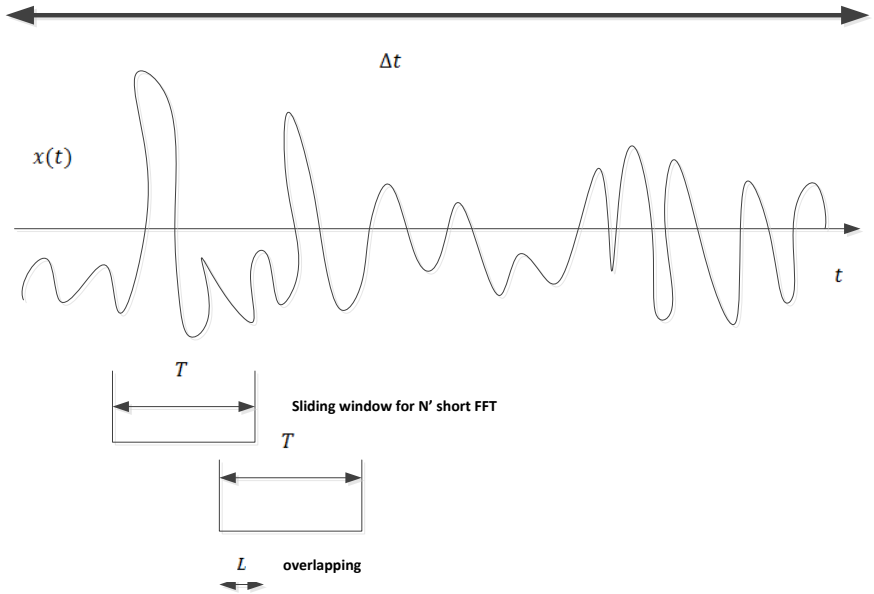


***Figure 6-3*** *Practical implementation of time smoothed FFT method*

The data tapering window is used to reduce the cyclic leakage [13]. The data tapering window is typically a rectangle function, $a(r)$. According to the theory in [13], there is a number of different windows that can be used instead of the rectangle function including, the Bartlett window (a triangle), the Hanning and the Hamming windows [145]. A data tapering window $a(r)$ with an observation length, $T$, slides over the data for $\Delta t$ time span with a size of $N'$sliding point FFT and it produce two spectral components in each FFT window. It is known that the frequency separation of certain spectral components which are correlated is called cyclic frequency. The cyclic frequency $\alpha$ expressed as $\alpha = f_1 - f_2$, where $f_1$ and $f_2$ are the spectral frequencies of spectral components of $x(t)$. The spectral components are then down-converted to frequency shifted versions (one shifted with $+\frac{\alpha}{2}$ and the other one with $-\frac{\alpha}{2}$).

The time smoothed FFT method implementation is illustrated in the block diagram of *Figure 6-4*. According to the *Figure 6-4*, once two frequency shifted (down-converted) versions are determined, the conjugate of one frequency shifted version is multiplied with another frequency shifted version over the observation time $\Delta t$. After that, the multiplication product is passed through an LPF (average over time: time smoothing) to form SCF, $S_x^{\alpha}(f)$, as shown in *Figure 6-4*.

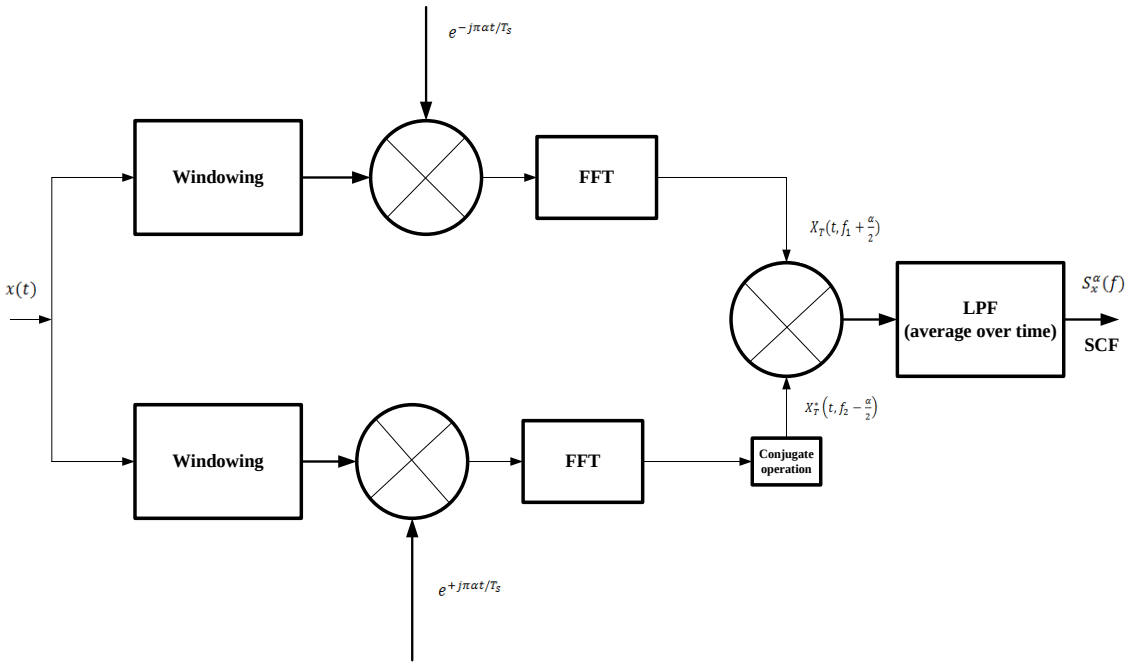


***Figure 6-4*** *Time smoothed FFT method [143], [7]*

If $\Delta f$ is the frequency resolution of SCF, then it relates with observation time as, $\Delta f = \frac{1}{T} = \frac{1}{\Delta t}$. The cyclic frequency resolution is $\Delta\alpha$ and this related with temporal resolution or observation time $\Delta t$ by $\Delta\alpha = \frac{1}{\Delta t}$. Substantial amount of smoothing is needed to be carried out in order to get a reliable SCF estimate [146]. If $N'$ is the length of short time FFT, $N$ is the length of the sequence or size of the data vector processed by FAM, $f_s$ is the sampling frequency, then $N > N'$ and $N' = \frac{f_s}{\Delta f}$. For a reliable SCF estimate,

$$\Delta t.\Delta f = \frac{N}{N'} \gg 1 \qquad (6\text{-}1)$$

The above eq. ( 6-1 ) criteria can achieved by $\Delta t \gg T$. In summary, for a reliable better smoothed SCF estimate the below expressed criteria need to be fulfilled.

$$\Delta\alpha << \Delta f$$
$$\frac{1}{\Delta\alpha} \cong \Delta t \gg T \cong \frac{1}{\Delta f}$$
$$\Delta f = \frac{1}{T} = \frac{1}{N' T_s} = \frac{1}{\Delta t}$$

The obtained spectral component, $X_T(t,f)$ of signals $x(t)$ and estimated SCF, $S_x^\alpha(f)$ can be written as in eq. ( 6-2 ) and eq. ( 6-3 ) respectively,

$$X_T(t,f) = \sum_{-N'/2}^{N'/2} a(r)x(t-r)e^{-j2\pi f(t-r)T_s} \quad (6\text{-}2)$$

$$S_x^\alpha(f) = \frac{1}{T}\langle X_T(t, f_1 + \frac{\alpha}{2}) X_T^*\left(t, f_2 - \frac{\alpha}{2}\right)\rangle \quad (6\text{-}3)$$

Where, $T_s$ is the sample duration, $f_s$ is the sampling frequency, $f$ is the spectral frequency, $\alpha$ is the cyclic frequency, $X_T^*$ is the complex conjugate of $X_T$ .

### 6.1.2 FFT Accumulation Method (FAM)

FAM is a particular algorithm based on time smoothing function in order to obtain spectral correlation function more efficiently through reducing the number of computation with a modification from time smoothed FFT method [13], [139] and [143]. The idea is to divide the bi-frequency plane into smaller areas and compute the cyclic estimate a block at a time using the efficient FFT [139]. The main signals sequence goes through short-time FFT and the spectral components are then evaluated. After that, frequency components are down-converted to baseband through multiplication with complex exponential [13]. One down-converted spectral component is multiplied with the conjugate of another down-converted spectral component. Finally, a second FFT is performed on the multiplication product sequence of down-converted spectral components to get SCF estimate [87], [143]. This second FFT is a unique feature of FAM in comparison with previously explained time smoothed FFT method.

The conceptual implementation block diagram considering above discussion on FAM is presented by *Figure 6-5*. *Figure 6-5* describes the processes involved in FAM with two step of FFT operation. The description of FAM in this section was intended to provide a brief overview of how the SCF estimate is generated through signal processing steps involved with FAM.

In FAM, smoothing is carried out to reduce the variance of the resulted estimate. Decimation and data tapering windowing are also taken into consideration for higher computational efficiency (reduced processing time) and they reduce cyclic and spectral leakage respectively. Decimation performs short time FFT on every $L$ sample of signals instead of every sample, where $L$ is an overlap parameter. If $N'$ is the length of short time FFT, we can choose $L \leq \frac{N'}{4}$ for better performance [143].

As a summary of *Figure 6-5* for FAM method, the frequency transform versions of signal are estimated by sliding $N'$ point FFT. Decimation (overlapping) took place by hopping over the data in block of $L$ samples while doing short FFT. The product sequences of frequency shifted or down-converted versions are time smoothed by another

$P$ point FFT to get the final version of SCF estimate, $S_x^{\alpha}(f)$ [6]. A better estimation of $N'$ and $P$ can be expressed below by eq. ( 6-4 **)** and eq. ( 6-5 ) [86].

$$N' = 2^{\left[\log_2(\frac{f_s}{\Delta f})\right]} \quad (6\text{-}4)$$

$$P = 2^{\left[\log_2(\frac{f_s}{L\Delta\alpha})\right]} \quad (6\text{-}5)$$

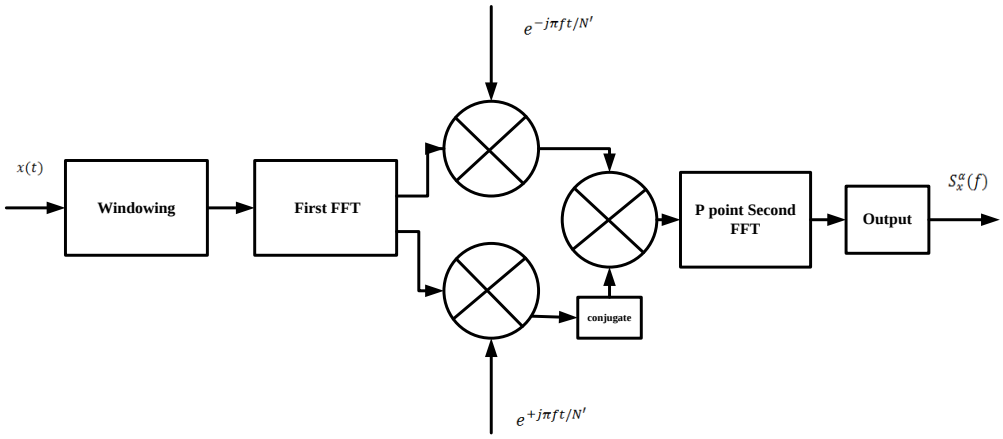


***Figure 6-5*** *FAM procedure [143]*

Finally, the design parameters for the cyclic spectral estimation are presented in a collective manner in *Table 6-1* from time smoothing method point of view, which is used in this thesis for simulation modeling. The specific value of these parameters used in the simulation will be presented in chapter 7.

**Table 6-1** *Time smoothed method design parameters*

| Name | Notation | Important criteria: at a glance |
|---|---|---|
| Time span or observation time | $\Delta t$ | $T = N' T_s$ <br> $T_s = \frac{1}{f_s}$ <br> $f = (\frac{f_1 - f_2}{2})$ <br> $\alpha = f_1 - f_2$ <br> $\Delta f = \frac{1}{T} = \frac{1}{N' T_s} = \frac{1}{\Delta t}$ <br> $\Delta t . \Delta f = \frac{N}{N'} \gg 1$ <br> $\frac{1}{\Delta\alpha} \cong \Delta t \gg T \cong \frac{1}{\Delta f}$ <br> $L \leq \frac{N'}{4}$ <br> $N = PL$ |
| Tapering window $a(r)$ length | $T$ | |
| Size of the sliding point FFT | $N'$ | |
| Sample duration | $T_s$ | |
| Sampling frequency | $f_s$ | |
| Spectral frequency | $f$ | |
| Cyclic frequency | $\alpha$ | |
| Frequency resolution of SCF | $\Delta f$ | |
| Cyclic frequency resolution | $\Delta\alpha$ | |
| Length of the sequence or size of the data vector | $N$ | |
| Decimation overlap parameter | $L$ | |
| Size of second FFT point | $P$ | |

In this thesis, FAM is adopted for implementation to get results on cyclostationary properties of OFDM and CDMA signal. FAM is much faster process than other methods as explained in [139], [143]. However, other methods should give similar kind of result and the reader can find further information in [120], [124]. A detailed implementation model of MATLAB based simulation test bench of the FAM algorithm will be presented in section 6.2.

### 6.1.3 Strip Spectral Correlation Algorithm (SSCA)

In SSCA method, the spectral component of signal $X_T(t,f)$ is described by eq. ( 6-2 **)**. $X_T(t,f)$ is directly multiplied with the conjugate of signal itself $x(t)^*$ and after that N-point FFT performed to explore the SCF, $S_x^\alpha(f)$ [21]. The SSCA method block diagram can be presented by *Figure 6-6.*

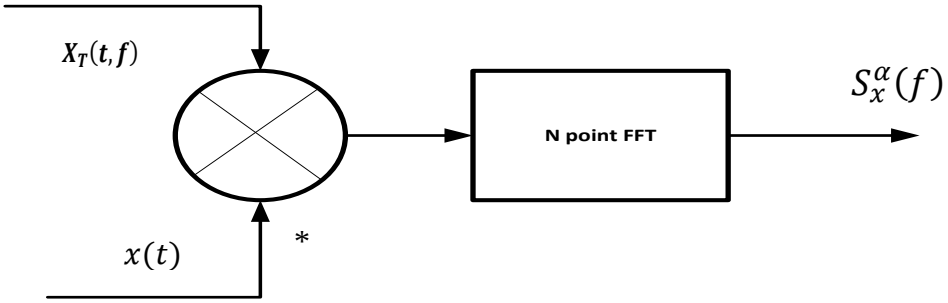


***Figure 6-6*** *SSCA block diagram [21], [120]*

## 6.2 Implementation model

CDMA or OFDM modulated test signals were passed through an AWGN channel and then time smoothing is performed based on FAM simulation model for the estimation of SCF. Test statistics of generated SCF are taken according to the SNR at specific cyclic frequency position of interest and then we apply binary hypothesis testing. The details of implemented model along with some of the selected parameters for the system signal generation is discussed in next section.

### 6.2.1 Simulation test bench chain

A block diagram of implemented MATLAB model through FAM based simulation is presented with process flow in *Figure 6-7.*

Firstly, BPSK modulated CDMA baseband signal or 16-QAM modulated OFDM baseband signal passed through AWGN channel. Then, FAM is used to evaluate signal's cyclostationary components, namely SCF test statistics under $H_1$ hypothesis. On the other hand, AWGN noise separately passed through FAM to produce SCF test sta-

tistics under $H_0$ hypothesis. In turn, this two SCF test statistics used in the binary hypothesis detection model described in section 4.2 to determine whether signal is present or absent in noise (decision). The decision is obtained from PDF under $H_1$ versus PDF under $H_0$. In our simulations, the PDF curves were obtained based on simulated data with high number of random realizations.

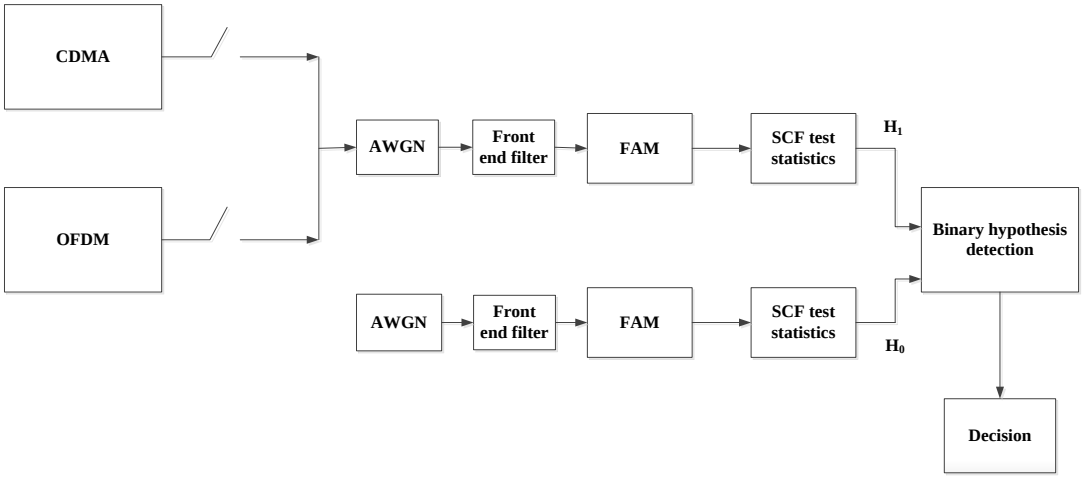


***Figure 6-7*** *Simulation test bench*

### 6.2.2 Simulation criteria and strategy

The simulation steps are described below:

- SCF test statistics are created for a predefined set of SNR values. For each SNR value, the simulations are repeated for 1000 random realizations, in order to get the test statistics.
- The test statistics of SCF are created at zero cyclic frequency position, single cyclic frequency position and multiple cyclic frequencies position while iterating for each SNR. As a result, the performance comparison of cyclic detector based on single (one) and multiple cyclic frequencies can be possible.
- In general, the maximum value of SCF over multiple number of cyclic frequencies position of interest are taken as test statistics.
- The obtained SCF statistics (for signal+noise and noise) act as input for binary hypothesis performance detector model described in section 4.2. The test statistics are compared with the threshold generated from a fixed probability of false alarm rate, and then the probability of detection is computed.
- The receiver front end filter designed and use to observe the effect on performance of detection.
- CDMA and OFDM modulated joint signal cyclic spectral analysis case is also observed, however this case will not be analysed in detail.

Results on performance detection obtained from the implemented set up will be presented in chapter 7.

# 7. SIMULATION RESULTS

This chapter presents the simulation results obtained from the simulation model described in chapter 6. This chapter focuses on the performance analysis of cyclostationarity-based detection for CDMA and OFDM signals, respectively. It also discusses the effect of parameter variation on the performance.

## 7.1 Simulation parameters

The simulated results are presented in such a way to highlight the cyclostationary properties of the modulated signal. We include the representation of different kind of statistical information, such as the Probability Distribution Function (PDF), the Cumulative Distribution Function (CDF), the cyclic spectral estimate figure from FAM simulation and the binary hypothesis detection performance curve of cyclostationary detection with a view of Receiver Operating Characteristics (ROC). MATLAB simulations were carried out to achieve the following results for each of signals cyclic analysis:

- Probability of detection ($P_d$) versus probability of false alarm ($P_{fa}$) at different Signal to Noise Ratio (SNR) for one specific cyclic frequency detection.
- Probability of detection ($P_d$) versus probability of false alarm ($P_{fa}$) at different cyclic frequencies for one fixed SNR.
- Probability of detection ($P_d$) versus SNR at fixed false alarm probability ($P_{fa}$) for different cyclic frequencies used in detection.
- Probability of detection ($P_d$) versus SNR at fixed false alarm probability ($P_{fa}$) for different SCF test statistics at one specific cyclic frequency.
- Receiver front-end filter effect on the detection performance is compared with unfiltered detection for both of the CDMA and OFDM signal in terms of ROC curve.

The SCF energy value based test statistics created for zero ($\alpha_0: \alpha = 0$) cyclic frequency, single ($\alpha_1: \alpha = 1$) cyclic frequency, non-cyclic frequency ($\alpha_{NC}$) and multiple cyclic frequencies ( $\alpha_{1:MC}$) of detection. In case of multiple cyclic frequencies detection ( $\alpha_{1:MC}$), we generally took the maximum value of SCF among the first $MC$ numbers of cyclic frequencies, unless otherwise specified. For CDMA, $MC$ is taken as $MC = \{2,4,6\}$ and for OFDM, $MC = \{3,5,10\}$.The variation on the energy data from SCF through taking mean, median and minimum among the SCF values of corresponding first $MC$ cyclic frequencies was considered for comparison purpose. The cyclostationary detection performance is also compared with the performance of the energy detector and

of the Higher Order Moment (HOM) detector in this binary hypothesis detection from AWGN noise. As the cyclic frequencies are affected by the simulation parameters, a list of important parameters with value for simulation system model is shown in *Table 7-1*.

***Table 7-1*** *List of simulation system parameters*

| **Simulation system parameter** | **value** |
|---|---|
| Number of random realizations | 1000 |
| SNR set | -20 dB to 5 db |
| Total processing time | 1 ms |
| Window type | Hamming |
| Generated noise type | AWGN |
| Sampling frequency, $f_s$ | 9.6 MHz |
| Frequency resolution, $\Delta f$ | 0.1 * $f_s$= 960 KHz |
| Cyclic frequency resolution, $\Delta\alpha$ | 0.00005 *$f_s$=480 Hz |
| Size of the sliding point FFT, $N'$ | 16 |
| Decimation overlap parameter, $L$ | 4 |
| Size of second FFT point, $P$ | 8192 |
| Size of the data vector, $N$ | 32768 |
| Bandwidth (BW) | 4 MHz |

## 7.2 Simulation results based on CDMA signals

This section presents the simulation results of CDMA signals with brief description on the obtained figures. In order to generate CDMA signal in MATLAB, some important simulation-specific parameters are shown in *Table 7-2*.

***Table 7-2*** *CDMA signal specific parameters selection*

| **CDMA parameters** | **value** |
|---|---|
| Modulation type | BPSK |
| Spreading factor, $S_F$ | 101 |
| Number of code epochs generated | 41 |
| Samples per code | 948 |
| Chip rate, $f_c$ | 1.023 MHz |
| Chip interval, $T_c$ | 9.7752 $e^{-07}$s |
| Sampling frequency, $f_s$ | 9.6 MHz |
| Sampling interval, $T_s$ | 1.0417 $e^{-07}$s |
| Doppler frequency shift | 0 Hz |
| Bit energy | 1 |
| Oversampling factor | 9.4 |

We have chosen BPSK modulation for CDMA signal generation, as BPSK is the widely used modulation techniques in most of the navigation applications for signal generation. Chip rate for CDMA signal is selected according to GPS signal and that is 1.023 MHz. Moreover, 1.023 MHz chip rate is chosen in GPS at the recommendation of J. Spilker in [147], [148] in order to avoid correlation problem associated with Doppler shifts. It is assumed that, the spreading factor long code is repeated from one code epoch to another, meaning that we use short codes in the simulations.
The simulation results described in next sections are divided into three categories, namely: CDMA test statistics, SCF figures and cyclostationary detection performance.

### 7.2.1 Statistical presentation of CDMA test statistics

Statistical presentation section includes the figures of the binary test statistics, and the PDF and CDF obtained from hypothesis detection model.

#### 7.2.1.1 Test statistics

*Figure 7-1* and *Figure 7-2* depict some examples of the CDMA test statistics for binary hypothesis detector model at $SNR = -12\ dB$ for zero cyclic frequency ($\alpha_0$) and for 2 cyclic frequencies ($\alpha_{1:2}$) respectively. For 2 cyclic frequencies ($MC = 2;\ \alpha_{1:2}$), the maximum SCF value over first 2 non-zero cyclic frequencies $\alpha_1$ and $\alpha_2$ ($\alpha = 2$) is considered. Test statistics are used to obtain PDF under each hypothesis. From these two figures, it is noticed that, the separation between $H_1$ hypothesis and $H_0$ hypothesis test statistics is reduced in ($\alpha_{1:2}$) when compared to $\alpha_0$.

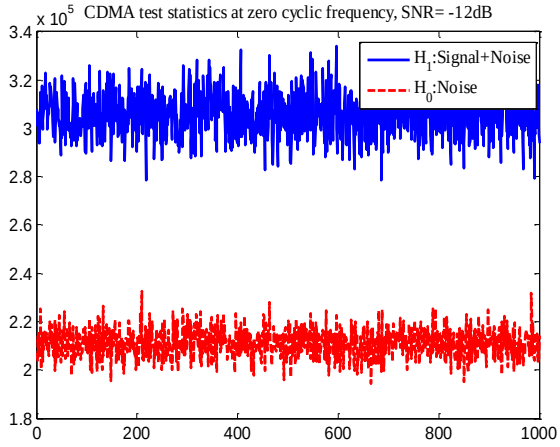


***Figure 7-1*** *CDMA statistics at zero cyclic frequency, $\alpha_0$*

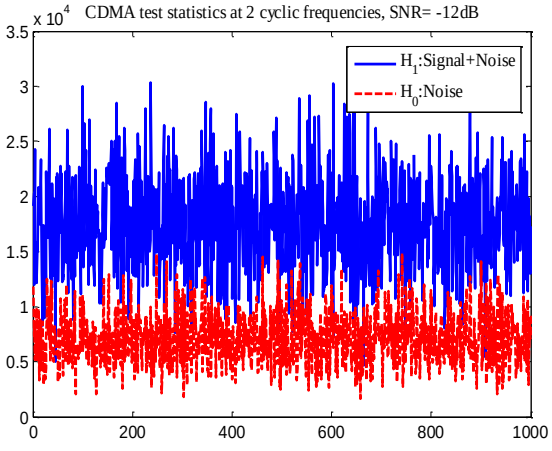


***Figure 7-2*** *CDMA statistics for maximum SCF over 2 non- zero cyclic frequencies, $\alpha_{1:2}$*

#### 7.2.1.2 Probability Distribution Function

*Figure 7-3* and *Figure 7-4* present some examples of the PDF distributions under $H_0$ and $H_1$ hypotheses, at fixed $SNR = -20\ dB$, for zero cyclic frequency ($\alpha_0$) and for 2

cyclic frequencies ($\alpha_{1:2}$) respectively. In case of $\alpha_{1:2}$, the maximum SCF value over first 2 non-zero cyclic frequencies ($\alpha_1, \alpha_2$) is considered. PDF distributions under $H_0$ and $H_1$ hypotheses at $\alpha_{1:2}$ exhibit more overlapping phenomenon than PDF distributions at $\alpha_0$, as shown in *Figure 7-3* and *Figure 7-4*.

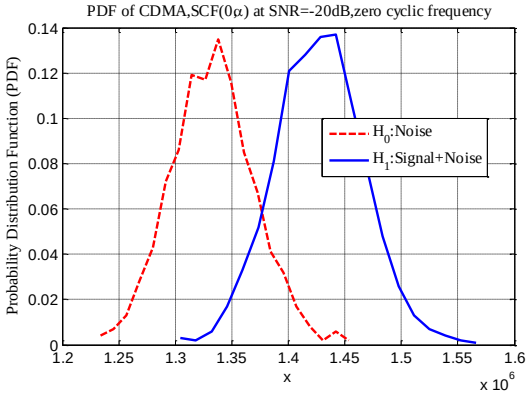


***Figure 7-3*** *CDMA test statistics PDF at zero cyclic frequency, $\alpha_0$ , SNR=-20 dB*

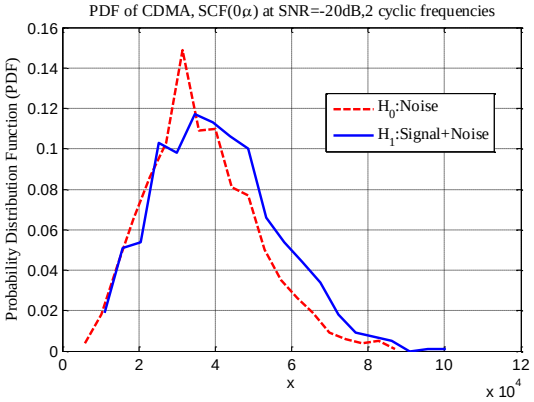


***Figure 7-4*** *CDMA test statistics PDF of maximum SCF over 2 non-zero cyclic frequencies, $\alpha_{1:2}$ , SNR=-20 dB*

### 7.2.1.3 Cumulative Distribution Function

*Figure 7-5* and *Figure 7-6* show an example CDF of CDMA detection at zero cyclic frequency ($\alpha_0$) and at 2 cyclic frequencies ($\alpha_{1:2}$), respectively at $SNR = -20\,dB$. For 2 cyclic frequencies ($MC = 2;\ \alpha_{1:2}$), the maximum SCF value over first 2 non-zero cyclic frequencies ($\alpha_1, \alpha_2$) is considered. According to these two figures, $H_1$ hypothesis CDF curve is following $H_0$ hypothesis CDF and this will give $P_d$ as, $P_d = 1 - CDF(H_1)$ and $P_{fa}$ as, $P_{fa} = 1 - CDF(H_0)$. As a result, $P_d$ can be higher than $P_{fa}$.

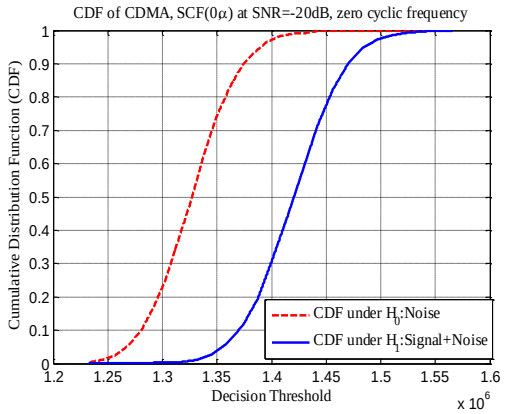


***Figure 7-5*** *CDMA CDF at zero cyclic frequency, $\alpha_0$, SNR=-20 dB*

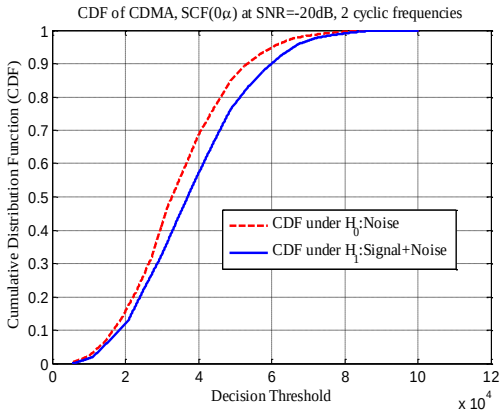


***Figure 7-6*** *CDMA CDF of maximum SCF over 2 non-zero cyclic frequencies, $\alpha_{1:2}$, SNR=-20 dB*

### 7.2.2 Spectral correlation density function plot

*Figure 7-7* provides an example of a SCF plot obtained from the cyclic spectral analysis of CDMA signal. The magnitude of the SCF is normalized for plotting purpose by the maximum value of the SCF and thus it ranges from 0 to 1. A SCF peak can be observed at several simulated CDMA cyclic frequencies. In addition, *Figure 7-7* also provides a comparison on simulated and theoretical SCF formation at cyclic frequencies. Simulated cyclic frequency positions gives more SCF peaks than theoretical cyclic frequency positions. However, theoretical CDMA cyclic frequencies can be used as a reference for better understanding of the simulated SCF pattern.

Theoretical CDMA cyclic frequencies set can be expressed as [124],

$$A = \{\alpha_0, \alpha_1, \alpha_2, \ldots., \alpha_m\}, m \in Z$$

Where, each cyclic frequency $\alpha_m$ is dependent on both the chip rate $f_c$ and the spreading factor $S_F$, given by,

$$\alpha_m \in \left\{ f_c * k, \frac{f_c}{S_F} * k \right\} \; where \; , k \in Z$$

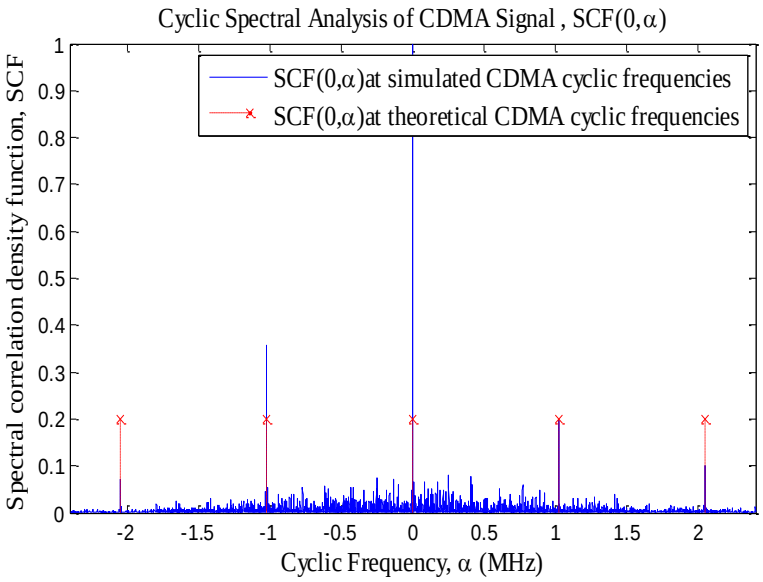


***Figure 7-7*** *Comparison of simulated and theoretical SCF of CDMA signal*

### 7.2.3 Cyclostationarity detection performance for CDMA signals

#### 7.2.3.1 $P_d$ versus $P_{fa}$ plots

*Figure 7-8* illustrates the probability of detection ($P_d$) versus the probability of false alarm ($P_{fa}$) at different SNR values and at two cyclic frequencies ($\alpha_{1:2}$). The maximum SCF value over first 2 non-zero cyclic frequencies ($\alpha_1$, $\alpha_2$) is considered for test statistics creation. The probability of detection increases as the probability of false alarm increases as expected.

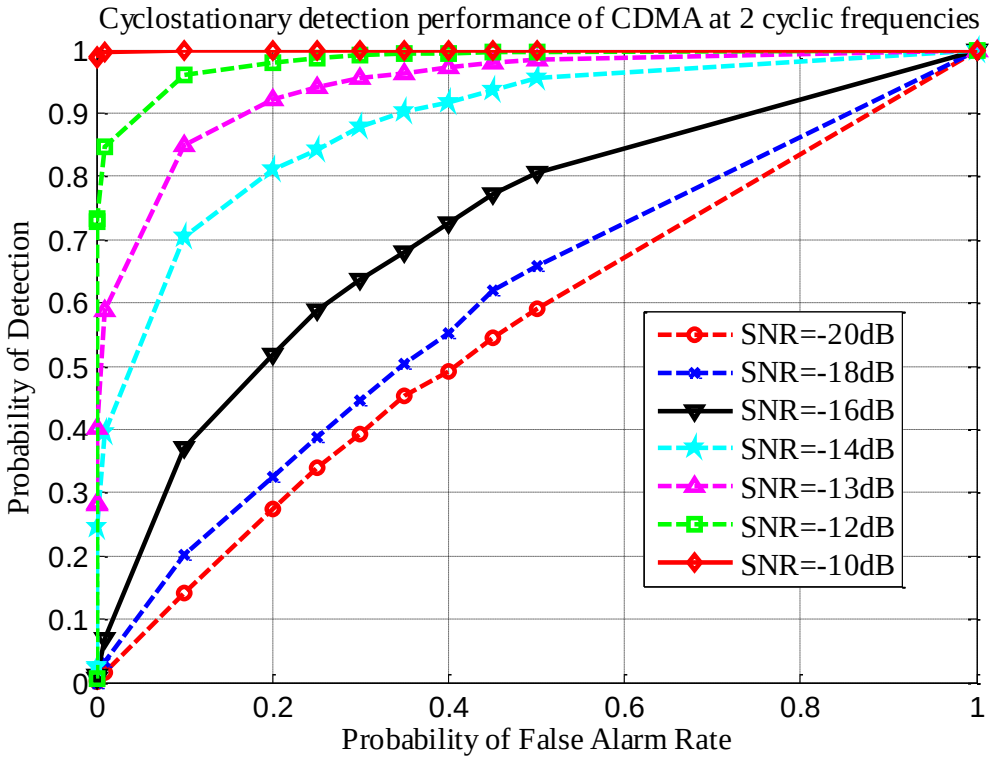


***Figure 7-8*** *$P_d$ versus $P_{fa}$ at different SNRs for CDMA signal*

*Figure 7-9* shows the $P_d$ versus $P_{fa}$ at different cyclic frequencies of detection, such as zero ($\alpha_0$) cyclic frequency, single ($\alpha_1$) cyclic frequency, 2 cyclic frequencies ($\alpha_{1:2}$), 4 cyclic frequencies ($\alpha_{1:4}$) and 6 cyclic frequencies ($\alpha_{1:6}$) at $SNR = -12\,dB$. In turns, multiple cyclic frequency detectors are compared with zero and single cyclic frequency detector. The SCF values at $\alpha = 0$ and $\alpha = 1$ are taken for $\alpha_0$ and $\alpha_1$ detection. On the other hand, as described earlier, $MC$ is taken as $MC = \{2,4,6\}$ for CDMA multiple cyclic frequencies detection. In this Figure 7-9, the maximum SCF values are computed over the 2, 4, 6 CDMA cyclic frequencies. In turns, we combine multiple cyclic frequencies by taking the maximum over first 2, 4, 6 cyclic frequencies.

For instance, when using 2 cyclic frequencies, the maximum value of SCF is taken between the first 2 SCFs at the first 2 cyclic frequency positions ($\alpha = 1, \alpha = 2$). For example, in the CDMA signal used in here, the first 2 cyclic frequencies appear at 1.023 MHz and 2.05 MHz respectively. When 2 cyclic frequencies are combined for the test statistic, we formed the test statistic as max (SCF_1_CDMA, SCF_2_CDMA), where SCF_1_CDMA and SCF_2_CDMA are the SCF values at the cyclic frequencies 1.023 MHz and 2.05 MHz.

From the results in *Figure 7-9*, it can be seen that the detection performance vary with the selection of the cyclic frequencies in which the cyclostationary detection is carried out.

The zero cyclic frequency position holds the highest-valued SCF amplitude among the other higher cyclic frequencies. Thus, a better performance is observed at zero cyclic frequency. It is common that the modulation scheme used in the signal generation

plays an important role in creation of the SCF at specific cyclic frequencies. It usually happens that, SCF has a higher energy at initial cyclic frequency positions than at a higher order cyclic frequency positions. In fact, this situation does not happen always, stronger SCF values can be observed at higher OFDM cyclic frequencies too, as shown for OFDM case in section 7.3.3.1.

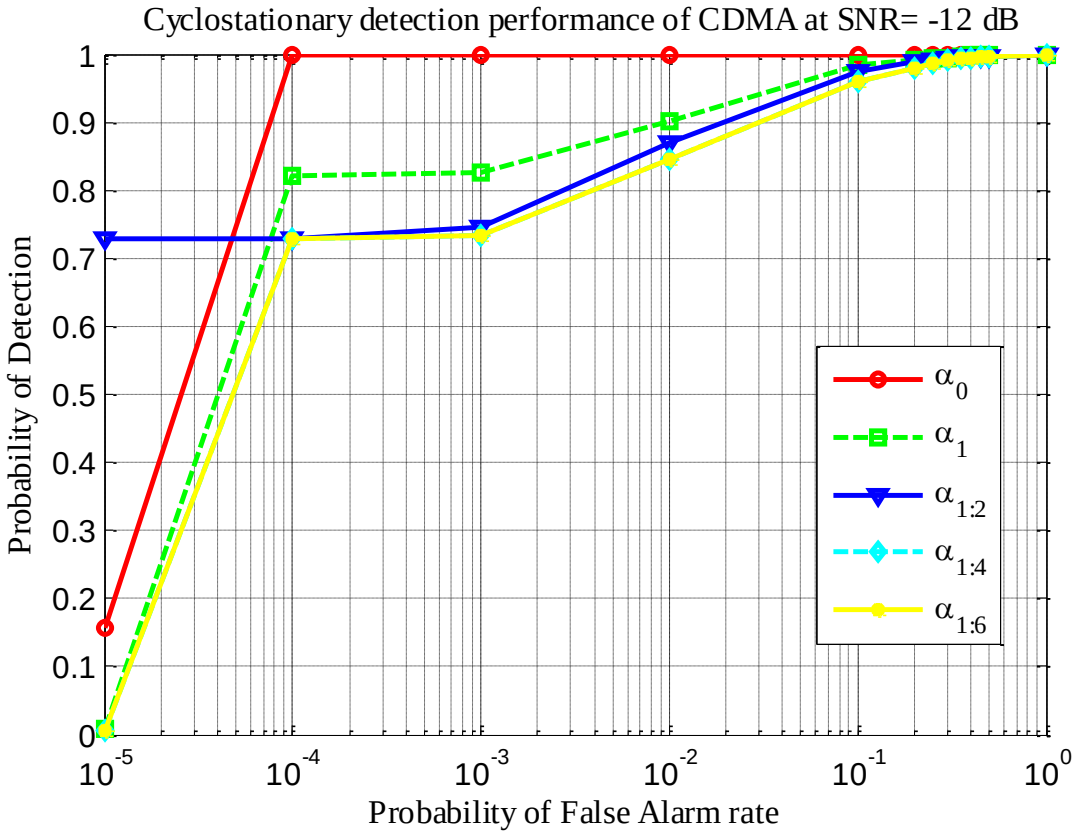


***Figure 7-9*** *$P_d$ versus $P_{fa}$ at different cyclic frequencies of CDMA signal*

### 7.2.3.2 $P_d$ versus SNR plots

*Figure 7-10* compares the cyclostationary detection performance with the performance of the energy detector and of the HOM detector. Cyclostationary detection conducted at zero cyclic frequency ($\alpha_0$), two cyclic frequencies($\alpha_{1:2}$), non-cyclic frequency ($\alpha_{NC}$) and single cyclic frequency ($\alpha_1$) are compared with the above-mentioned (in chapter 4) classical detectors (energy and higher order moment).

For instance, non-cyclic frequency $\alpha_{NC}$ was derived as the mean of $\alpha_1$ and $\alpha_2$, which is expressed as below,

$$\alpha_{NC} = \frac{\alpha_{2+}\alpha_1}{2}$$

Regarding the non-cyclic frequency considered, this is taken from the middle point, between the first 2 consecutive cyclic frequencies, $\alpha_1$ and $\alpha_2$, after $\alpha_0$. For CDMA its value is 511.5 KHz.

$P_d$ versus SNR is plotted in *Figure 7-10* at mentioned different cyclic frequencies of CDMA signal and at a fixed false alarm value of 0.01. Single cyclic frequency detection outperforms the 2 cyclic frequencies detection as the first cyclic frequency position SCF holds much higher amplitude than the second cyclic frequency SCF. The SCF values are basically determined by the signal parameter such as the chip rate, modulation order, symbol rate etc. The detection performance at zero cyclic frequency is showing better result than the detection at other multiple cyclic frequencies. The detection performance at non-cyclic frequency is showing the worst result among all detection which is obvious, but it is nevertheless surprising that even at a non-cyclic frequency there is some information pertaining to the signal presence. This points out towards the fact that there is indeed a certain spectral leakage, no doubt due to a finite block length processing and noise presence. A more thorough explanation of the fact with the energy detector and zero-order cyclic frequency detectors outperform the other cyclostationarity detectors is given in section 7.5, by introducing the notions of the deflection coefficient and its relationship with the noise variance and the noise creation for binary hypothesis detection.

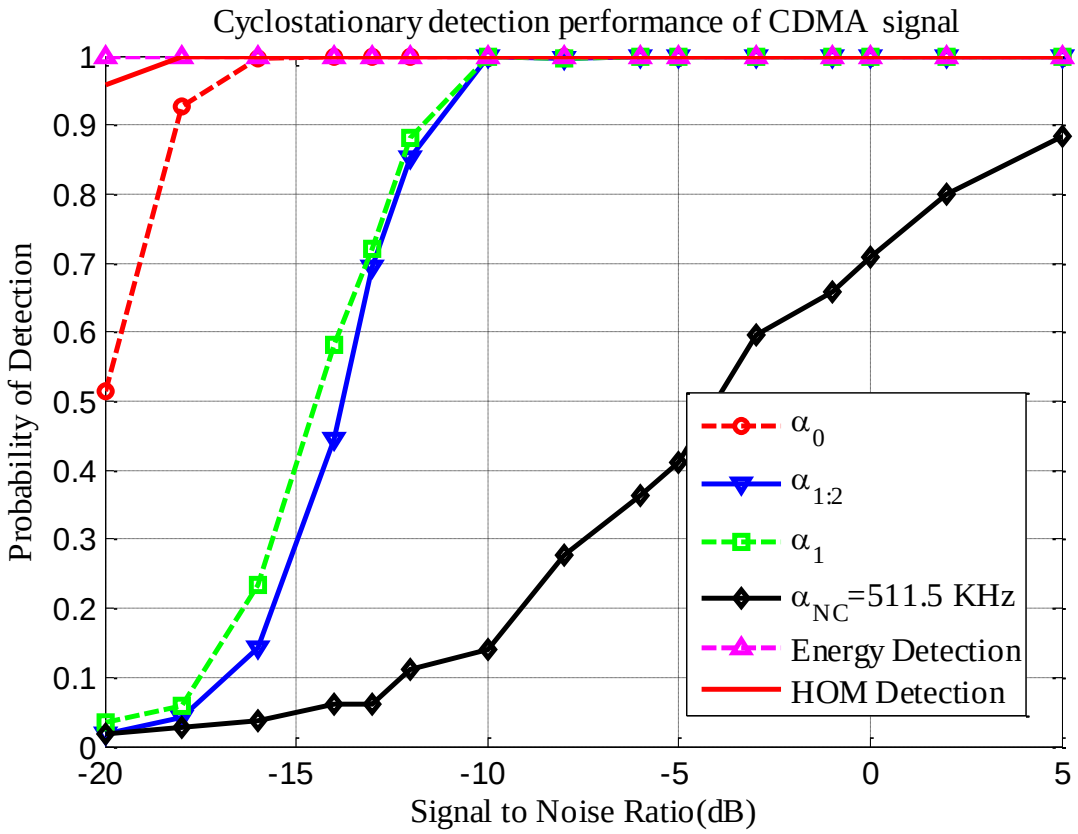


***Figure 7-10*** *$P_d$ versus SNR at different cyclic frequencies of CDMA signal*

*Figure 7-11* shows a comparative performance among several multiple cyclic frequencies detection for CDMA signals. In addition, multiple cyclic frequency ($\alpha_{1:MC}$) detectors are compared with single cyclic frequency ($\alpha_1$) detector. The test statistics when more than one cyclic frequency was used were taken as the maximum values of SCF over the first 2, 4, or 6 CDMA cyclic frequencies, respectively. The first single cyclic

frequency detection again provides better performance than the multiple cyclic frequency detection due to the fact that the SCF at first cyclic frequency has the highest amplitude than the other SCF values at non-zero cyclic frequencies.

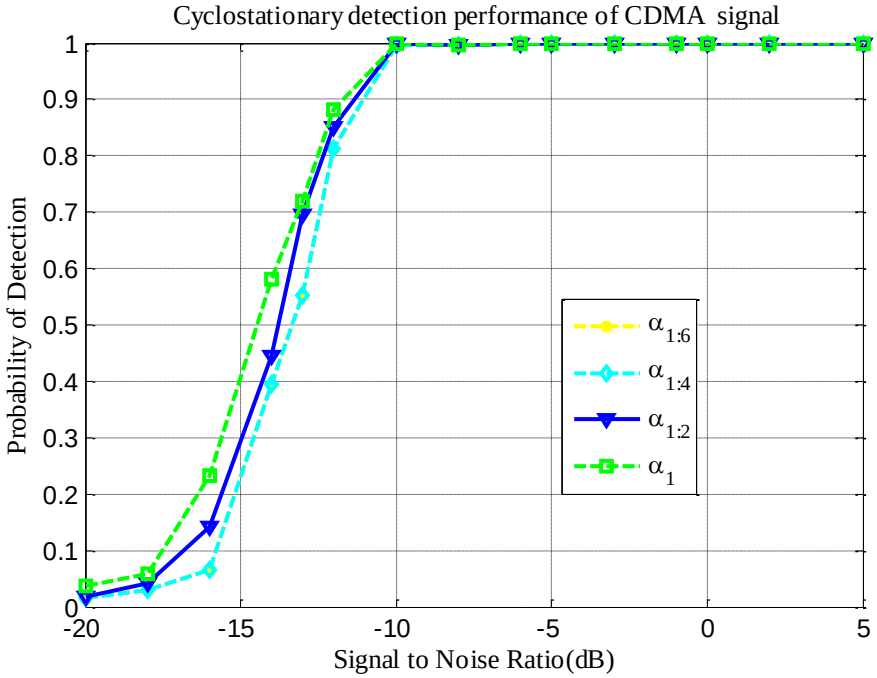


***Figure 7-11*** *$P_d$ versus SNR at different cyclic frequencies of CDMA signal: comparison of signal cyclic frequency detection with multiple cyclic frequency detection*

*Table 7-3* illustrates obtained SCF values corresponding to the used CDMA cyclic frequencies. As the order of cyclic frequency increases, the value of cyclic frequency increases. However, the SCF values are decreasing as the order of cyclic frequency increases, which also clarified the presented result on higher order multiple cyclic frequency detection.

***Table 7-3*** *SCF values corresponding to the cyclic frequency for CDMA cyclic analysis*

| **Cyclic frequency,** $\alpha = 1,2 \ldots ,6$ | **Cyclic frequency value[MHz]** | **SCF value** |
|---|---|---|
| 1 | 1.023 | 1.9918e+04 |
| 2 | 2.05 | 7.2160e+03 |
| 3 | 2.4 | 8.5891e+03 |
| 4 | 2.4 | 8.5891e+03 |
| 5 | 2.4 | 8.5891e+03 |
| 6 | 2.4 | 8.5891e+03 |

In *Figure 7-11*, detection performance at four cyclic frequencies ($\alpha_{1:4}$) is overlapping with detection performance at six cyclic frequencies ($\alpha_{1:6}$). *Figure 7-12* shows the same plot in details for this overlapping performance between $\alpha_{1:4}$ and $\alpha_{1:6}$. The reason be-

hind this overlapping in this plot is having the same value of SCF test statistics for both of this multiple cyclic frequencies, which can also be observed from *Table 7-3*.

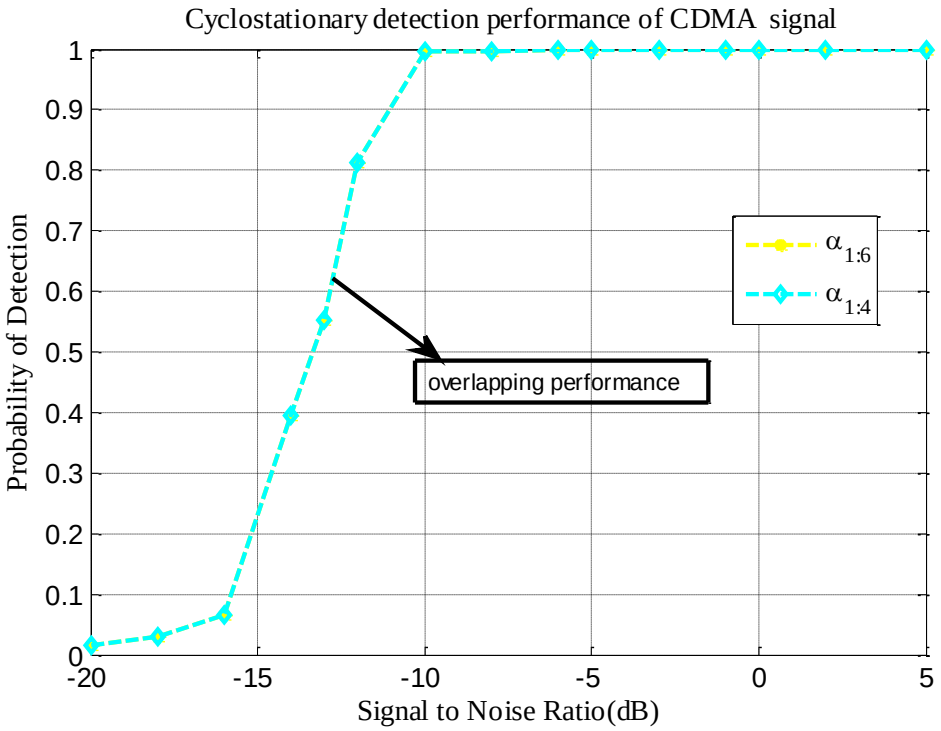


***Figure 7-12*** *$P_d$ versus SNR plot with overlapping performance of $\alpha_{1:6}$ and $\alpha_{1:4}$ of CDMA signal*

#### 7.2.3.3 The choice of the SCF test statistics

The test statistics formation procedure from the SCF energy is also an important factor in order to have better cyclostationary detection. In general, for the non-zero cyclic frequency detection, we used the maximum value of SCF, obtained from the multiple cyclic frequencies of interest. It is observed that, in cyclostationary detection at a specific non-zero cyclic frequency for a long observation time, the maximum value of SCF will give the best test statistics. For example, *Figure 7-15* and *Figure 7-16* are showing test statistics comparison between maximum and mean SCF value over 6 CDMA cyclic frequencies. Maximum SCF value based test statistics is giving best statistics in term of SCF energy value and gap between two hypotheses, as shown in *Figure 7-15* and *Figure 7-16*. Whereas for a limited observation window or in the case where all SCF values are almost equal for specific multiple cyclic frequencies, this may be different and this raises the necessity of investigating the detection performance by varying the formulation of SCF test statistics. The test statistics can be taken, for example from the maximum, mean, median, or minimum value of SCF over the multiple cyclic frequencies of interest.

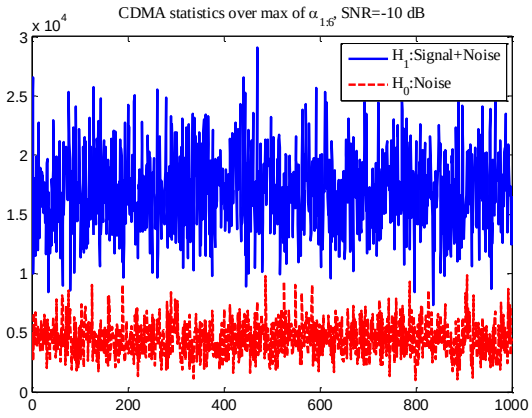


***Figure 7-13*** *CDMA statistics of maximum SCF over 6 cyclic frequencies ($\alpha_{1:6}$), SNR= -10 dB*

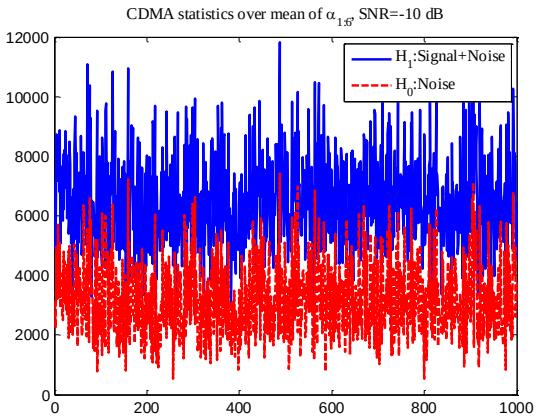


***Figure 7-14*** *CDMA test statistics of mean SCF over 6 cyclic frequencies ($\alpha_{1:6}$), SNR=-10 dB*

*Figure 7-15* shows the detection performance at 2 CDMA cyclic frequencies ($\alpha_{1:2}$) with variation on SCF test statistics formulation. This particular result indicates an overlapping performance of median SCF detection with mean SCF detection. The mean based detection is giving better result than maximum SCF based detection performance. This type of performance can be explained by the fact that, the mean value of two SCF over first 2 cyclic frequencies is more stable than the maximum value of SCF over the same.

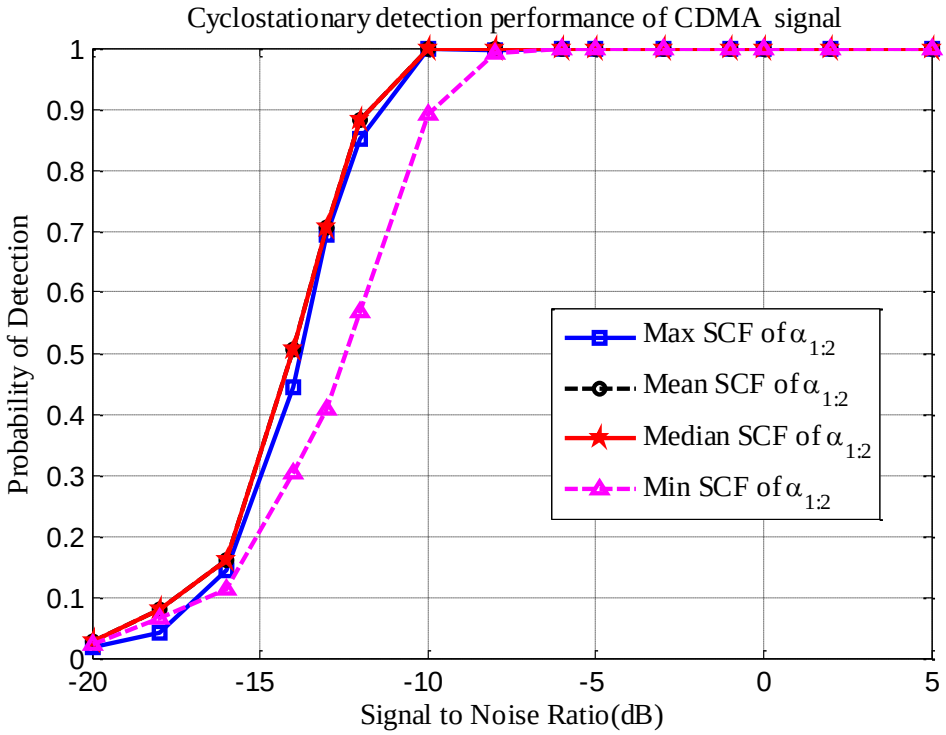


***Figure 7-15*** *Detection performance at 2 CDMA cyclic frequencies ($\alpha_{1:2}$) with variation on SCF test statistics formulation*

*Figure 7-16* provides the detection performance at 4 CDMA cyclic frequencies ($\alpha_{1:4}$) with the variation on SCF test statistics formulation. The result indicates that for this detection, maximum SCF give the best performance while mean, median and min statis-

tics, respectively, follow the maximum statistics. The minimum SCF based detection is placed here for a comparison purpose and it certainly shows degraded performance compared to the other statistics formulations, as expected.

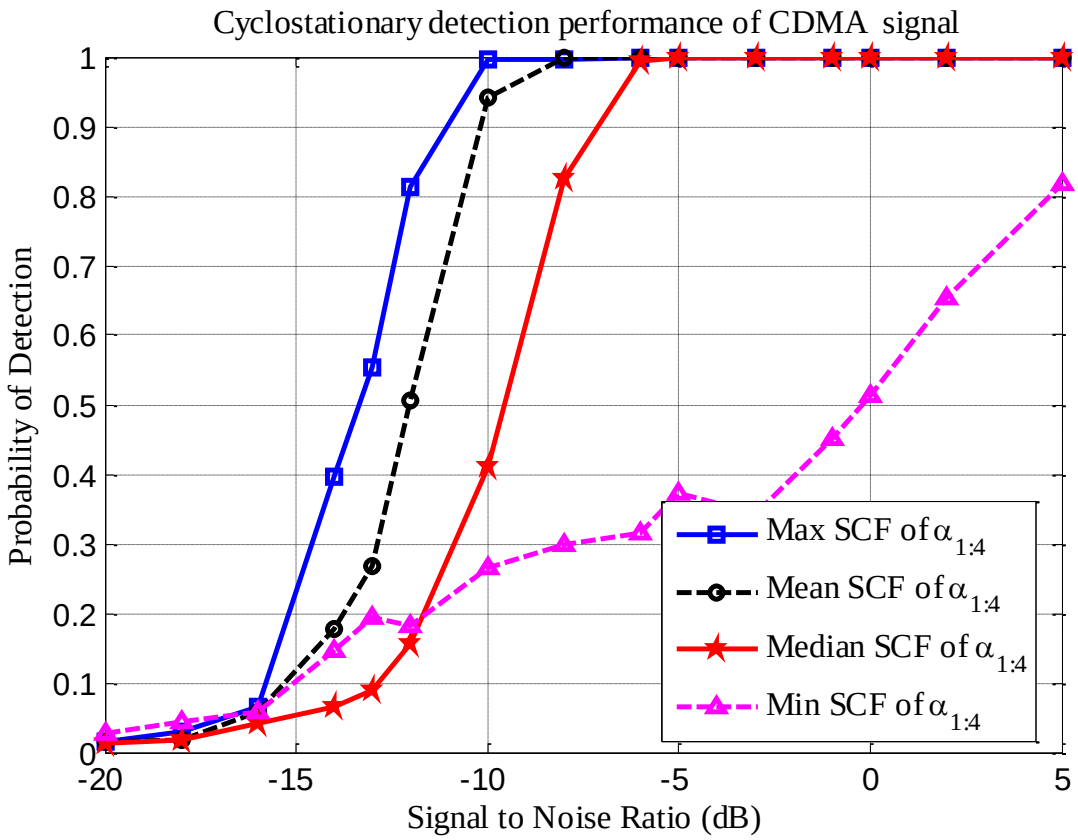


***Figure 7-16*** *Detection performance at 4 CDMA cyclic frequencies ($\alpha_{1:4}$) with variation on SCF test statistics formulation*

*Figure 7-17* shows performance detection at six CDMA cyclic frequencies ($\alpha_{1:6}$) with a variation of SCF test statistics creation. The figure provides a similar pattern characteristic as in *Figure 7-16*, where the maximum SCF provides best result and the other choices have smaller detection probabilities. However, median SCF gives exceptionally poor performance, which is even smaller than minimum SCF based detection performance.

In summary, the detection performance actually depends on which cyclic frequency the detection is carried out and what is the combining rule when several cyclic frequencies are used. Choosing the maximum SCF values among a set of considered cyclic frequencies proved to be the best option.

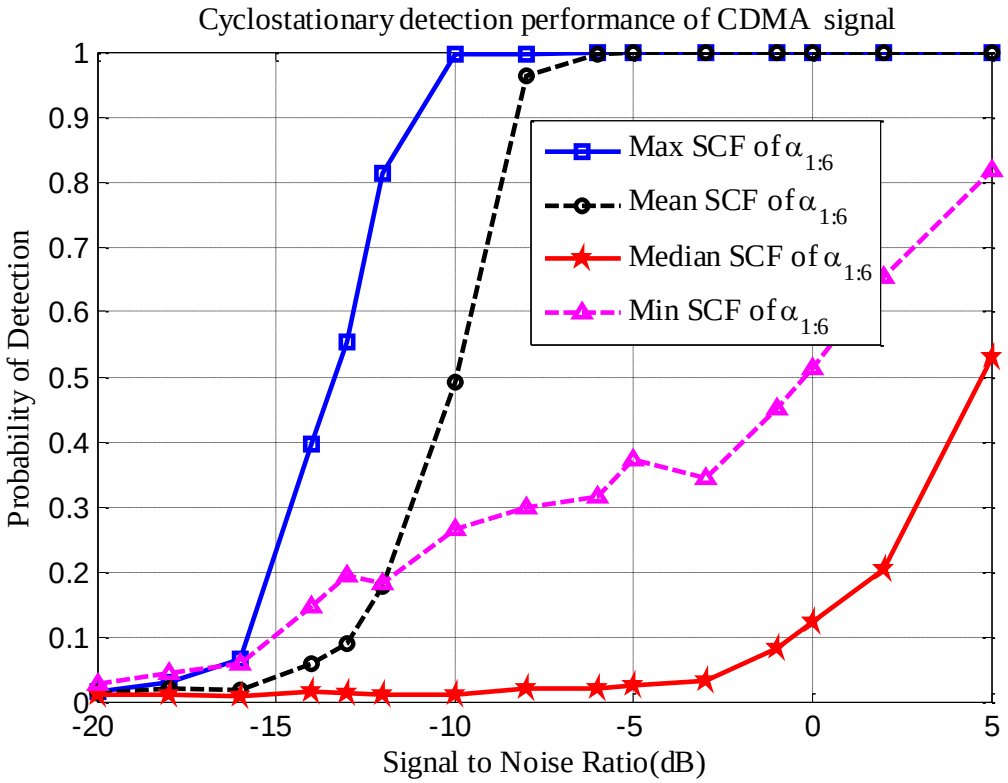


***Figure 7-17*** *Detection performance at 6 CDMA cyclic frequencies ($\alpha_{1:6}$) with variation on SCF test statistics formulation*

#### 7.2.3.4 Receiver front-end filter effect on performance

A FIR filter was included in the simulations to model the receiver front-end filter. The filter parameters are given below in *Table 7-4.*

***Table 7-4*** *List of receiver front end filter design parameters*

| Receiver Filter Parameter Name | Value |
|---|---|
| Filter Type | FIR |
| Loss in passband | 0.1dB |
| Attenuation in stopband | 40 dB |
| Transition bandwidth, TBW | BW/8,BW/4,BW/2 |

*Figure 7-18* shows the effect of filtering with three types of transition bandwidth (TBW) in the cyclostationarity-based detection. The result shows better performance in the case of using a filter in the initial low false alarm region than in the case with no filtering. Detection at $\alpha_{1:2}$ with $TBW = 2MHz$ is showing best result than filtering with $TBW = 0.5\ MHz$ and $TBW = 1MHz$. This is a MATLAB simulation result which has several design-related influencing factors and may affect the desire outcome. In a real navigation receiver implementation filter is used as an integrated part of receiver front end.

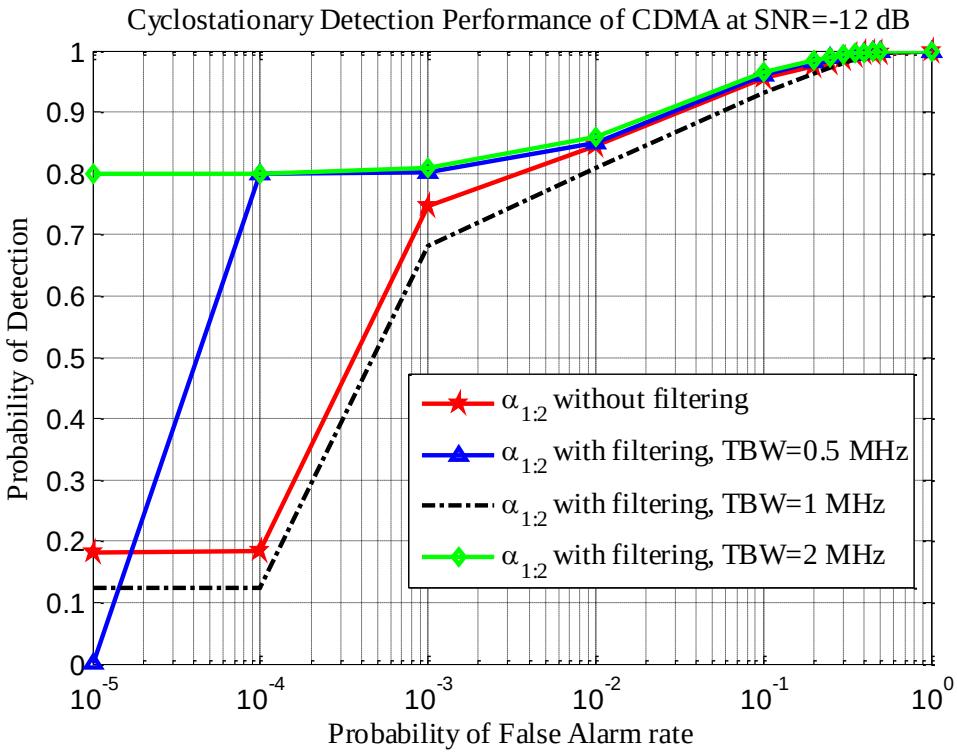


***Figure 7-18*** *Effect of receiver front end filter on cyclostationarity-based detection performance for CDMA signal*

## 7.3 Simulation results based on OFDM signals

This section presents the simulation results for OFDM signals. The important parameters are presented in *Table 7-5* for the generation of this OFDM signal in MATLAB.

***Table 7-5*** *OFDM signal specific parameters selection*

| OFDM signal parameter | Value |
|---|---|
| Bandwidth | 4 MHz |
| Sampling Frequency | 9.6 MHz |
| OFDM symbol duration | $1.3333e^{-04}s$ |
| Number of FFT carrier | 1024 |
| Guard interval | $3.3333e^{-05}s$ |
| Number of subcarrier in guard interval | 256 |
| Pilot subcarrier | Every $8^{th}$ data subcarrier |
| Subcarrier modulation | 16-QAM |
| Generated OFDM symbols | 30 |

The simulation results described in next sections are divided into three categories, namely: OFDM test statistics, SCF figures and cyclostationary detection performance.

### 7.3.1 Statistical presentation of OFDM test statistics

Statistical presentation section includes the figures of binary test statistics, PDF and CDF obtained from hypothesis detection model.

#### 7.3.1.1 Test statistics

*Figure 7-19* and *Figure 7-20* depict examples of OFDM test statistics for binary hypothesis detector model at $SNR = -12\ dB$ for zero cyclic frequency ($\alpha_0 : \alpha = 0$) and 10 cyclic frequencies ($MC = 10; \alpha_{1:10}$), respectively. For $\alpha_{1:10}$ , the maximum SCF value over first 10 non-zero cyclic frequencies is considered. Test statistics presented in here are used to obtain PDF under each hypothesis. From these two figures, it is noticed that, the separation between $H_1$ hypothesis and $H_0$ hypothesis test statistics is reduced in ($\alpha_{1:10}$) when compared to $\alpha_0$ , which is similar to CDMA cases presented earlier.

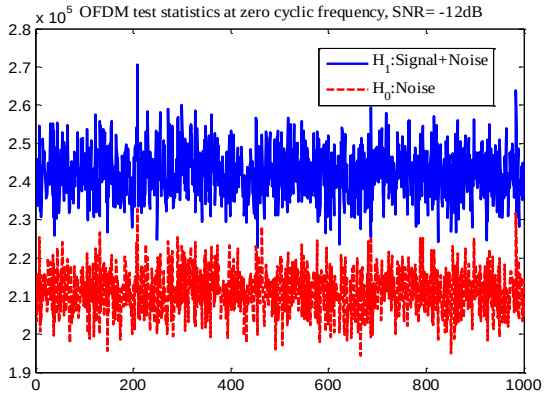


***Figure 7-19*** *OFDM statistics at zero cyclic frequency ($\alpha_0$),SNR= -12 dB*

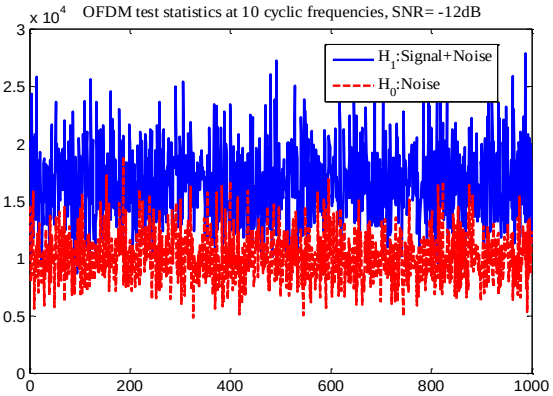


***Figure 7-20*** *OFDM test statistics of maximum SCF over 10 non-zero cyclic frequencies ($\alpha_{1:10}$), SNR=-12 dB*

#### 7.3.1.2 Probability Distribution Function

*Figure 7-21* and *Figure 7-22* present examples of PDF curves for OFDM binary hypothesis test statistics at fixed $SNR = -20\ dB$ for zero cyclic frequency ($\alpha_0$) and 10 cyclic frequencies ($\alpha_{1:10}$). In case of $\alpha_{1:10}$, the maximum SCF value over first 10 non-zero cyclic frequencies is considered. According to these figures, PDF distributions under $H_0$ and $H_1$ hypotheses at $\alpha_{1:10}$ exhibit more overlapping phenomenon than PDF distributions at $\alpha_0$ , as shown in *Figure 7-21* and *Figure 7-22*.

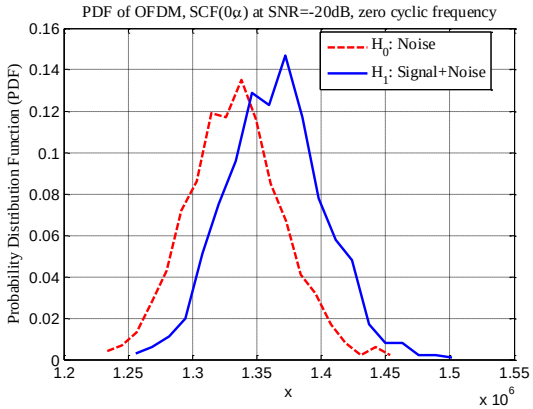


***Figure 7-21*** *OFDM test statistics PDF at zero cyclic frequency ($\alpha_0$), SNR= -20 dB*

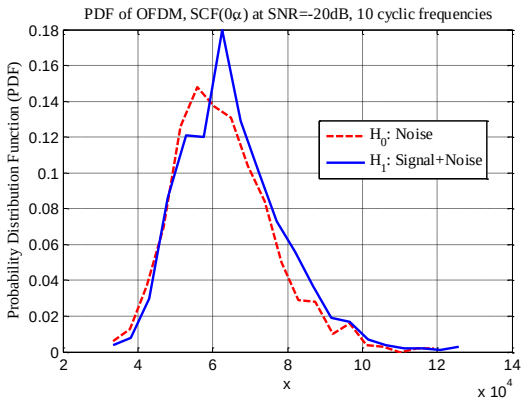


***Figure 7-22*** *OFDM Test statistics PDF of maximum SCF over 10 non-zero cyclic frequencies ($\alpha_{1:10}$), SNR= -20 dB*

### 7.3.1.3 Cumulative Distribution Function

*Figure 7-23* and *Figure 7-24* shows examples of CDF of OFDM test statistics at zero cyclic frequency $(\alpha_0)$ and 10 cyclic frequencies $(\alpha_{1:10})$ respectively at $SNR = -20\ dB$. According to these two figures, $H_1$ hypothesis CDF curve is following $H_0$ hypothesis CDF curve and this will give $P_d$ as, $P_d = 1 - CDF(H_1)$ and $P_{fa}$ as, $P_{fa} = 1 - CDF(H_0)$. As a result, $P_d$ can be higher than $P_{fa}$. However, in comparison to CDMA, the gap between two hypotheses CDF curve decreases in each of this OFDM cases.

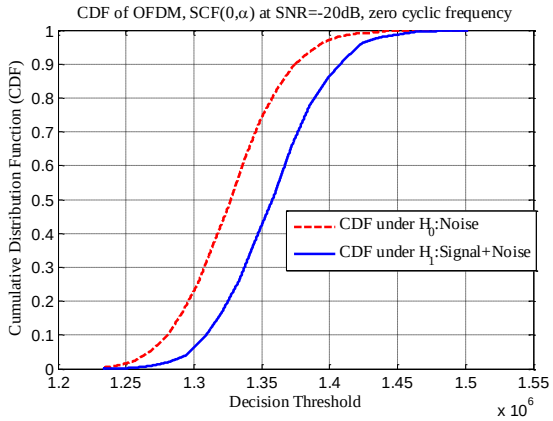


***Figure 7-23****OFDM CDF at zero cyclic frequency ($\alpha_0$), SNR=-20 dB*

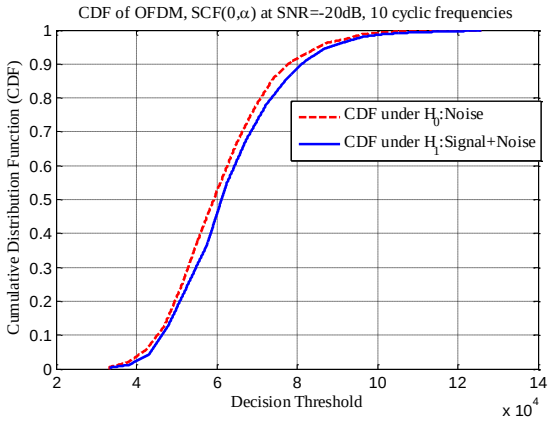


***Figure 7-24*** *OFDM CDF at 10 cyclic frequencies, maximum SCF over $(\alpha_{1:10})$ is taken, SNR= -20 dB*

### 7.3.2 Spectral correlation density function plot

*Figure 7-25* shows the SCF plot obtained from the cyclic spectral analysis of OFDM signal. The magnitude of the SCF is normalized for plotting purpose by the maximum value of the SCF and thus ranges from 0 to 1. SCF peaks can be observed at several

cyclic frequencies. According to theory, the OFDM cyclic frequencies are at integer multiples of sampling frequency [124]. The set of theoretical OFDM cyclic frequencies can be expressed as,

$$B = \{\alpha_0, \alpha_1, \alpha_2, \ldots., \alpha_n\}, n \in Z$$

Where, each cyclic frequency $\alpha_n$ location is related to OFDM symbol period, $T_{sym}$, given by,

$$\alpha_m \in \left\{ \frac{1}{T_{sym}} * k \right\} \; where \; , k \in Z$$

*Figure 7-25* also provides a comparison between simulated SCF and theoretical SCF corresponding to pilots at cyclic frequencies. According to this figure, Simulated OFDM cyclic frequencies are more frequently appearing and closer to each other than theoretical OFDM cyclic frequencies. More spectral peaks in simulation are related to the spectral correlation between OFDM spectral components with certain frequency shifts. However, theoretical OFDM cyclic frequencies can be used as a reference for better understanding of the simulated SCF pattern.

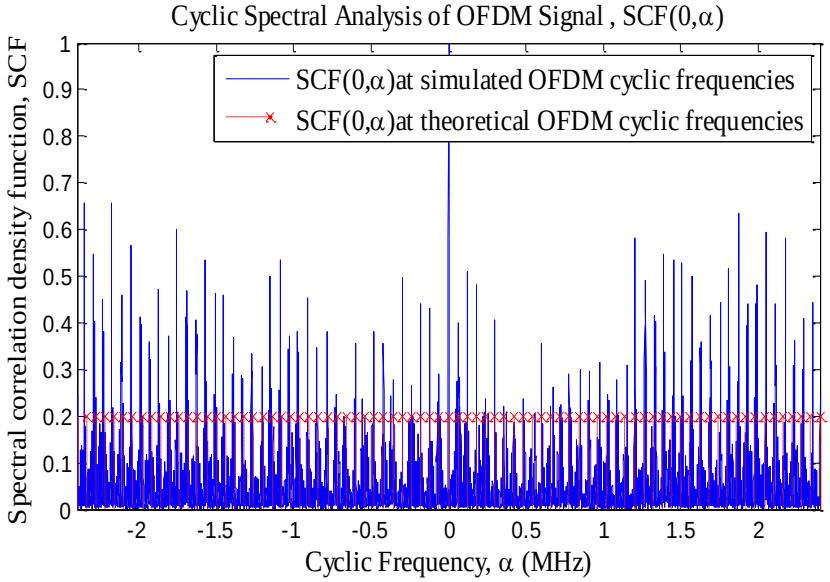


***Figure 7-25*** *Comparison of simulated and theoretical SCF of OFDM signal*

### 7.3.3 Cyclostationary detection performance for OFDM signals

#### 7.3.3.1 $P_d$ versus $P_{fa}$ plots

*Figure 7-26* illustrates the $P_d$ versus $P_{fa}$ at different SNR and at maximum SCF over first 10 cyclic frequencies detection ($\alpha_{1:10}$). The $P_d$ increases as the $P_{fa}$ increases as expected. *Figure 7-26* shows similar kind of performance in comparison to CDMA signal, as shown in *Figure 7-8*.

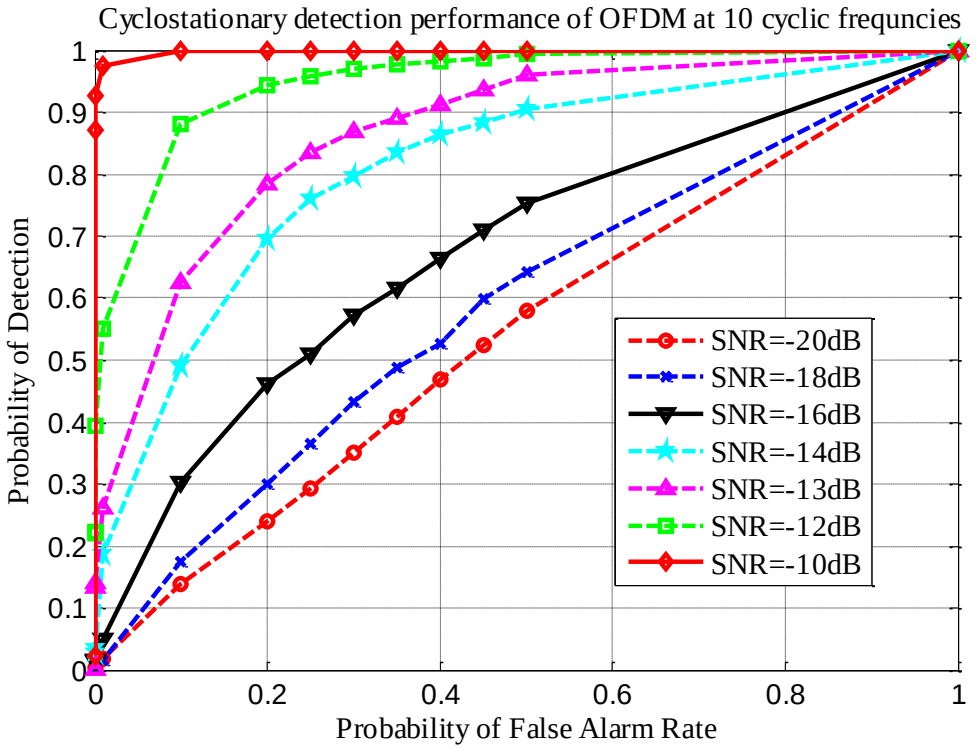


***Figure 7-26*** *$P_d$versus $P_{fa}$ at different SNR of OFDM signal*

*Figure 7-27* shows the $P_d$ versus $P_{fa}$ at different cyclic frequencies of detection, such as zero cyclic frequency ($\alpha_0$), single cyclic frequency ($\alpha_1$), 3 cyclic frequencies ($\alpha_{1:3}$), 5 cyclic frequencies ($\alpha_{1:5}$), 10 cyclic frequencies ($\alpha_{1:10}$) at $SNR = -12\,dB$. In turns, multiple cyclic frequency detectors are compared with zero and single cyclic frequency detector. The SCF values at $\alpha = 0$ and $\alpha = 1$ are taken for $\alpha_0$ and $\alpha_1$ detection. On the other hand, as described earlier, $MC$ is taken as $MC = \{3,5,10\}$ for OFDM multiple cyclic detection and in this *Figure 7-27* the maximum SCF values are computed over the 3, 5, 10 OFDM cyclic frequencies.

For instance, when using 3 cyclic frequencies, the maximum value of SCF is taken over the first 3 SCFs at the first 3 cyclic frequency positions ($\alpha = 1, \alpha = 2, \alpha = 3$). For example, in the OFDM signal used in here, the first 3 cyclic frequencies appear at 0.0076172 MHz, 0.014941 MHz, and 0.022559 MHz respectively. When 3 cyclic frequencies are combined for the test statistic, we formed the test statistic as max (SCF_1_OFDM, SCF_2_OFDM, SCF_3_OFDM), where SCF_1_OFDM, SCF_2_OFDM and SCF_3_OFDM are the SCF values at the cyclic frequencies 0.0076172 MHz, 0.014941 MHz, 0.022559 MHz respectively.

In OFDM cyclic spectral analysis case, the simulated cyclic frequencies are found closer to each other. To obtain an optimum detection and extraction of higher order cyclostationary features of OFDM signal, we made a choice of using up to 10 OFDM cyclic frequencies. However, learning of much higher order cyclic frequency (e.g. $MC = \{\ldots\ldots,11,12,13\ldots.\}$) may lead to better detection. On the other hand, in CDMA cyclic spectral analysis, we made an optimum choice of using up to 6 CDMA cyclic

frequencies. In the simulation context, the selection of the elements of $MC$ set (multiple cyclic frequencies) can be taken in more constructive way by having a prior knowledge of SCF values obtained from cyclic spectral analysis.

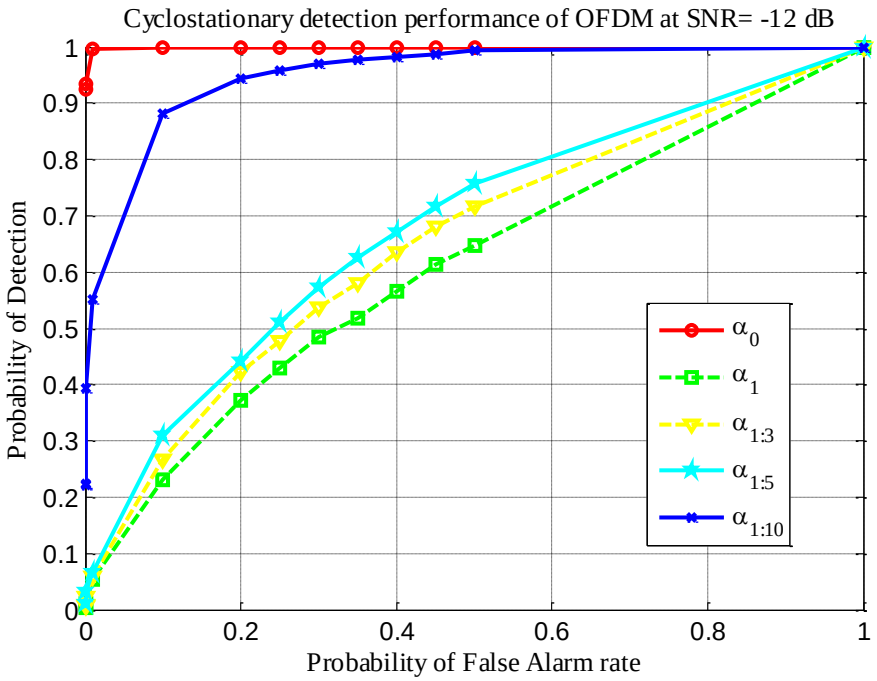


***Figure 7-27*** *$P_d$versus $P_{fa}$ at different cyclic frequencies of OFDM signal*

From the result, it can be seen that, detection performance is increasing as the number of multiple cyclic frequencies increases. However, in CDMA case, first single cyclic frequency detection provides better performance than the multiple cyclic frequency detection due to the fact that the CDMA SCF at first cyclic frequency has the highest amplitude than the other SCF values at non-zero cyclic frequencies.

### 7.3.3.2 $P_d$ versus SNR plots

*Figure 7-28* compares OFDM cyclostationarity-based detection performance with the performance of energy detection and of HOM detection. We show the cyclostationarity-based detector at zero cyclic frequency ($\alpha_0$), at ten cyclic frequencies ($\alpha_{1:10}$), at a non-cyclic frequency ($\alpha_{NC}$) and at single cyclic frequency ($\alpha_1$). The $P_d$ versus SNR is plotted in *Figure 7-28* at different cyclic frequencies of OFDM signal at a fixed false alarm value of 0.01. The energy detector and the HOM detector outperform the other cyclic detectors as those energy based detectors provide better result in an AWGN environment with a comparison of cyclic detectors (this will be further explained in Section 7.5). The detection performance at zero cyclic frequency is showing better result than the detection at 10 cyclic frequencies. On the other hand, multiple cyclic frequencies ($\alpha_{1:MC}$) detection provides better result than detection at single first cyclic frequency. However, in CDMA, first single cyclic frequency detection provides better performance than the multiple cyclic frequency detection.

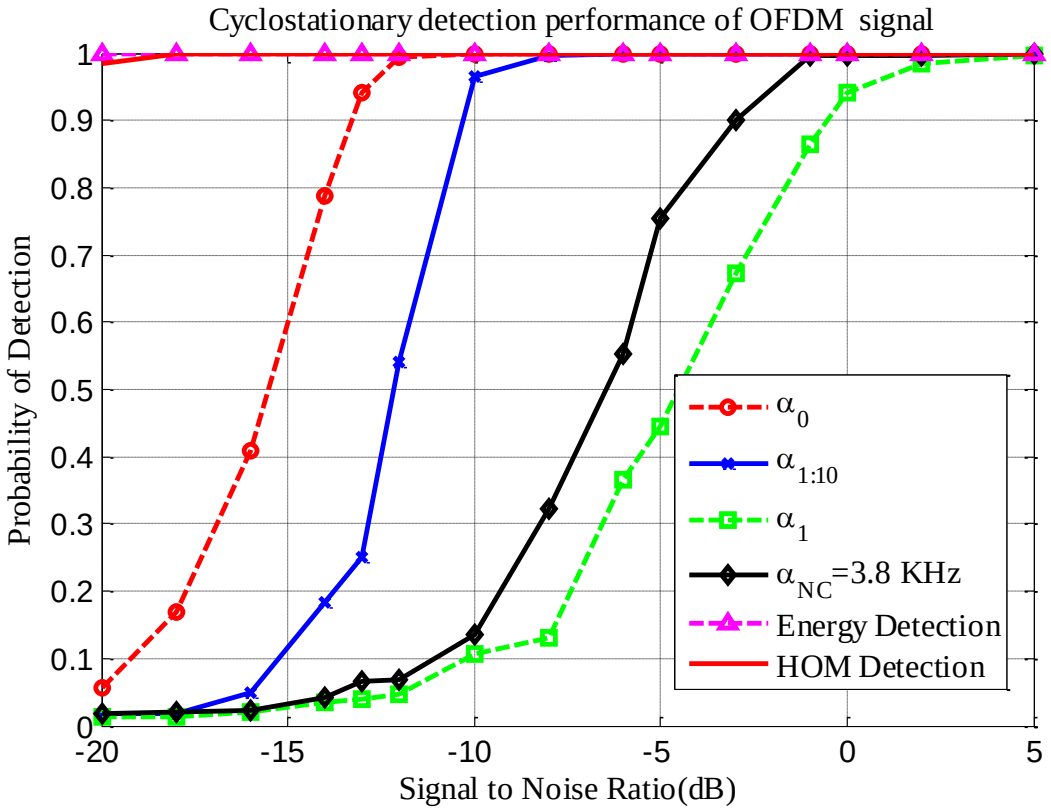


***Figure 7-28*** *$P_d$ verses SNR at different cyclic frequencies of OFDM signal*

It is interesting to observe that, non-cyclic frequency provides even better result than detection at single cyclic frequency. This result indicates that, there is certainly spectral leakage exists while doing cyclic spectral analysis of OFDM signal. On the other hand, in case of CDMA, non-cyclic frequency detection provides the worst result. It seems that, according to our cyclostationary simulation settings, OFDM signal is more sensitive to spectral leakage than CDMA signal. So, proper spectral leakage prevention steps need to take in consideration according to the received signals type while doing cyclic spectral analysis. In turns, prevention of spectral leakage will lead to better detection.

*Figure 7-29* shows a comparative performance among several multiple cyclic frequencies ($\alpha_{1:MC}$) detection for OFDM signals. In addition, multiple cyclic frequency detectors are compared with single cyclic frequency ($\alpha_1$) detector. The test statistics when more than one cyclic frequency was used were taken as the maximum values of SCF over the first 3, 5, or 10 OFDM cyclic frequencies, respectively. It follows that, for OFDM, the probability of detection increases as the cyclic frequencies further from zero cyclic frequency ($\alpha = 0$) are considered. We recall that the SCF values are related to the pilot pattern, guard interval and sampling frequency.

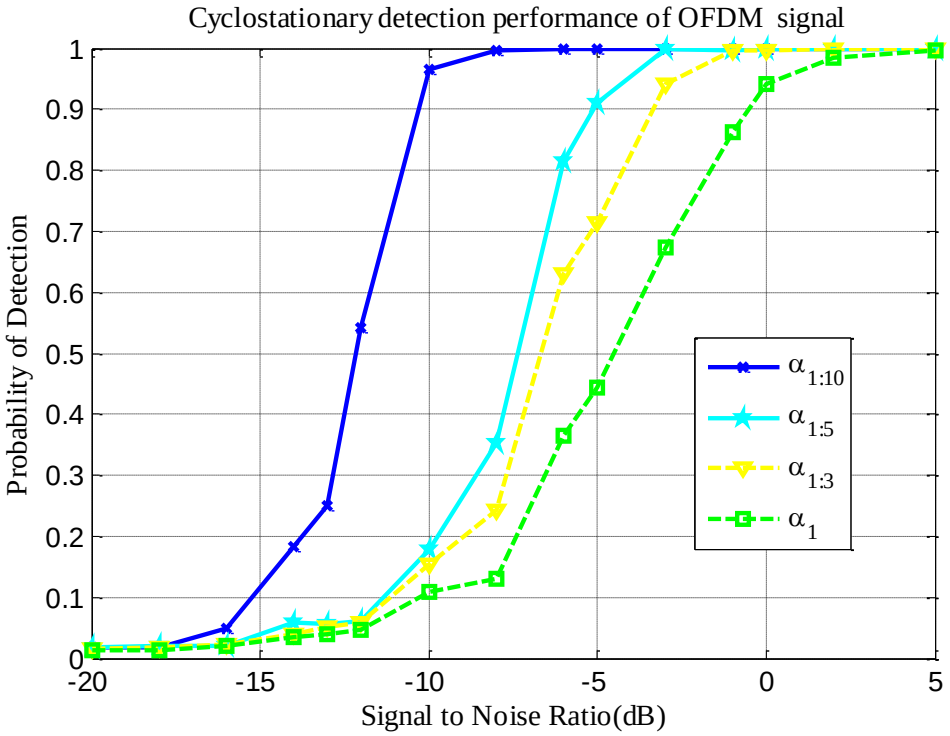


***Figure 7-29*** *$P_d$ versus SNR at different cyclic frequencies of OFDM signal: comparison of signal cyclic frequency detection with multiple cyclic frequencies detection*

*Table 7-6* points out obtained SCF values corresponding to the used OFDM cyclic frequencies for one random iteration. As the order of OFDM cyclic frequency increases, the value of cyclic frequency showing a increasing trend. The SCF values of corresponding cyclic frequencies is also showing increasing trend as the order of cyclic frequency increases.

***Table 7-6*** *SCF values corrosponding to the cyclic frequency for OFDM cyclic analysis*

| **Cyclic frequency,** $\alpha = 1,2 \ldots ,10$ | **Cyclic frequency value[MHz]** | **SCF value** |
|---|---|---|
| 1 | 0.0076172 | 2.5873e+03 |
| 2 | 0.014941 | 1.9653e+03 |
| 3 | 0.022559 | 6.1831e+03 |
| 4 | 0.029883 | 3.9441e+03 |
| 5 | 0.0375 | 2.2014e+03 |
| 6 | 0.045117 | 5.6034e+03 |
| 7 | 0.052441 | 9.6567e+03 |
| 8 | 0.060059 | 1.8771e+04 |
| 9 | 0.067383 | 1.0031e+04 |
| 10 | 0.075 | 7.0397e+03 |

#### 7.3.3.3 The choice of the SCF test statistics

*Figure 7-30* provides the detection performance at 10 OFDM cyclic frequencies ($\alpha_{1:10}$) with variation on the choice of the SCF test statistics, namely by using mean, minimum, median or maximum among the SCF values at the first 10 cyclic frequencies. The result indicates that the mean test statistic gives the best performance while the maximum, median and minimum statistics follow the mean statistics in decreasing order. The minimum SCF based detection placed here for the comparison purpose shows, as expected, much lower performance than the other test statistics. It is clear that, the fluctuations of the maximum value of SCF over several cyclic frequencies are significant if they are observed for a high enough number of random realizations (in this thesis, 1000 random iterations were used for test statistics generation). The mean-based SCF test statistics provides better result than the maximum SCF test statistics; because the mean fluctuations are smaller (the mean test statistic is more stable than the maximum test statistic). *Figure 7-31* and *Figure 7-32* also clearly show better result with mean based test statistics than maximum test statistics for OFDM cyclostationary detection at 5 ($\alpha_{1:5}$) and 3 cyclic frequencies ($\alpha_{1:3}$) respectively. The median based detection remains around the range of maximum SCF value based detection. The minimum SCF value based detection provides always a worse performance than the other choices, which is obvious. It is interesting to note that, the gap between worst and best performance is closing when the number of considered multiple cyclic frequencies is getting smaller.

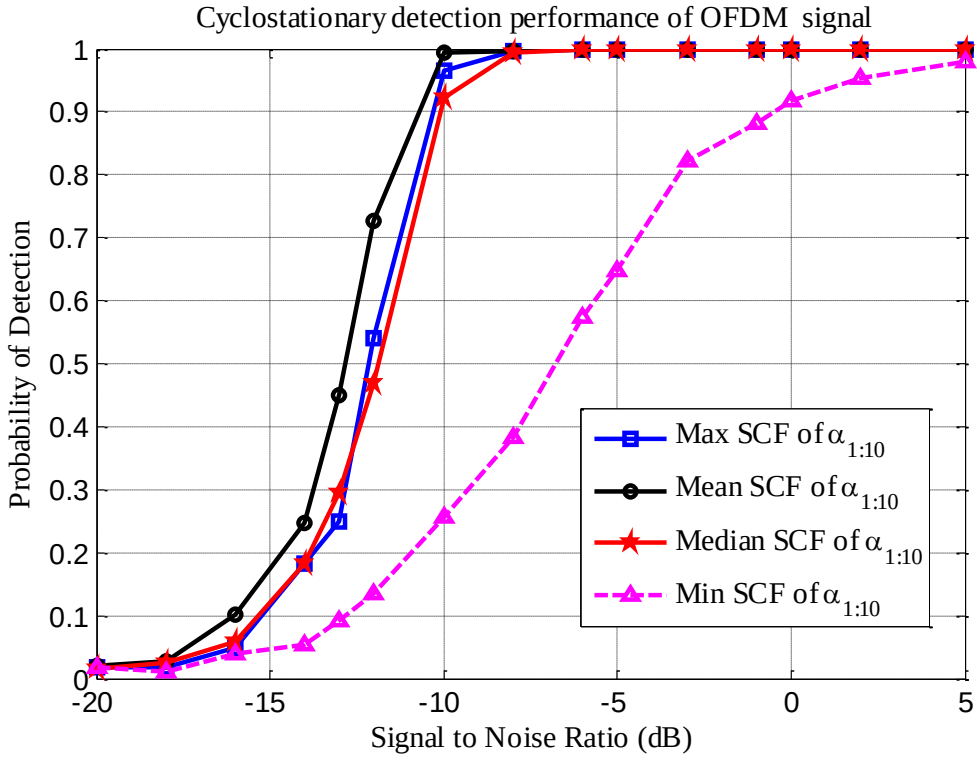


***Figure 7-30*** *Detection performance at 10 OFDM cyclic frequencies with variation on SCF test statistics formulation*

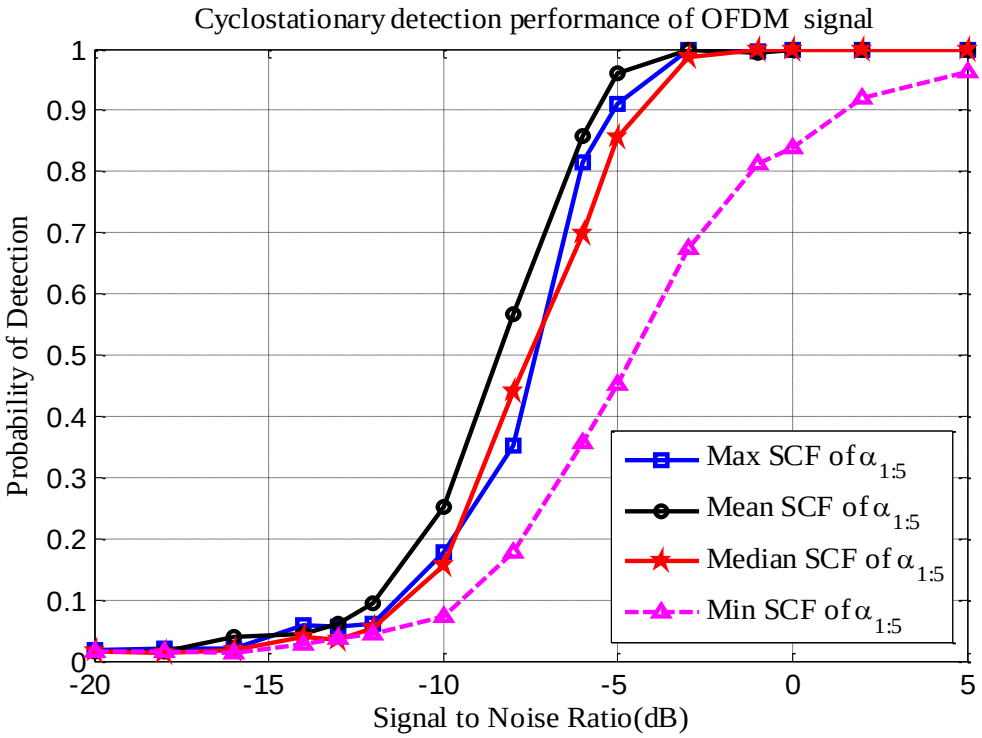


***Figure 7-31*** *Detection performance at 5 OFDM cyclic frequencies with variation on SCF test statistics formulation*

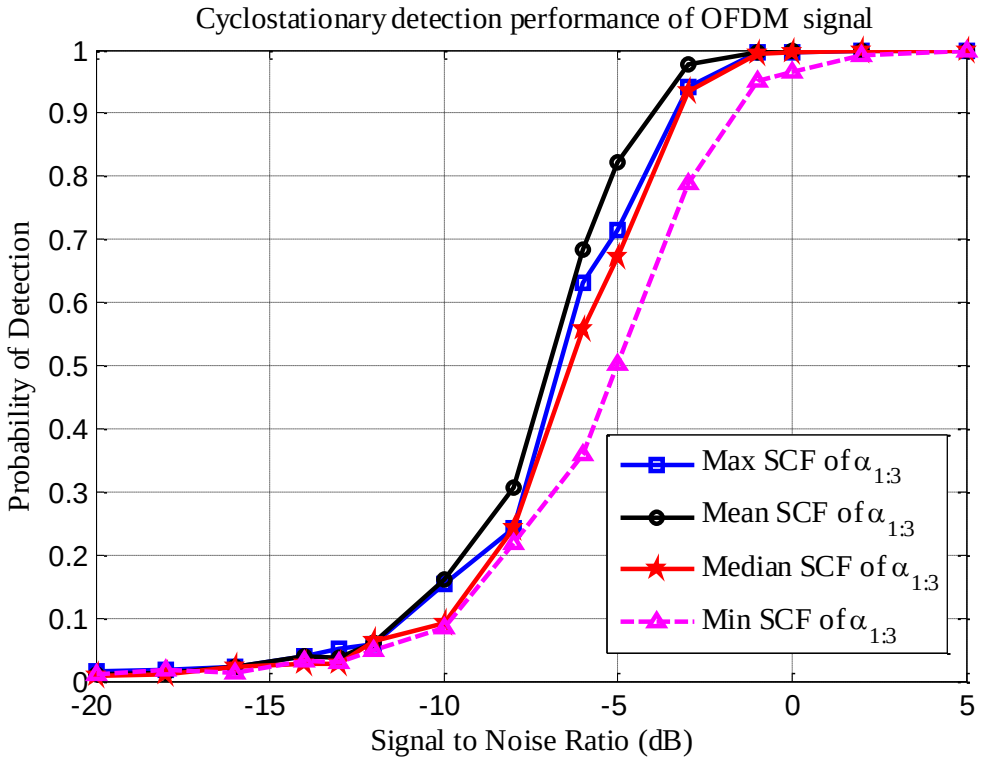


***Figure 7-32*** *Detection performance at 3 OFDM cyclic frequencies with variation on SCF test statistics formulation*

#### 7.3.3.4 Receiver front-end filter effect on performance

*Figure 7-33* illustrates a comparative view of using filter for cyclostationary detection of OFDM signal. In this simulation, the FIR filter parameter presented in *Table 7-4* is used to observe filtering effect on cyclostationary detection for OFDM signal. The result shows a similar performance with and without filtering. However, in the case of CDMA, filtering with higher TBW shows better result than without filtering detection performance. In a real navigation receiver, RF front end filter is used as an integrated part for suppressing unwanted signal.

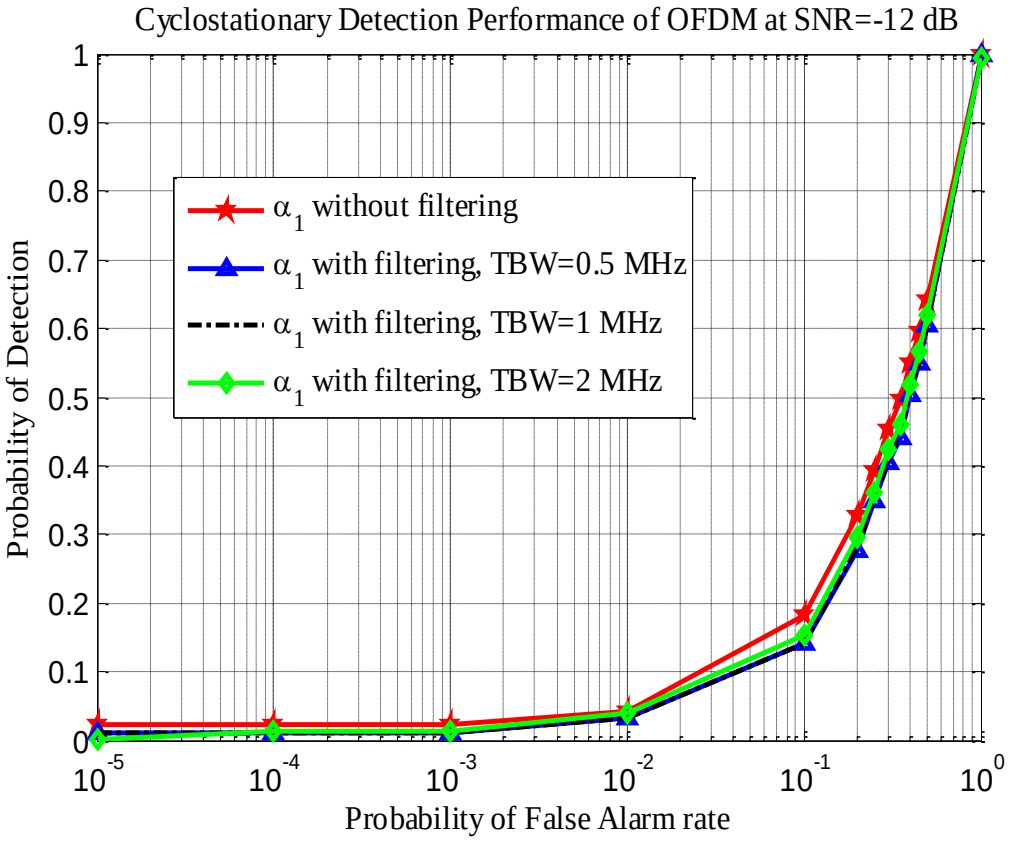


***Figure 7-33*** *Effect of the receiver front-end filter on cyclostationarity-based detection performance for OFDM signal*

## 7.4 Cyclic spectral analysis of mixture of signals

*Figure 7-34* shows the Spectral Correlation Density Function (SCF) of when an OFDM signal is superposed with a CDMA signal, forming a signal mixture. This type of joint analysis has the purpose of the signal identification based on SCF pattern and modulation scheme used. *Figure 7-34* also provides a comparison of simulated SCF at joint cyclic frequencies with the individual theoretical SCF at individual theoretical cyclic frequencies as a reference. From this figure it can be seen that, OFDM signal exhibits more theoretical cyclic frequencies than CDMA, if we consider a specific window (e.g. from 0 MHz to 2 MHz in x axis of *Figure 7-34*).

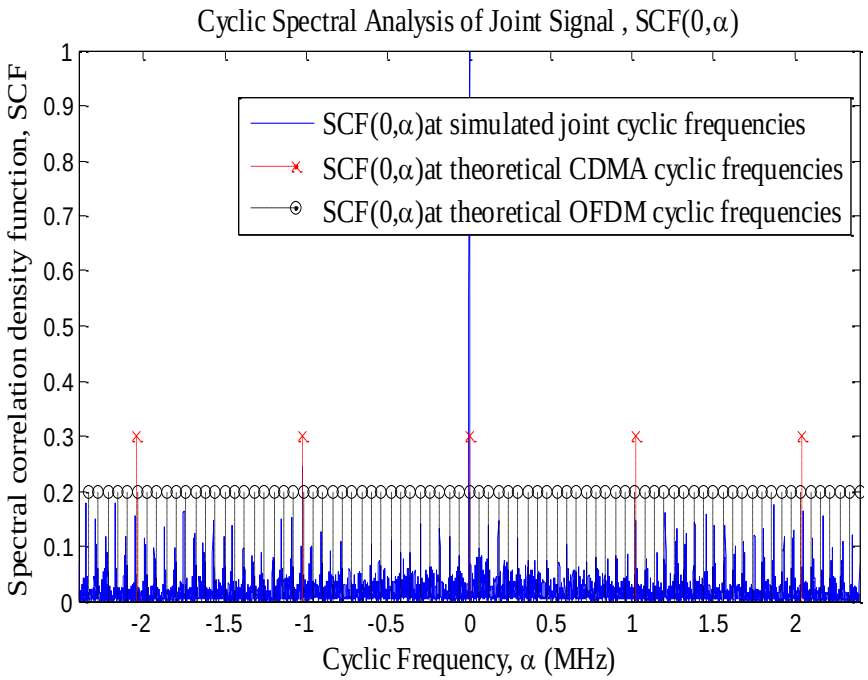


***Figure 7-34*** *SCF of joint (OFDM+CDMA) signal*

Table *7-7* summarizes the important parameters which are used in this particular joint cyclic spectral analysis.

***Table 7-7*** *Summary of CDMA and OFDM signal parameters used in forming mixture*

| **Parameters** | **CDMA specific value** | **Parameters** | **OFDM specific value** |
|---|---|---|---|
| Modulation | BPSK | Modulation | 16-QAM |
| Chip rate | 1.023 MHz | Symbol period | 133 $\mu$s |
| Spreading factor | 101 | Pilot position | Every $8^{th}$ sub-carrier |
| Sampling frequency | 9.6 MHz | Sampling frequency | 9.6 MHz |

We assume that, spectral peaks will appear at the cyclic frequencies those are integer multiple of sampling frequency. In case of the signal mixture, some SCF of CDMA signal overlap with OFDM signal in some common cyclic frequency positions. For example, 1.02 MHz is the first common cyclic frequency for both. For CDMA, 1.02 MHz corresponds to $\alpha_1$, whereas for OFDM 1.02 MHz corresponds to $\alpha_{136}$. The SCF values for CDMA and OFDM at the common cyclic frequency are different. On the other hand, the source of remaining (non-overlapping) SCF on the cyclic frequency axes whether generated from OFDM or CDMA can be determined by classification information. This type of joint detection based on classification of signal from the mixture of signal will open a new research area for future work.

## 7.5 Discussion on the spectral analysis of CDMA and OFDM signals

In general, cyclostationary detectors are designed to achieve the signal detection in varying noise power situations, including the low SNR cases. The comparison performance presented in earlier sections for CDMA and OFDM signal raise the question about the effectiveness of cyclostationary detection. A brief overall discussion on the comparison of simulated cyclostationary higher multiple cyclic frequency detection performance of OFDM and CDMA, respectively, signal with zero cyclic frequency and other classical detectors is presented below and the performance is argued from four points of view, namely the deflection coefficient, the non-stationary noise, the noise mean and variance and the simulation parameters.

### 7.5.1 Deflection issues

The deflection coefficient $d_x$ can be defined as below:

$$d_x = \frac{|E(H_1) - E(H_0)|^2}{var(H_0)}$$

Where $E(.)$ stand for the expected value operator and in this case used to calculate the mean value of the binary test statistics at, and $var(.)$ for the signal variance under $H_0$ hypothesis. Here $H_1$and $H_0$ represents the alternative and null hypothesis test statistics, respectively. The deflection is a measure of the signal detection performance in low SNR with Gaussian distribution cases [120], [149]. According to the theory presented in [120] and [149] if the value of deflection coefficient $d_x$ increases, then the probability of detection increases as well. In this thesis, as per the MATLAB generated Gaussian statistics in AWGN noise scenario with $(\alpha_0)$ and $(\alpha_1)$ detection, the value of $d_x$ is decreasing from zero cyclic frequency $(\alpha_0)$ to single cyclic frequency $(\alpha_1)$ at a specific initial low SNR. The deflection coefficient is decreasing as the noise variance is increasing from $(\alpha_0)$ to $(\alpha_1)$ at a specific initial low SNR. This is why, according to the deflection theory, the signal detection performance at zero cyclic frequency is higher than the detection at single cyclic frequency. As the SNR increases, the deflection value at single cyclic frequency is getting higher than that of zero cyclic frequency. This fact clearly justified the earlier presented performance for detection at single cyclic frequency, when compared with zero cyclic frequency detection.

*Table 7-8* and *Table 7-9* provide the numerical observation of deflection value related with cyclic analysis for both of the CDMA and OFDM signal. As seen in these tables, zero cyclic frequency has much higher deflection coefficient than single cyclic frequencies at initial low SNR (e.g. -20 dB, -10 dB). For example, in CDMA case, at $SNR = -20\ dB$, the deflection value at $\alpha_0$ is 23.8178, while at $\alpha_1$ the deflection value is 0.1327. As a result, CDMA cyclostationary detection performance at $\alpha_0$ is higher than detection at $\alpha_1$. Similarly, for example, in case of OFDM detection at $SNR = -20\ dB$, the deflection value at $\alpha_0$is 1.5571 while at $\alpha_1$, the deflection is 7.00093e-3.

As a result, signal detection performance at $\alpha_0$ is slightly better than detection at $\alpha_1$. As the SNR increases, deflection value at single cyclic frequency is getting higher than at $\alpha_0$ for both of the CDMA and OFDM.

***Table 7-8*** *CDMA deflection transition*

| SNR/Deflection value | Zero cyclic frequency, $(\alpha_0)$ | Single cyclic frequency,$(\alpha_1)$ |
|---|---|---|
| SNR=-20dB | 23.8178 | 0.1327 |
| SNR=-10dB | 2.2071e3 | 94.99 |
| SNR= 0 dB | 2.3781e5 | 12.97e3 |

***Table 7-9*** *OFDM deflection transition*

| SNR/Deflection value | Zero cyclic frequency, $(\alpha_1)$ | Single cyclic frequency, $(\alpha_1)$ |
|---|---|---|
| SNR=-20dB | 1.5571 | 7.00093e-3 |
| SNR=-10dB | 141.8350 | 0.64074 |
| SNR= 0 dB | 1.5323e4 | 87.6601 |

### 7.5.2 Non-stationary noise issues

In this thesis, the MATLAB based simulations were conducted with additive white random stationary noise, for which the variance was assumed known. This was because we wanted to test the cyclostationarity properties under more controlled conditions and in 'best cases scenarios' and because the thesis timeframe was too short to include the non-stationary modeling. In a real scenario, the communication signals may get involved with non-stationary noise and this noise will introduce uncertainty with the noise power [150]. The primary concern of the cyclostationary detectors is to detect a signal under such uncertainty produced by the non-stationary noise. In such a case, the cyclostationary detector is expected to perform better than the energy detector [150].

We expect that, in the presence of non-stationary noise, the performance of the cyclostationary detector will be better than the one of the energy detector or with the zero-cyclic frequency detector. If we apply binary testing at zero cyclic frequency detection with non-stationary noise, as the noise power is varying, the SCF energy-based detection is expected to fail compared to higher multiple cyclic frequencies detection. Guoqing JI and Hongbo Zhu have made a study about this in [151] and they analyzed the negative effect on energy detector performance due to the noise uncertainty. In a varying noise power situation, it is impossible to have an exact knowledge of noise power in order to detect the signal. Moreover, higher multiple cyclic frequencies detection with varying noise power will create zero-valued SCF for non-stationary noise at higher cyclic frequencies, while the signal of interest will create non-zero SCF estimate at those cyclic frequencies. As a result, higher order cyclostationary detection reduces the detection problem of signal in case signal with non-stationary noise, as compared with energy detection.

### 7.5.3 Mean and noise variance issues

In the analysis of the cyclostationary signals in this thesis, the test statistics were generally taken from the amplitude of SCF values at several cyclic frequencies and this SCF values are still indicating signals energy on that particular cyclic frequency positions. We noticed, based on our simulations, the noise mean was decreasing and the noise variance was increasing from zero cyclic frequency towards non-zero higher order cyclic frequency detection. We know that, if the noise variance is increasing, then the energy based detector will have a decreasing performance [150]. Under these circumstances, the performance of the cyclostationary detection at higher multiple cyclic frequencies indicated worse result than the energy detector or with the zero-cyclic frequency detector. *Table 7-10* and *Table 7-11* provide the noise mean and variance values on the generated stationary noise for both CDMA and OFDM signals respectively. The statistical information presented in the two tables is obtained from $H_0$ hypothesis histograms presented in *Figure 7-35* to *Figure 7-38*. The noise mean is decreasing by the amount of $\Delta M$ and noise variance is increasing by the amount of $\Delta V$ from zero cyclic frequency towards non-zero higher order cyclic frequency detection for both of the signals.

***Table 7-10*** *Noise mean and variance analysis for CDMA signal*

| **SNR (dB)** | **Noise mean at zero cyclic frequency (dB)** | **Noise variance at zero cyclic frequency (dB)** | **Noise mean at 2 cyclic frequencies (dB)** | **Noise variance at 2 cyclic frequencies (dB)** | **ΔM (dB)** | **ΔV (dB)** |
|---|---|---|---|---|---|---|
| -20 | 6.4563 | 6.5569e-05 | 4.8397 | 0.0143 | 1.6166 | 1.42e-2 |
| -10 | 5.4564 | 7.1217e-05 | 3.8242 | 0.0153 | 1.6322 | 1.52e-2 |
| 0 | 4.4563 | 6.6105e-05 | 2.8296 | 0.0150 | 1.6267 | 1.49e-2 |
| 10 | 3.4568 | 6.8857e-05 | 1.8344 | 0.0142 | 1.6224 | 1.41e-2 |

***Table 7-11*** *Noise mean and variance analysis for OFDM signal*

| **SNR (dB)** | **Noise mean at zero cyclic frequency (dB)** | **Noise variance at zero cyclic frequency (dB)** | **Noise mean at 10 cyclic frequencies (dB)** | **Noise variance at 10 cyclic frequencies (dB)** | **ΔM (dB)** | **ΔV (dB)** |
|---|---|---|---|---|---|---|
| -20 | 6.4563 | 6.5569e-05 | 4.9718 | 0.0089 | 1.4845 | 8.83e-3 |
| -10 | 5.4564 | 7.1217e-05 | 3.9658 | 0.0084 | 1.4906 | 8.33e-3 |
| 0 | 4.4563 | 6.6105e-05 | 2.9632 | 0.0083 | 1.4931 | 8.23e-3 |
| 10 | 3.4568 | 6.8857e-05 | 1.9670 | 0.0078 | 1.4898 | 7.73e-3 |

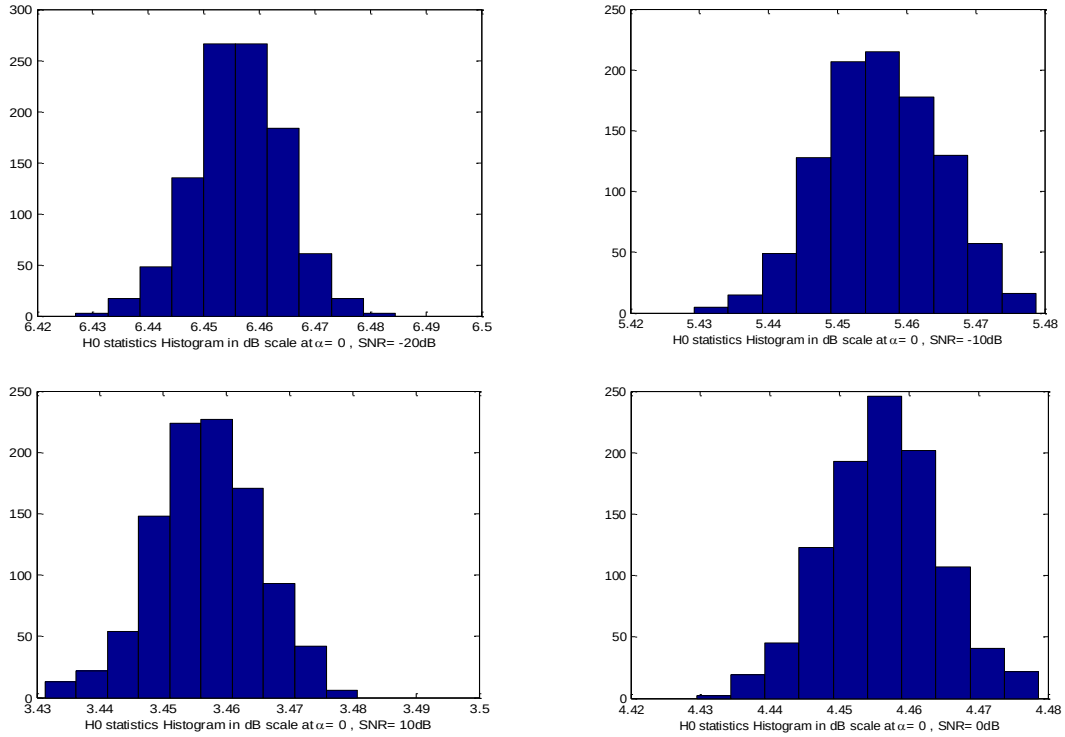


***Figure 7-35*** *$H_0$ statisitcs based noise histogram used in noise mean and variacne calculation for CDMA cyclostatioanry detection at zero cyclic frequency ($\alpha = 0$), top left : SNR=-20 dB, top right: SNR=-10 dB, bottom right: 0 dB, bottom left: SNR=10 dB*

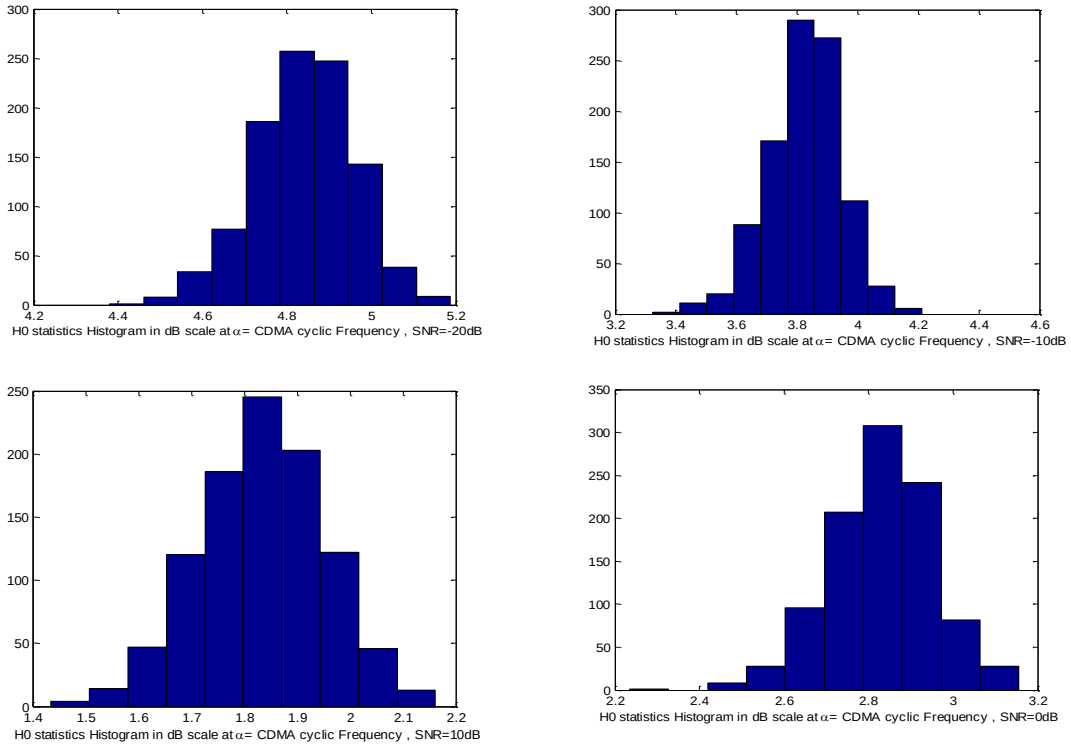


***Figure 7-36*** *$H_0$ statisitcs based noise histogram used in noise mean and variacne calculation for CDMA cyclostatioanry detection at 2 cyclic frequencies ($\alpha_{1:2}$), top left : SNR=-20 dB, top right: SNR=-10 dB, bottom right: 0 dB, bottom left: SNR=10 dB*

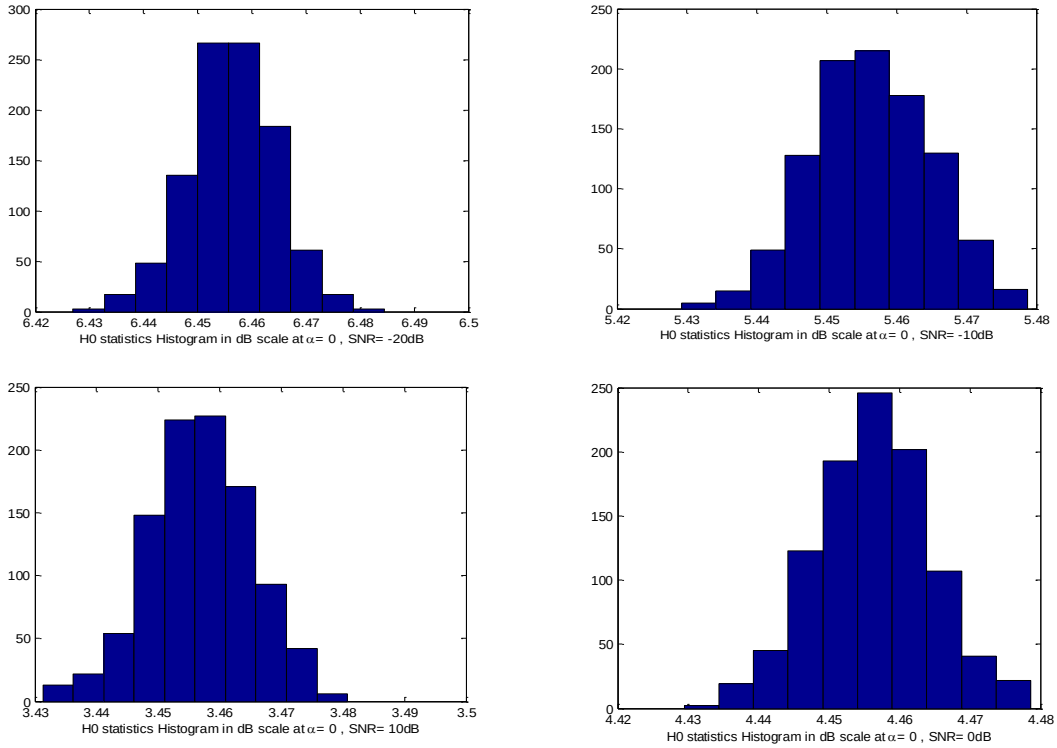


***Figure 7-37*** *$H_0$ statisitcs based noise histogram used in noise mean and variacne calculation for OFDM cyclostatioanry detection at zero cyclic frequency ($\alpha = 0$), top left : SNR=-20 dB, top right: SNR=-10 dB, bottom right: 0 dB, bottom left: SNR=10 dB*

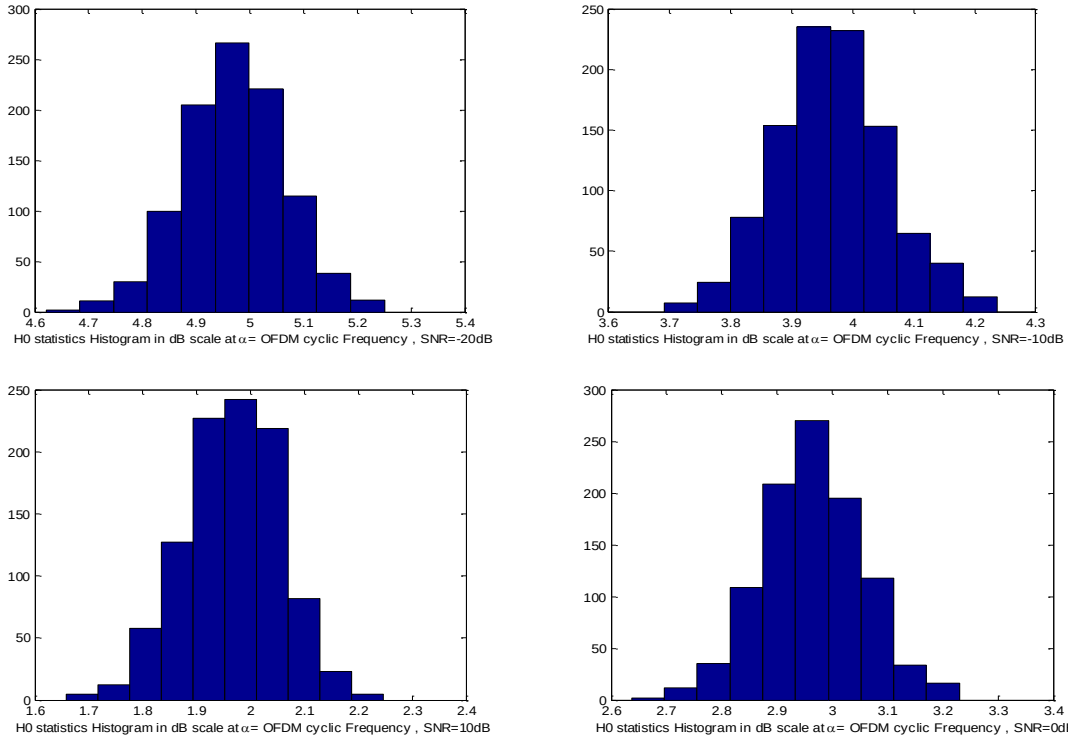


***Figure 7-38*** *$H_0$ statisitcs based noise histogram used in noise mean and variacne calculation for OFDM cyclostatioanry detection at 10 cyclic frequencies ($\alpha_{1:10}$), top left : SNR=-20 dB, top right: SNR=-10 dB, bottom right: 0 dB, bottom left: SNR=10 dB*

### 7.5.4 Simulation parameters issues

The following simulation parameters are expected to influence the results:

- The threshold selection: the threshold is used according to the fixed false alarm value of 0.01 to obtain binary detection performance. More adaptive selection of threshold according to SNR and test statistics will lead a better result.
- The number of random realizations: currently we used 1000 random iterations for test statistics generation from SCF value. More number of random realizations (e.g. 2000, 30000) would influence the detection performance.
- FAM Window: we used Hamming window for all types of cyclic spectral analysis performed in this thesis. However, using of other kinds of windows (e.g. Hanning, Kaiser etc) will influence the detection performance.
- The SCF test statistics choice (discussed in section 7.2.3.3 and section 7.3.3.3) and selection of cyclic frequency are also important influencing factors for getting better detection
- In this thesis, cyclic resolution is selected as $0.00005 *$ sampling frequency and spectral resolution is selected as $0.1 *$ sampling frequency. Selection of these particular values are also playing key role in SCF estimation.

.

# 8. CONCLUSIONS AND FUTURE WORKS

## 8.1 Conclusions

This thesis gave an overview of the signals of opportunity concepts and briefly illustrated the potential of signals of opportunity for positioning. The author presented a generic model for the signals of opportunity-based positioning system in chapter 2. This thesis reviewed the system specific models of the majority of the wireless signals who are available indoors, in order to evaluate their potential in positioning. Furthermore, in order to fully realize the spectrum awareness criteria of future cognitive positioning, several methods for spectrum sensing and signal classification were presented. While presenting the spectrum sensing methods in chapter 4, significant emphasis was given to cyclostationary detection and classification. The thesis addressed the importance of selecting the suitable signal from a pool of signals and mentioned possible solutions to that. The main contribution of this thesis is two-folds: providing a review of cyclostationary signal theory in the context of SoO and the application of cyclostationarity properties to signal detection in noise (for the purpose of identifying the signals available for positioning). Additionally, in chapter 6, this thesis discussed about all kinds of existing spectral correlation methods which can be used for cyclic spectral analysis. In the simulation section of chapter 6, the most effective method, namely FAM, was selected for spectral analysis of CDMA and OFDM signals. Chapter 7 showed the detection results and the last sections of chapter 7 discussed about the results obtained on individual cyclostationary detection of CDMA and OFDM. The results indicated how to do the selection of a cyclic frequency from a set of cyclic frequencies at which the cyclostationary detection can be performed in order to achieve desirable detection performance. Moreover, effects of various data reduction techniques for spectral correlation on cyclostationary detection were examined. Summing up, the thesis explained the usage of cyclostationary analysis for signal detection and compared it with other spectrum sensing techniques including energy detection. The conclusion was that cyclostationarity features can be indeed used to select the available SoO in noise and they have potential into detecting the SoO into a mixture of signals as well (a work that has been further developed in [124].

However, several areas can still be explored further, since the testing set of multiple cyclic frequencies was selected on a random manner so far. Moreover, the lengths of the observation interval, the length of the FAM window and the threshold choice also have

an impact in the results. A better understanding of the cyclic frequencies and spectral correlation pattern can lead to a better reliability in cyclostationary-based detection.

## 8.2 Future works

Further investigation on cyclostationary detection performance can be done by taking into account variations in the simulation parameter (e.g. bandwidth, pilot power, processing time, modulation order). Moreover, in the simulation of cyclostationary signal detection, the presence of multipath and fading channel, the cyclic frequency offset due to Doppler shift, the interference associated with the channel and noise power uncertainty involvements are yet to discover. It will be very interesting to observe the cyclostationary detection performance with the presence of non-stationary noise as well. As future work, signal detection from combination of signals should be analyzed. The pattern of signals cyclostationary features statistical distribution can be checked with chi-square distribution and this verification can provide a result whether simulation based generated spectral correlation follow chi-square distribution or not. A completely new dimension can be given to this research by starting the analysis on signal classification through this cyclostationary signal analysis. As a continuation of this work, cyclostationary properties of ultra wideband signals will also be investigated in the context of cognitive positioning. Finally, a development of a MATLAB Simulink based simulator model with process blocks for cyclostationary analysis can be taken into consideration for future work purposes which will be generic in terms of multiple signal processing and proving output on signal detection and classification performance.

# REFERENCES


[1] D. Skournetou, "Delay estimators for tracking low CNR GNSS signals", Master thesis, Tampere University of Technology, August 2007.

[2] A. Dammann, S. Sand and R. Raulefs, "Signals of opportunity in mobile radio positioning", in *Proceedings 20th European Signal Processing Conference (EUSIPCO 2012)*, Bucharest, Romania, pp. 549- 553, August 2012.

[3] M. A. Enright and C. N. Kurby, "A Signals of Opportunity Based Cooperative Navigation Network", in *NAECON, 2009 IEEE Aerospace & Electronics Conference*, pp. 213- 218, 2009.

[4] M. Robinson, R. Ghrist, "Topological Localization via Signals of Opportunity", *IEEE Transactions on Signal Processing*, vol. 60, no. 5, pp. 2362-2373, 2012.

[5] S. Hadzic, J. Rodriguez, "Cooperative Positioning for Heterogeneous Wireless Systems: Proposed Framework", *2010 6th International Conference on Wireless and Mobile Communications*, pp. 215-218, 2010.

[6] J. Zhang, "Advanced Signal Processing in Multi-mode Multi-frequency Receivers for Positioning Applications", PhD thesis, Tampere University of Technology, Tampere, 2013.

[7] E. S. Lohan, J. Lunden, G. Seco-Granados, J. A. Lopez-Salcedo, and V. Koivunen, "Cyclic Frequencies of GNSS Signals and their Potential within a Cognitive Framework", *ION Navigation journal*, [in press], 2014.

[8] H. Celebi and H. Arslan, "Cognitive Positioning Systems", *IEEE Transactions on Wireless Communications*, vol. 6, no. 12, pp. 4475–4483, Dec. 2007.

[9] K. W. Kim, "Exploiting Cyclostationarity for Radio Environmental Awareness in Cognitive Radios Awareness in Cognitive Radios", PhD thesis, Virginia Polytechnic Institute and State University, Blacksburg, VA, USA, 2008.

[10] E. Like, V. Chakravarthy, P. Ratazzi and Z. Wu, "Signal Classification in Fading Channels Using Cyclic Spectral Analysis", *EURASIP J. Wirel. Commun. Netw*, vol. 2009, no. 1, p. 879812, 2009.

[11] C. Watson, "Signal Detection and Digital Modulation Classification based Spectrum Sensing for Cognitive Radio", PhD thesis, Northeastern University, 2014.

[12] K. Kim, I. Akbar, and K. Bae, "Cyclostationary Approaches to Signal Detection and Classification in Cognitive Radio", in *New Frontiers in Dynamic Spectrum Access Networks*, Dublin, no. 6, pp. 212–215, 2007.

[13] E. L. Costa, “Detection and Classification of Cyclostationary Signals”, Master thesis, Naval Postgraduate School, Monterey, CA, US, March 1996.

[14] A. Dammann, S. Sand and R. Raulefs, “On the benefit of observing signals of opportunity in mobile radio positioning”, in *Proceedings 9th International ITG Conference on Systems, Communications and Coding (SCC 2013)*, Munich, Germany, pp. 1-6, January 2013.

[15] W. A. Gardner, “Exploitation of spectral redundancy in cyclostationary signals”, *Signal Processing Magazine, IEEE*, vol. 8, no. 2, pp. 14-36, 1991.

[16] W. A. Gardner, A. Napolitano and L. Paura, “Cyclostationarity: Half a century of research”, *Signal Processing*, vol. 86, no. 4, pp. 639–697, Apr. 2006.

[17] G. Giannakis, “Cyclostationary Signal Analysis”, University of Virginia, CRC Press LLC, 1999.

[18] W. A. Gardner, “Cyclostationarity in Communications and Signal Processing”, Ed. W. A. Gardner. IEEE Press, New York, 1994.

[19] J. Lunden and V. Koivunen, “Spectrum sensing in cognitive radios based on multiple cyclic frequencies”, in *Proc. 2nd Int. Conf. Cognitive Radio Oriented Wireless Netw. Commun. (CrownCom)*, pp. 37–43, Orlando, FL, USA, July 31–August 3, 2007.

[20] R. Thoma, “Spectral Correlation Measurement”, Department of Communication and Measurement, Technical University of Ilmenau, Germany, Tech. Rep., 1993.

[21] C. Tom, “Cyclostationary spectral analysis of typical satcom signals using the FFT accumulation method”, space systems and technology section, defense research establishment Ottawa, Ottawa, Canada, Tech. Rep., 1995.

[22] T. Asai, A. Benjebbour, H. Yoshino, “Recognition of CDMA signals with orthogonal codes using cyclostationarity”, *IEEE 6th Workshop on Signal Processing Advances in Wireless Communications*, pp. 480- 484, 2005.

[23] S. Sohn and N. Han, J. kim “OFDM Signal Sensing Method Based on Cyclostationary Detection”, in *Proc. ICST, Conference on Cognitive Radio Oriented Wireless Networks and Communications*, USA, pp. 63 – 68, Aug. 2007.

[24] H. Liu, H. Darabi, P. Banerjee, and J. Liu, "Survey of Wireless Indoor Positioning Techniques and Systems", *IEEE Transactions on systems ,man, and cybernetics-part c:application and reviews*, vol. 37, no. 6, pp. 1067–1080, 2007.

[25] F. Gustafsson, F. Gunnarsson, "Mobile positioning using wireless networks: possibilities and fundamental limitations based on available wireless network measurements", *IEEE Signal Processing Mag.*, vol. 22, no. 4, pp. 41-53, Jul. 2005.

[26] S. Shrestha, "RSS-Based Position Estimation in Cellular and WLAN Networks", Master of Science Thesis, Tampere University of Technology, January 2012.

[27] P. Prasithsangaree, P. Krishnamurthi and P. K. Chrysanthis, "On indoor position with wireless LANs", in *Proc. IEEE Int. Symp. Pers. Indoor, Mobile Radio Commun*, vol. 2, pp. 720–724, Sep. 2002.

[28] M. Vossiek, M. Wiebking, L. Gulden, P. Weighardt and J. Hoffmann, "Wireless local positioning—Concepts, solutions, applications", in *Proc. IEEE Wireless Commun. Netw. Conf.*, pp. 219–224, Aug. 2003.

[29] A. K. M. M. Hossain and W.S. Soh, "A comprehensive study of Bluetooth signal parameters for localization", The *18th Annual IEEE International Symposium on Personal, Indoor and Mobile Radio Communications (PIMRC'07)*, Athens, Greece, pp.1-5, 2007.

[30] N. Mair and Q. H. Mahmoud, "A Collaborative Bluetooth-Based Approach to Localization of Mobile Devices", *8th International Conference on Collaborative Computing: Networking, Applications and Worksharing*, *Collaboratecom 2012*, Pittsburgh, PA, United States, pp. 362-371, October, 2012.

[31] A. Cangialosi, J.E. Monaly and S.C. Yang, "Leveraging RFID in hospitals: Patient life cycle and mobility perspectives", *IEEE Communications Magazine*, vol. 45, no. 9, pp. 18–23, Sept. 2007.

[32] R. Want, "An introduction to RFID technology", *IEEE Pervasive Computing*, vol. 5, no. 1, pp. 25–33, Jan.-March 2006.

[33] J. L. Brchan, Z. Lianlin, W. Jiaqing, R. E. Williams, L. C. P´erez, "A Real-time RFID Localization Experiment Using Propagation Models*", IEEE International Conference on RFID (RFID)*, pp. 141- 148, Orlando, FL, 2012.

[34] T. Sanpechuda and L. Kovavisaruch, "A review of RFID Localization: Applications and Techniques", National Electronics and Computer Technology Center, Thailand, *Proceedings of ECTI-CON 2008*, vol. 2, pp. 769-772, 2008.

[35] Z. Qinghui, L. Wei, "Research on the Three Dimensional Indoor RFID Positioning Algorithm", *ICCMS '10. Second International Conference on Computer Modeling and Simulation*, vol. 10, pp.93- 95, 2010

[36] J. Hightower, R. Want, and G. Borriello, "SpotON: An indoor 3D location sensing technology based on RF signal strength", Univ. Washington, Seattle, Tech. Rep. UW CSE 2000–02-02, Feb. 2000.

[37] S. Gezici, H. V. Poor, "Position Estimation via Ultra-Wideband Signals Federal Communications Commission", First Report and Order 02-48, Feb. 2002.

[38] Z. Sahinoglu, S. Gezici, and I. Guvenc, "Ultra-Wideband Positioning Systems: Theoretical Limits, Ranging Algorithms, and Protocols", Cambridge University Press, 2008.

[39] R. J. Fontana, "Recent system applications of short-pulse ultra-wideband (UWB) technology", *IEEE Trans. Microw. Theory Tech.*, vol. 52, no. 9, pp. 2087–2104, Sep. 2004.

[40] J. Huang , L. Lo Presti , R. Garello and B. Sacco, "Study of Positioning Methods in DVB-T Single Frequency Networks", in *Proceedings of the Fourth International Conference on Communications and Electronics*, Hue, Vietnam, pp. 263–268, August 2012.

[41] J. Huang, L. Lo Presti and R. Garello, "Article on Digital Video Broadcast-Terrestrial (DVB-T) Single Frequency Networks Positioning in Dynamic Scenarios", in *Sensors 2013*, vol. 13(8), August 2013.

[42] H. Celebi, "Location awareness in cognitive radio networks", PhD thesis, University of South Florida, 2008.

[43] H. Celebi and H. Arslan, "Utilization of Location information in Cognitive Wireless Networks", *IEEE Wireless Communications Magazine- Special Issue on Cognitive Wireless Networks*, vol. 14, no. 4, pp. 6-13, August 2007.

[44] A. Gorcin, K. A. Qaraqe, H. Celebi, and H. Arslan, "Location-Aware Cognitive Communication Systems for Public Safety," pp. 1–41, in "Telecommunications in Disaster Areas" book, River, Nov. 2010.

[45] D. Skournetou, “Mitigation of Dominant Channel Propagation Effects in GNSS-based Positioning”, PhD thesis, Tampere University of Technology, 2012.

[46] V. Juarez-leria, “Timing-based location estimation for OFDM signals with applications in LTE, WLAN and WiMax”, Master thesis, Tampere University of Technology, February 2012.

[47] D. A. Streight, “Application of cyclostationary signal selectivity to the carry on multi-platform GPS assisted time difference of arrival system”, Mater thesis, Naval Postgraduate school, Monterey, California, USA, March 1997.

[48] V. Moghtadaiee, S. Lim, and A. G. Dempster, “System-Level Considerations for Signal-of-Opportunity Positioning”, *2010 International Symposium on GPS/GNSS*, Taipei, Taiwan, pp. 1–7, October 2010.

[49] L.A. Latiff, A. Ali, O. Chia-Ching, N. Fisal, “Development of an indoor GPS-free self-positioning system for mobile ad hoc network (MANET)”, *The IEEE 7th Malaysia International Conference on Communication*, vol. 2, 2005.

[50] S. Chang, S. Ham, S. Kim, D. Suh, H. Kim, “Ubi-Floor: Design and Pilot Implementation of an Interactive Floor System”, *2010 2nd International Conference on Intelligent Human-Machine Systems and Cybernetics (IHMSC)*, vol. 2, pp. 290- 293, 2010.

[51] C.R. Yu, C.L. Wu, C.H. Lu, L.C. Fu, “Human Localization via Multi-Cameras and Floor Sensors in Smart Home”, *IEEE International Conference on systems, Man and Cybernetics, 2006*, vol. 5, pp. 3822- 3827, 2006.

[52] F. Ellinger, R. Eickhoff, A. Ziroff, J. Huttner, R. Gierlich, J. Carls, G. Bock, "European project RESOLUTION-local positioning systems based on novel FMCW radar", *IEEE, Microwave and Optoelectronics Conference*, Brazil, pp. 499- 502, 2007.

[53] E. S. Lohan, G. Seco-Granados, “C/N0-Based Criterion for Selecting BOC-Modulated GNSS Signals in Cognitive Positioning”, *IEEE Comm. Letters*, vol. 17, no. 3, pp. 537–540, 2013.

[54] O. Zakaria, “Blind signal detection and identification over the 2.4 GHz ISM band for cognitive radio”, Master thesis, University of south Florida, USA, 2009.

[55] J. Larranaga, L. Muguira, J. M. Lopez-Garde, J. I. Vazquez, “An environment adaptive ZigBee-based indoor positioning algorithm”, *2010 International Con-*

*ference on Indoor Positioning and Indoor Navigation (IPIN)*, pp. 1- 8, Zurich, 2010.

[56] T. Luftner, C. Kropl, R. Hagelauer, M. Huemer, R. Weigel, J. Hausner, "Wireless infrared communications with edge position modulation for mobile devices", *Wireless Communications, IEEE,* vol. 10, no. 2, pp. 15-21, 2003.

[57] Q. Wang, G. Ren, "Novel positioning scheme with single base station for high speed train in WiMax systems", *ICCE-China Workshop (ICCE-China), 2013 IEEE,* pp. 63- 66, 2013.

[58] F. Xiangning, T. Sailang, Z. Xiaodong, "Networking and routing for mesh wireless network", in *Proceedings International Conference on Wireless Communications, Networking and Mobile Computing,* vol. 2, pp. 1068- 1071, 2005.

[59] H. Nurminen, J. Talvitie, S. Ali-Löytty, P. Muller, E.S. Lohan, R. Piché, M. Renfors, "Statistical path loss parameter estimation and positioning using RSS measurements", accepted to *Journal of Global Positioning Systems*, 2013.

[60] S. Shrestha, J. Talvitie, and E.S. Lohan, "Deconvolution-based indoor localization with WLAN signals and unknown access point locations", in *Proc. of IEEE ICL-GNSS*, Jun 2013, Italy.

[61] H. Nurminen, S. Ali-Löytty, R. Piché, J. Talvitie, E.S. Lohan, M. Renfors, "Statistical Path Loss Parameter Estimation and Positioning Using RSS Measurements in Indoor Wireless Networks", in *Proc. of IPIN*, Nov 2012, Australia.

[62] V. Kelly, "New IEEE 802.11ac™ Specification Driven by Evolving Market Need for Higher, Multi-User Throughput in Wireless LANs", report, *2014 International CES*, USA, 2014.

[63] X. Feng, Q. Zhang, B. Li , "Enabling Co-channel Coexistence of 802.22 and 802.11af Systems in TV White Spaces", *2013 IEEE International Conference on Communications (ICC)*, Budapest, pp. 6040- 6044, June 2013.

[64] E. Perahia, C. Cordeiro, M. Park and L. L. Yang, "IEEE 802.11ad: Defining the Next Generation Multi-Gb/s Wi-Fi*," 2010 7th IEEE Consumer Commun. and Net. Conf.*, pp. 1–5, Jan. 2010,

[65] P. Bigioi, A. Ionas, G. Susanu, P. Corcoran, "Connectivity Solution to Link a Bluetooth Camera to the Internet", in *Proceedings of IEEE Consumer Electronics*, vol. 47, no. 9, pp. 294 – 299, August 2001.

[66] M. Bouet, A.L. dos Santos, "RFID tags: Positioning principles and localization techniques, Wireless Days", *2008 WD '08*. 1st IFIP, pp. 1- 5, 2008.

[67] Axcess International Inc., [WWW], [Accessed on 20.3.2013], Available: http://www.axcessinc.com

[68] B. Witwer, "Developing the 777 airplane information management system (AIMS): a view from program start to one year of service", *IEEE Transactions on Aerospace and Electronic Systems*, vol. 33, no. 2, Part: 2, pp. 637- 641, 1997.

[69] J. Iinatti, I. Oppermann, and M. Ha, Eds., *UWB Theory and Applications*, New York: Wiley, 2004.

[70] Z. Sahinoglu, S. Gezici, and I. Guvenc, "Ultra-Wideband Positioning Systems: Theoretical Limits, Ranging Algorithms, and Protocols", Cambridge University Press, 2008.

[71] S. Gezici, H.V. Poor, "Position Estimation via Ultra-Wide-Band Signals", *Proceedings of the IEEE*, vol. 97, no. 2, pp. 386- 403, 2009.

[72] U.H. Reimers, "DVB-The Family of International Standards for Digital Video Broadcasting", *Proceedings of the IEEE*, vol. 94, no.1, pp. 173-182, 2006

[73] U. Reimers and A. Morello, "DVB-S2, the second generation standard for satellite broadcasting and unicasting", *Int. J. Satell. Commun. Network*, vol. 22, no. 3, May–Jun. 2004.

[74] M. A. Abu-Rgheff, *Introduction to CDMA*, 1st ed. Academic, pp. 153–194, 2007

[75] A. Lakhzouri, "Channel Estimation and Mobile Phone Positioning in CDMA Based Wireless Communication Systems", Master thesis, Tampere University of Technology, 2005.

[76] S. de J. Silván, "Nomothetic Approaches for Spectrum Sensing," Master thesis, Tampere University of Technology, 2012.

[77] D. Lee, H. Lee, and L. B. Milstein, "Direct Sequence Spread Spectrum Walsh-QPSK Modulation", *IEEE Transactions on communications*, vol. 46, no. 9, September 1998.

[78] B.J. Ku, H.Y. Yang, S.H. Yoon, S.C. Han , C.E. Kang , "Turbo code and star 16-QAM for DS/SSMA communications", *IEEE Pacific Rim Conference on Communications, Computers and Signal Processing*, pp. 337- 340, 1999.

[79] R. L. Peterson, R. E. Ziemer, and D. E. Borth, "Introduction to Spread Spectrum Communications", Prentice Hall, Inc., 1995.

[80] T. F. Wong, *Spread Spectrum & CDMA*, eBook, lecture notes, University of Florida, Chapter 2. Available : http://wireless.ece.ufl.edu/twong/Notes/CDMA/ch2.pdf

[81] C. Quintana, J. Rabadan, J. Rufo, F. Delgado and R. Perez-Jimenez, "Time-Hopping Spread-Spectrum System for Wireless Optical Communications", *IEEE Transactions on Consumer Electronics*, vol. 55, no. 3, August, 2009.

[82] J. H. Baik, M. Sherman, F. Wajid, "Come toward the Light: A Post Biblical Project in Luminal Navigation" eBook, Rutgers 332 428, Dec. 2010, available: http://www.winlab.rutgers.edu/~crose/428_html/proposals_various/OverheadlightNav.pdf

[83] M. Laner, "Evaluation and modeling of power control information in a 3G cellular mobile network," Master's thesis, TU Wien, 2009. [WWW]. Available: http://publik.tuwien.ac.at/files/PubDaU77941.pdf

[84] A. Ziani, A. Medouri, "Implementation and performance of the RAKE receiver for CDMA", *2011 International Conference on Multimedia Computing and Systems (ICMCS)*, pp. 1- 4, 2011.

[85] M. Z. H. Bhuiyan, E. S. Lohan, and M. Renfors, "Code Tracking Algorithms for Mitigating Multipath Effects in Fading Channels for Satellite-Based Positioning," *EURASIP J. Adv. Signal Process*, vol. 2008, pp. 1–18, 2008.

[86] S. R. Schnur, "Identification and Classification of OFDM based Signals Using Preamble Correlation and Cyclostationary Feature Extraction", Master Thesis, Naval post graduate school, California, USA, 2009.

[87] M. E. Castro, "Cyclostationary Detection for OFDM in Cognitive Radio Systems.", Master thesis, University of Nebraska-Lincoln, August 2011.

[88] H. A. Suraweera, K. R. Panta, M. Feramez, and J. Armstrong, "OFDM Peak-to-Average Power Reduction Scheme with Spectral Masking." *Proc. Symp. on Communication Systems, Networks and Digital Signal Processing*, pp.164-167, July 2004.

[89] A. S Kang, V. Sharma, “Pulse Shape Filtering in Wireless Communication-A Critical Analysis”, *(IJACSA) International Journal of Advanced Computer Science and Applications*, vol. 2, no.3, March 2011.

[90] M. K. Simon, “Bandwidth-Efficient Digital Modulation with Application to Deep-Space Communications”, issued by the Deep-Space Communications and Navigation Systems, California Institute of Technology, June 2001.

[91] F. Xiong, *Digital Modulation Techniques*. Boston, MA: Artech House, 2000.

[92] S. Ranvier, "Modulation methods", Radio Laboratory/ TKK, Helsinki University of Technology, 16 November 2004, [WWW], [accessed on 15.04.2014], Available: http://www.comlab.hut.fi/opetus/333/2004_2005_slides/modulation_methods.pdf

[93] S. Hinedi, M. Simon, D. Raphaeli, “The performance of non-coherent orthogonal M-FSK in the presence of timing and frequency errors”, *IEEE Transactions on Communications*, vol. 43, no. 2/3/4, pp. 922- 933, 1995.

[94] A. Y. Wang, C. G. Sodini, “On the Energy Efficiency of Wireless Transceivers”, *IEEE International Conference on Communications*, vol. 8, pp.3783- 3788, 2006.

[95] B. Kim, V. Stojanovic, “An Energy-Efficient Equalized Transceiver for RC-Dominant Channels”, *IEEE Journal of Solid-State Circuits*, vol.45, no. 6, pp. 1186- 1197, 2010.

[96] M. M. Hasan, L. H. Jiun, N. W. Cheun , M. S. Shahid, “Smart telephone design-caller identification and answering machine”, *1998 IEEE International Conference on Semiconductor Electronics, 1998. Proceedings. ICSE '98*. pp. 217 - 222, Bangi, 1998

[97] T. Wescott, “A DGPS/Radiobeacon Receiver for Minimum Shift Keying with Soft Decision Capabilities”, Master of Science Thesis, Worcester Polytechnic Institute, 1990.

[98] Differential Global Positioning System (DGPS), Canadian Coast Guard, [WWW], Available: http://www.ccg-gcc.gc.ca/eng/CCG/DGPS_Home

[99] J. B. Anderson, T. Aulin, and C.E. Sundberg, *Digital Phase Modulation*, New York: Plenum Press, 1986.

[100] P. K. Govindaiah, "Design and Development of Gaussian Minimum Shift Keying (GMSK) Demodulator for Satellite Communication", *International Journal of Research in Communication Engineering*, vol. 2, no. 2, June 2012.

[101] F. Jondral, R. Machauer, and A. Wiesler, "Comparison of GMSK and linear approximated GMSK for use in Software Radio." *In Proceedings 1998 IEEE 5th International Symposium on Spread Spectrum Techniques and Applications*, vol. 2, pp. 557-559, Sun City, 1998.

[102] K. Murota and K. Hirade, "GMSK Modulation for Digital Mobile Radio Telephony," *IEEE Transactions on Communications*", vol. COM-29, no. 7. pp. 1044-1050, July 1981.

[103] University of Hull, report, "Appendix D – Digital Modulation and GMSK", [WWW], Available: http://www.emc.york.ac.uk/reports/linkpcp/appD.pdf

[104] Automatic Identification system overview, USA coast guard, report, [WWW], [accessed on 15.04.2014], Available: http://www.navcen.uscg.gov/?pageName=AISworks

[105] D. Cimarusti, R. Ives, "Development of an automatic identification system of spoken languages: Phase I", *IEEE International Conference on Acoustics, Speech, and Signal Processing, ICASSP '82*, vol. 7, pp. 1661- 1663, 1982

[106] W. A. Kissick, "The temporal and spectral characteristics of Ultra wideband s ignals", U.S. Department of Commerce, NTIA report 01-383, Jan. 2001, Available: http://www.wireless.ece.ufl.edu/uwb/signalpapers/01-383.pdf

[107] J. Harvey and R. Harjani, "Pulse Generator Design for UWB IR Communication Systems," Dept of ECE, University of Minnesota, MN 55455, USA, *2005 IEEE Int. Symp. Circuits Syst.*, vol. 2, pp. 4381–4384, 2005.

[108] T. K. K. Tsang and M. N. El-Gamal, "Ultra –Wideband (UWB) communications systems : An overview," in *The 3rd International IEEE-NEWCAS Conference, 2005*, pp. 381-386, 2005.

[109] A. Conti, M. Guerra, D. Dardari, N. Decarli, M.Z. Win, "Network Experimentation for Cooperative Localization", *IEEE Journal on Selected Areas in Communications*, vol. 30, no. 2, pp. 467- 475, 2012.

[110] M. Z. Win, A. Conti, S. Mazuelas, Y. Shen, W.M. Gifford, D. Dardari, M. Chiani, "Network localization and navigation via cooperation", *IEEE Communications Magazine*, vol. 49, no. 5, pp. 56- 62, 2011.

[111] Y. Saito, Y. Kishiyama, A. Benjebbour, T. Nakamura, A. Li, and K. Higuchi, "Non-Orthogonal Multiple Access (NOMA) for Future Radio Access", *2013 IEEE 77th Vehicular Technology Conference (VTC Spring)*, pp. 1- 5, 2013.

[112] T. Nakamura, "LTE Enhancements and Future Radio Access", NTT DOCOMO, INC, *The 5th Future of Wireless International Conference*, 2013 [WWW], [accessed on 25.04.2014], Available: http://www.cambridgewireless.co.uk/Presentation/TakehiroNakamura020713.pdf

[113] S. Haykin, D. J. Thomson, and J. H. Reed, "Spectrum Sensing for Cognitive Radio," *Proc. IEEE*, vol. 97, no. 5, pp. 849–877, May 2009 .

[114] D. Rawat and G. Yan, "Spectrum Sensing Methods and Dynamic Spectrum Sharing in Cognitive Radio Networks: A Survey", *International Journal of Research and Reviews in Wireless Sensor Networks*, vol. 1, no. 1, 2011.

[115] A. B. MacKenzie, J. H. Reed, P. Athanas, C. W. Bostian, R. M. Buehrer, L. A. DaSilva, S. W. Ellingson, Y. T. Hou, M. Hsiao, C. Patterson, S. Raman, and C. da Silva, "Cognitive Radio and Networking Research at Virginia Tech", *Proc. IEEE*, vol. 97, no. 4, pp. 660–688, Apr. 2009.

[116] M. Sherman, A. N. Mody, R. Martinez and C. Rodriguez, "IEEE Standards Supporting Cognitive Radio and Networks, Dynamic Spectrum Access, and Coexistence," in *Journal IEEE Communications Magazine*, vol. 46, pp. 72–79, July 2008.

[117] S. D. Barnes, "Cognitive Radio Performance Optimization through Spectrum Availability Prediction", Master Thesis, University of Pretoria. March 2012.

[118] R. R. Thomas, B. Zayen, R. Knopp, B.T. Maharaj, "Multiband Time-of-Arrival positioning technique for cognitive radio systems", *2011 IEEE 22nd International Symposium on Personal Indoor and Mobile Radio Communications (PIMRC)*, pp. 2315- 2319, 2011.

[119] W. Guibène and D. Slock, "Cooperative Spectrum Sensing and Localization in Cognitive Radio Systems Using Compressed Sensing", *Journal of Sensors*, vol. 2013, article ID 606413, 9 pages, 2013.

[120] A. M. Gillman, "Non Co-operative Detection of LPL/LPD Signals via Cyclic Spectral Analysis", Master Thesis, Air Force Institute of Technology, Canberra, Australia, March 1999.

[121] T. Yucek and H. Arslan, "A survey of spectrum sensing algorithms for cognitive radio applications", *IEEE Commun. Surv. Tutorials*, vol. 11, no. 1, pp. 116–130, 2009.

[122] B. A. Siddiqui, "Simulink-based acquisition unit for Galileo E1 CBOC modulated signals", Master Thesis, Tampere University of Technology, November 2009.

[123] M. F. Samad, "Effects of MBOC Modulation on GNSS Acquisition Stage", Master Thesis, Tampere University of Technology, 2009.

[124] P. Figueiredo e Silva, M. L. Rahman, G. Seco-Granados and E.S. Lohan, "Detection of cyclic frequencies in a mixed CDMA and OFDM signal for cognitive positioning systems", submitted to *International Conference on Localization and GNSS 2014.*

[125] R. R. Thomas and B. T. Maharaj, "Towards a bandwidth efficient cognitive positioning system", *IET Electronic Letters*, vol. 48, no. 12, pp. 787–788, June 2012.

[126] R. R. Thomas, B. Zayen, R. Knopp and B. T. Maharaj, "Multiband Time-of-Arrival Positioning Technique for Cognitive Radio Systems", in *22nd PIMRC 2011 workshop on cognitive radio and networking: solutions and challenges ahead*, Toronto, Canada, pp.2315-2319, September 2011.

[127] K. Sithamparanathan and A. Giorgetti, "Cognitive Radio Techniques: Spectrum Sensing, Interference Mitigation, and Localization", Artech House, Sep. 2012, chapter 3: Introduction to Spectrum Sensing Techniques, [WWW], Available: http://www.artechhouse.com/static/sample/Sith-203_CH03.pdf

[128] S. B. Sadkhan, N. A. Abbas, "Higher Order Statistics and Their Roles in Blind Source Separation (BSS)", *MASAUM Journal of Computing*, vol. 1, no. 2, September 2009.

[129] H. B. Guan, C. Z. Ye, M. Y. Li, "Modulation classification based on spectrogram", *Proceedings of the Third International Conference on Machine Learning and Cybernetics*, Shanghai, vol. 6, pp. 3551-3556, August 2004.

[130] A. Kubankova, "Examination of Digital Modulations Classification Method based on Spectrogram Analysis on Signals Corrupted by Different Noises and Interferences," *Proc. 8th WSEAS Int. Conf. Signal Process*. pp. 90–93, 2009.

[131] J. Mendel, "Tutorial on higher-order statistics (spectra) in signal processing and system theory: Theoretical results and some applications," *Proc. IEEE*, vol. 79, pp. 278-305, Mar. 1991.

[132] F.J. Massey, "The Kolmogorov-Smirnov Test for Goodness of Fit", *Journal of the American Statistical Association*. vol. 46, no. 253, pp. 68–78, March, 1951.

[133] Y. Li, F. Wang, and G. Zhu, "Hybrid digital modulation classification", *8th Int. Wirel. Commun. Mob. Comput. Conf.*, no. 1, pp. 990–993, August, 2012.

[134] C.K. Chiu, *An Introduction to Wavelets*, Academic Press, San Diego, 1992.

[135] E. Hernandez, and G. L. Weiss, *A First Course on Wavelets*, CRC Press Inc., 489, 1996.

[136] K.C. Ho, W. Prokopiw and Y.T. Chan, "Modulation identification of digital signals by the wavelet transform", *IEEE Pruc.-Radur; Sonar Navig.*, vol. 147, no. 4, pp. 169-176, August, 2000.

[137] L. Hong and K. C. Ho, "Identification of digital modulation types using the wavelet transform," in *Proc. IEEE MILCOM*, pp. 427-431, 1999.

[138] F. K. Faek, "Digital Modulation Classification Using Wavelet Transform and Artificial Neural Network", *J. Zankoy Sulaimani*, vol. 13, no. 1, 2010.

[139] B. E. Guenther, "Multi-User Signal Classification via Cyclic Spectral Analysis", Master Thesis, Wright State University, USA, 2009.

[140] W.A. Gardner, *Introduction to Random Processes with Applications to Signals and Systems*, 2nd Ed., MacGraw-Hill, New York, 1986.

[141] A. Papoulis, "Probability, Random variables, and Stochastic Processes", 3rd edition, McGraw-Hill, 1991.

[142] D. A. Streight, "Application of cyclostationary signal selectivity to the carry on multi-platform GPS assisted time difference of arrival system", Mater Thesis, Naval Postgraduate school, Monterey, California, USA. March 1997.

[143] R. Roberts, W. Brown, and H. Loomis, "Computationally Efficient Algorithms for Cyclic Spectral Analysis", *Signal Processing Magazine, IEEE*, vol. 8, no. 2, pp. 38-49, 1991.

[144] W.A. Brown, and H. H. Loomis, "Digital Implementations of Spectral Correlation Analyzers", *IEEE Transactions on signal processing*, vol. 41, no. 2, February 1993.

[145] J. Mishra, D. K. Barik, C. M. K. Swain, "Cyclostationary Based Spectrum Sensing in Cognitive Radio: Windowing Approach", *International Journal of Recent Technology and Engineering (IJRTE)* ISSN: 2277-3878, vol. 3, no. 1, March 2014.

[146] P. D. Sutton, K. E. Nolan, and L. E. Doyle, "Cyclostationary Signatures in Practical Cognitive Radio Applications", *IEEE Journal on selected areas in communications*, vol. 26, no. 1, January 2008.

[147] B. Parkinson, J. Spilker, P. Axelrad, P. Enge, "Global Positioning System: Theory and Applications", volume II, American Institute of Aeronautics and Astronautics, Washington, DC, 1996.

[148] J. Bao-Yen Tsui, "Fundamentals of Global Positioning System Receivers: A Software Approach", Copyright 2000 John Wiley & Sons, Inc. Print ISBN 0-471-38154-3 Electronic ISBN 0-471-20054-9.

[149] M. Derakhshani, T. Le-Ngoc, M. Nasiri-Kenari, "Efficient Cooperative Cyclostationary Spectrum Sensing in Cognitive Radios at Low SNR Regimes", *IEEE Transactions on wireless communications*, vol. 10, no. 11, November 2011.

[150] R. Tandra and A. Sahai, "Fundamental limits on detection in low SNR under noise uncertainty", *2005 International Conference on Wireless Networks, Communications and Mobile Computing*, vol. 1, pp. 464–469, 2005.

[151] G. Ji, and H. Zhu, "On the noise power uncertainty of the low SNR energy detection in cognitive radio", *J. Computational Information Systems*, vol.6, no.8, pp. 2457-2463, 2010, Available at http://www.Jofcis.com